AD-A245 715

(2)

Second Annual Report for Perception for Outdoor Navigation

Charles Thorpe and Takeo Kanade
Principal Investigators

CMU-RI-TR-91-28

DTIC
ELECTE
FEB 11 1992
S D
D

The Robotics Institute
Carnegie Mellon University
Pittsburgh, Pennsylvania 15213

This document has been approved for public release and sale; its distribution is unlimited.

December 1991

DEFENSE TECHNICAL INFORMATION CENTER
9203340

© 1991 Carnegie Mellon University

This report reviews progress at Carnegie Mellon from August 16, 1990 to August 15, 1991 on research sponsored by DARPA, DOD, monitored by the US Army Engineer Topographic Laboratories under contract DACA 76-89-C-0014, titled "Perception for Outdoor Navigation". Parts of this work were also supported by a Hughes Fellowship, by a grant from NSF titled "Annotated Maps for Autonomous Underwater Vehicles," and by a grant from Fujitsu Corporation.

92 2 10 092

REPORT DOCUMENTATION PAGE

Form Approved
OMB No. 0704-0188

Public reporting burden for this collection of information is estimated to average 1 hour per response including the time for reviewing instructions, searching existing data sources gathering and maintaining the data needed, and completing and reviewing the collection of information. Send comments regarding this burden estimate or any other aspect of this collection of information, including suggestions for reducing this burden to Washington Headquarters Services, Directorate for information Operations and Reports, 1215 Jefferson Davis Highway, Suite 1204, Arlington, VA 22202-4302, and to the Office of Management and Budget, Paperwork Reduction Project (0704-0188), Washington, DC 20503

1. AGENCY USE ONLY (Leave blank)	2. REPORT DATE	3. REPORT TYPE AND DATES COVERED
	December 1991	technical

4. TITLE AND SUBTITLE

Second Annual Report for Perception for Outdoor Navigation

5. FUNDING NUMBERS

DACA 76-89-C-0014

6. AUTHOR(S)

Charles Thorpe and Takeo Kanade

7. PERFORMING ORGANIZATION NAME(S) AND ADDRESS(ES)

The Robotics Institute
Carnegie Mellon University
Pittsburgh, PA 15213

8. PERFORMING ORGANIZATION REPORT NUMBER

CMU-RI-TR-91-28

9. SPONSORING / MONITORING AGENCY NAME(S) AND ADDRESS(ES)

DARPA, DoD

10. SPONSORING / MONITORING AGENCY REPORT NUMBER

11. SUPPLEMENTARY NOTES

12a. DISTRIBUTION / AVAILABILITY STATEMENT

Approved for public release;
Distribution unlimited

12b. DISTRIBUTION CODE

13. ABSTRACT *(Maximum 200 words)*

This report reviews progress at Carnegie Mellon from August 16, 1990 to August 15, 1991 on research sponsored by DARPA, DoD, monitored by the U.S. Army Engineer Topographic Laboratories under contract DACA 76-89-C-0014, titled "Perception for Outdoor Navigation."

Research supported by this contract includes perception for road following, terrain mapping for off-road navigation, and ssytems software for building integrated mobile robots. We overview our efforts for the year, and list our publications and personnel, then provide further detail on several of our subprojects.

14 SUBJECT TERMS	15. NUMBER OF PAGES
	87 pp
	16. PRICE CODE

17. SECURITY CLASSIFICATION OF REPORT	18 SECURITY CLASSIFICATION OF THIS PAGE	19 SECURITY CLASSIFICATION OF ABSTRACT	20 LIMITATION OF ABSTRACT
unlimited	unlimited	unlimited	unlimited

Table of Contents

Accesion For
NTIS CRA&I
DTIC TAB
Unannounced
Justification
By
Distribution /
Availability Codes
Dist | Avail and / or Special
A-1

DTIC COPY INSPECTED

List of Figures

List of Tables

Abstract

This report reviews progress at Carnegie Mellon from August 16, 1990 to August 15, 1991 on research sponsored by DARPA, DOD, monitored by the US Army Engineer Topographic Laboratories under contract DACA 76-89-C-0014, titled "Perception for Outdoor Navigation".

Research supported by this contract includes perception for road following, terrain mapping for off-road navigation, and systems software for building integrated mobile robots. We overview our efforts for the year, and list our publications and personnel, then provide further detail on several of our subprojects.

1. Introduction

1.1 Introduction

This report reviews progress at Carnegie Mellon from August 16, 1990 to August 15, 1991 on research sponsored by DARPA, DOD, monitored by the US Army Engineer Topographic Laboratories under contract DACA 76-89-C-0014, titled "Perception for Outdoor Navigation".

During this second year of the contract we have made significant progress across a broad front on the problems of computer vision for outdoor mobile robots. We have built new algorithms (in neural networks, range data analysis, object recognition and road finding); we have integrated our perception modules into new systems (including onroad and off road, notably on the new Navlab II vehicle); and we have participated in notable programmatic events, ranging from generating two new thesis proposals to playing a major role in the "Tiger Team", shaping the architecture for the new DARPA program in Unmanned Ground Vehicles.

This report begins with a summary of the year's activities and accomplishments, in this chapter. Chapter 2, "3-D Landmark Recognition from Range Images", provides more detail on object recognition from multiple sensor locations. Chapter 3, "Representation and Recovery of Road Geometry in YARF", discusses geometry issues in YARF, our symbolic road tracking system. The last two chapters discuss systems issues that are important in providing cues and constraints for an active vision approach to robot driving. "A Computational Model of Driving for Autonomous Vehicles", Chapter 4, introduces the complexities of reasoning for driving in traffic. The fifth and final chapter, "Combining artificial neural networks and symbolic processing for autonomous robot guidance", shows how we combine neural nets with map data in a complete system.

1.2 Algorithms and Modules

YARF (Yet Another Road Follower) tracks roads in color images, using specialized feature detectors to find white lines, yellow lines, and other road markings. Individually detected features are used to update a model of road location and curvature. There are several new ideas implemented in YARF this year. First, the SHIVA system now automatically initializes YARF by finding consistent candidate lines and edges in the first image processed. Thereafter, YARF can use known vehicle motion between frames to position feature trackers in subsequent images.

Secondly, YARF now uses robust statistics to reduce its sensitivity to errors in individual trackers. Robust statistics methods look for consistent subsets of data, rather than always using all the data as is typical of least-squares curve fitting. Thus, a few outliers (mistakes in reported feature location) will be ignored, rather than possibly skewing the estimated road location. More details on the geometric reasoning of YARF, and its use of robust statistics, are given in Chapter 3.

Finally, YARF now has the capability to group features detected or noted as missing in multiple images. Finding a consistent gap in, for instance, a double yellow center line, is a first step in intersection detection.

SCARF, or Supervised Classification Applied to Road Following, has been reimplemented and extended. SCARF uses color clustering to derive typical colors of on- and off-road pixels in a labeled image, then uses those clusters to classify pixels in an unknown image as "most likely road" or "most likely non-road". The classified images must them be searched to find the most probable location of the road in the image. Previous implementations of SCARF ran in about 4 seconds per image on a Sun-4, or 2 second per image on a 10-cell Warp. By making some simplifying assumptions, our current version runs in 0.5 seconds on a Sun-4, or 0.1 second (without I/O) on a 4 thousand processor MASSPAR. The simplifications come partly from not collecting new color classes for each new image, but instead using one set for as long as they are valid. The trick is to determine when

road and off-road colors change enough that new color statistics need to be computed. We have investigated several methods, with promising but not yet conclusive results.

ALVINN, the Autonomous Land Vehicle In a Neural Net, continues to expand its capabilities for road following. The highlights of its performance this year include new top speed of 20 mph (which is the top speed mechanically of the Navlab); runs on new types of road (dirt and 4-lane paved); and driving a new vehicle (the Navlab II, a converted HMMWV). Technically, the biggest new thrust for ALVINN is using multiple nets to handle different situations. An individual network, trained for a particular type of road (say a single-lane paved road), will not be able to handle different scenes (such as a multi-lane road). Furthermore, a neural net will not usually give a good indication of failure; instead, it will cheerfully suggest a steering direction, even if incorrect. Recent work with ALVINN shows that it is possible to derive confidences for individual nets on individual scenes, and thus to select which network is best for each scene. The intuition behind the approach is to use the output of a network to recreate the expected input, and to compare the recreated input with the actual image. If the recreated input is a single-lane road, while the actual scene is multi-lane, the images will have a large mismatch, and that network may be ignored. The subtleties of making this work have to do with appropriate weighting of each pixel.

The other continuing effort with ALVINN, detailed in Chapter 5, involves building large systems that include both connectionist and symbolic processing. Our approach uses a combination of cues, including map information, for vehicle positioning and guidance.

Obstacle Detection

The Navlab has been used to demonstrate computationally efficient obstacle detection using sonar and giga-hertz radar. Using an array of sonars mounted on the Navlab, the system has demonstrated stopping for obstacles; steering around obstacles; and tracking guard rails and parked cars. Each of these applications uses the same underlying data structure, a grid of cells in vehicle coordinates containing the location of detected objects. At each time step, the object locations stored in the grid are updated to account for vehicle motion. New sonar or radar returns are then entered into the grid. A confidence is stored with each entry. If the same grid cell contains an object for more than one time steps, its confidence increases. If an occupied grid cell does not get a new return, its confidence is diminished. After a user-specified interval, the confidence goes to zero, and the object is considered to have disappeared. This gives us a primitive mechanism for handling moving objects.

Starting with the grid data structure, there are several additional processing steps used by particular applications. The obstacle detection module calculates which grid cells the vehicle will sweep as it drives along its intended course. If any of those cells are marked occupied, it decelerates the vehicle to a smooth stop before hitting the object. Obstacle avoidance uses the same algorithm as obstacle detection, but examines several arcs, and chooses an arc that misses the obstacles. This module has been integrated with road following, to track arcs that stay near the center of the road while avoiding obstacles. Tracking linear objects, such as guard rails, starts by fitting a line to the occupied cells that are near the vehicle's path. If the line fits the data well, and is in approximately the predicted location, the module has high confidence that it has correctly tracked the linear feature. It calculates the correct arc along which to steer in order to keep the vehicle at the desired distance from the feature.

Sign Recognition

We have begun a new effort in recognizing road signs. Our first task was to hand-craft a Stop sign recognizer. We use the red color as a cue to sign location, then look for color edges, then use a variety of techniques to fit the octagonal shape. A verification step tries to check for an appropriate number of red pixels in the detected shape, making allowance for the white lettering. The results are excellent on our small number of test samples. We will try

to generalize this work to detect a variety of traffic control and caution signs. Our intent is to build a more general program, rather than to hand-craft individual recognizers.

3-D Object Recognition

We have been working of building maps of the environment of a mobile robot using an laser range finder. Our previous work involved building maps of simple objects represented by their location and the uncertainty on their location, and using the map information for navigation. We have extended the map building to build explicit three-dimensional models of the landmarks and to use those models for navigation by matching the models with observed object models. Including explicit shape models allows for selective landmark identification and for a more detailed map of the environment.

The object models are built by gathering range data from several closely-spaced images. The features and data collected on each object are used to fit a discrete surface, represented by a mesh of points, which constitutes the object model stored in the map. This approach does not involve an explicit segmentation of the observed scene. Instead, features extracted from individual range and reflectance images are grouped in clusters corresponding to objects in the scene. The features are range and reflectance edges and near-vertical regions. Data points that are within a given distance of the cluster are included as well as features. Each cluster is assumed to correspond to one object. Clusters are tracked from image to image using a previously developed matching algorithm. For each object, the surface fitting process is iterated using data and features from the previous images and from the corresponding cluster in the new image. This leads to a refined model of each object in the scene that takes into account the new data. This approach to building object models has many attractive features. First, it incorporates the natural idea of object refinement since the model is progressively refined as more data is acquired. Second, it avoids the problem of segmentation by going directly from only low-level features and data points to object model. Finally, it is applicable to a wide class of object shapes since it is not restricted to particular surfaces such as planar surfaces. The initial selection of objects in the image may be done automatically by identifying clusters of features, or manually by pointing to the approximate locations of the objects. The latter may be appropriate when building a map for robot navigation in which only a few landmarks are relevant.

Once stored in a map, the object models can be used for navigation by using a matching algorithm. The algorithm assumes that the approximate position of the vehicle in the map is known so that the approximate location of the predicted models in sensor space can be computed. A search through the pose space based on correlation between stored model and observed data gives an refined approximation of object position with respect to vehicle. Using this approximation as a starting point, a gradient descent yields the final estimate of the transformation between map model and observed object.

We have implemented and tested those algorithms using either Navlab or Navlab II as testbed vehicles, and the Erim laser range finder as sensor. The Perceptron range finder, which has better spatial resolution, was also used for off-line experimentation only. Models of natural and man-made objects were successfully built. The models were matched with observations during vehicle travel yielding correct vehicle position. In those experiments, the perception system was tested in isolation, gathering image and position data, building and matching models without actually sending driving commands or position corrections to the vehicle. Our goal is now to incorporate the algorithms in the existing Navlab navigation environment to eventually demonstrate improved mission capabilities. Several issues have to be addressed toward this goal. First, model building has to be performed off-line since it is currently very computationally demanding. Similarly, even though the time required for matching models is small enough that it can be used while the vehicle is in continuous motion, it is currently limited to low vehicle speeds. Second, we need to identify a class of objects for which the algorithms performs best so that they can be used as landmarks for navigation. Theoretically, the algorithms are applicable to objects representable by a single closed

surface. However, their performance vary widely depending on the characteristics of the objects. Third, we need to develop ways to automate map building since the initial object selection is currently done manually in order to retain only a small number of objects in the map.

Further information on 3-D data processing is found in Chapter 2.

Active Vision. We are studying active vision (control of sensors and focus of attention) in the context of "driving models", used to describe perceptual behavior for driving in traffic. Driving models are needed by many researchers to improve traffic safety and to advance autonomous vehicle design. To be most useful, a driving model must state specifically what information is needed and how it is processed. Such models are called computational because they tell exactly what computations the driving system must carry out. To date, detailed computational models have primarily been developed for research in robot vehicles. Other driving models are generally too vague or abstract to show the driving process in full detail. However, the existing computational models do not address the problem of selecting maneuvers in a dynamic traffic environment.

In our Pharos / Ulysses work we study dynamic task analysis and use it to develop a computational model of driving in traffic. This model has been implemented in a driving program called Ulysses as part of our research program in robot vehicle development. Ulysses shows how traffic and safety rules constrain the vehicle's acceleration and lane use, and shows exactly where the driver needs to look at each moment as driving decisions are being made. Ulysses works in a simulated environment provided by our new traffic simulator called PHAROS, which is similar in spirit to previous simulators (such as NETSIM) but far more detailed. Our new driving model is a key component for developing autonomous vehicles and intelligent driver aids that operate in traffic, and provides a new tool both for traffic research and for active vision.

Details of Pharos and Ulysses are given in Chapter 4.

1.3 Program

Theses and Proposals

During the past year, we have had two new thesis proposals, both of which should be complete within the next year: "Neural Network Based Perception for Mobile Robot Guidance", by Dean Pomerleau, and "YARF: A System for Adaptive Navigation of Structured City Roads", by Karl Kluge. In addition, we expect the completion within the next year of the thesis "A Tactical Control System for Robot Driving", by Douglas Reece.

Connections with other CMU programs

The work done on this contract has influenced, and been influenced by, other projects at CMU. The most obvious connection is with the related contract "Unmanned Ground Vehicle Systems", which provides the vehicles, operations, systems architectures, and some high-speed navigation support. During the past year, the UGV contract has built a new vehicle, the Navlab II. The Navlab II is a converted HMMWV. It has been equipped for high-speed navigation, both on and off roads. The design includes high-protection occupant seats with 4-point harnesses; suspended equipment racks for rough terrain; hard-mounted monitors; and other features for safe high-speed driving. It has driven autonomously at speeds greater than 50 mph on highways, 15 mph on dirt roads, and 6 mph on moderate off-road terrain. Other work under that contract involves integrating perception results with a planner and controller that understand vehicle dynamics, for high-speed cross-country runs.

Other related projects include the NASA-sponsored AMBLER and NSF work in underwater vehicles. The AMBLER is a 6-legged walking machine for planetary exploration. Much of the 3-D terrain mapping work is

shared between AMBLER and Navlab. In addition, the AMBLER researchers have done important work on calibrating range scanners, which will be very useful in evaluating future sensors for Navlab. Under NSF support, we are working on two projects involving cooperation with Florida Atlantic University on underwater vehicles. The most direct connection is in the area of underwater map building. The side-scan sonar data available underwater has somewhat different characteristics than the 3-D data from the Navlab's scanning laser rangefinder. In particular, side-scan data is reflectance as a function of time, in a narrow vertical plane. Measuring time of reflectance gives range in a series of concentric rings, but does not localize position along one of those rings. So converting range data to x, y, z points requires reasoning about surface normals from reflectance, as well as merging multiple scans. Some of these techniques are closely related to techniques and insights gained from working with laser data on the Navlab.

Finally, there continue to be strong connections with our basic Image Understanding work. In particular, new work this past year in stereo vision and in motion analysis appear to be promising for future Navlab application. The stereo work involves multi-baseline stereo, using as many as five images on the same axis to get redundant information about depth. The calculations are simple and regular, so this method has good potential for parallel implementation. The motion work, which is Carlo Tomasi's thesis, starts by finding differential motion between different points. The difference in motion between adjacent points is algebraically related to the difference in their depths. This method directly calculates shape (difference in depth) without first calculating depth, which gives much more accurate results.

Connections with other programs

The new DARPA program on Unmanned Ground Vehicles will be the framework for this Perception work. We have participated in the UGV workshops, including hosting the May 1991 workshop at CMU. In addition, we (Thorpe) have been involved in the Tiger Team, created by Erik Mettala to define the architecture of the UGV. The Tiger Team met during the summer of 1991 in Denver, in Monterey, again in Denver before the August UGV workshop, and numerous times by telephone, email, and FAX.

In addition, we (Thorpe) organized the DARPA ISAT Summer Study on Autonomous Agents. This study investigated the challenges and opportunities in building both physical agents, such as mobile robots, and synthetic agents, such as simulated forces in SIMNET.

1.4 Personnel

Supported by this contract or doing closely related research:

Faculty: Martial Hebert, Takeo Kanade, Chuck Thorpe

Staff: Mike Blackwell, Thad Druffel, Jim Frazier, Eric Hoffman, Ralph Hyre, Jim Moody, Bill Ross, Hans Thomas

Graduate students: Omead Amidi, Jill Crisman, Jennie Kay, Karl Kluge, InSo Kweon, Dean Pomerleau, Doug Reece, Tony Stentz

1.5 Publications

Selected publications by members of our research group, supported by or of direct interest to this contract.

Autonomous Navigation of Structured City Roads. D. Aubert, K. Kluge, and C. Thorpe. In Proceedings of SPIE

Mobile Robots V, 1990.

Building Object and Terrain Representation for an Autonomous Vehicle. M. Hebert. American Control Conference, June 1991.

3-D Measurements from Imaging Laser Radars. M. Hebert and E. Krotkov. IROS'91 (also accepted for publications in IJIVC).

Neural network-based vision processing for autonomous robot guidance. D. Pomerleau. In Proceedings of SPIE Conference on Aerospace Sensing, Orlando, Fl.

Rapidly Adapting Artificial Neural Networks for Autonomous Navigation. D. Pomerleau. In Advances in Neural Information Processing Systems 3, R.P. Lippmann, J.E. Moody, and D.S. Touretzky (ed.), Morgan Kaufmann, pp. 429-435.

Combining artificial neural networks and symbolic processing for autonomous robot guidance. D. Pomerleau, J. Gowdy, and C. Thorpe. To appear in Journal of Engineering Applications of Artificial Intelligence, Chris Harris, (Ed.).

A Computational Model of Driving for Autonomous Vehicles, CMU-CS-91-122, D. Reece & S. Shafer, April 1991.

Toward Autonomous Driving: The CMU Navlab. Part I: Perception. C. Thorpe, M. Hebert, T. Kanade, and S. Shafer. IEEE Expert, V 6 # 4 August 1991.

Toward Autonomous Driving: The CMU Navlab. Part II: System and Architecture. C. Thorpe, M. Hebert, T. Kanade, and S. Shafer. IEEE Expert, V 6 # 4 August 1991.

Annotated Maps for Autonomous Land Vehicles. C. Thorpe and J. Gowdy. In Proceedings of DARPA Image Understanding Workshop, 1990.

UNSCARF, A Color Vision System for the Detection of Unstructured Roads. C. Thorpe and J. Crisman. In Proceedings of IEEE International Conference on Robotics and Automation, 1991.

Outdoor visual navigation for autonomous robots. C. Thorpe. In Robotics and Autonomous Systems 7 (1991).

2. 3-D Landmark Recognition from Range Images

2.1 Introduction

Landmark recognition is an important component of a mobile robot system. It is used to compute vehicle position with respect to a map and to carry out a complex mission. The definition of what is a landmark varies depending on the application, ranging from visual features, to simple objects described by their locations, to complex objects. In this chapter, landmarks are objects that can be represented by a closed surface. To restrict the definition, the objects are assumed to be entirely visible in one sensor frame. This is to rule out cases in which only a small part of the object can be visible in one sensor frame. Two issues that have to be addressed in this context. First, the representation of the objects must be general enough to allow for a large set of landmarks. Object models are built from sequences of images. Second, finding landmark in images must be fast enough to be used while the vehicle is traveling in continuous motion at moderate speeds.

Many different techniques may be used for modeling and recognizing landmarks. The techniques described in this chapter are based on a general map-based navigation scenario. In the remainder of this Section, the scenario is described in detail in Section 2.1.1. The sensing used in those experiments in briefly described in Section 2.1.2. The rest of the chapter is divided in two parts, an algorithm for building object models from sequences of range images is introduced in Section 2.2, and an algorithm for finding landmarks in range images is described in Section 2.3.

2.1.1 A Scenario for Map-Based Navigation

In this chapter, landmark recognition is addressed in the context of map-based navigation defined as follows: A vehicle navigates autonomously through a partially mapped environment. The map has been built through previous traversal of the same environment. The map contains a set of landmarks, that is object models and their location in the map. The vehicle has internal sensors that measure its approximate location and orientation. Knowing the field of view of the sensor, it is possible to predict which map objects may be visible from the current vehicle position. By comparing the models with the image of the current, the position of the landmarks with respect to the vehicle may be computed. Equivalently, the pose of the vehicle with respect to the map coordinate system may be computed. Recognizing map landmarks as the vehicle travels can be used in two ways in this scenario: First, the estimated pose of the vehicle may be updated based on the landmarks, thus correcting for errors in the internal positioning system of the vehicle. Second, it can be used to raise an alarm when a specific landmark is reached and to take some action defined in the mission description. An example of the first case is a vehicle traveling autonomously on a road. As the distance traveled increases, the accuracy of the vehicle's internal estimate of its position decreases. The estimate can be reinitialized to a more accurate value, the uncertainty of which does not depend on distance traveled. This is an example of the use of landmarks as positioning beacons. As an example of the second case, let us consider a vehicle traveling through a network of roads using a road following algorithm. Assuming that the road follower is optimized for a particular type of road, it cannot handle intersections and must therefore be turned off as it traverses an intersection. The problem is to accurately predict when the vision system should be turned off. This may be achieved by finding a landmark close to the intersection, correcting vehicle position accordingly, and turning off vision as the vehicle turns in the intersection. In this example, it is critical to have a very accurate position estimate so that the vehicle can go through the intersection relying only on dead reckoning. In general a variety of actions such as switching perception modules, adjusting vehicle speed, or stopping may be triggered whenever the vehicle encounters a specific landmark.

As part of the Navlab project, an initial system was built [10] in which landmarks are stored as (x,y) positions in a 2-D map. The map is built through an initial traverse of the terrain. In this system, the user can specify "alarms" that instruct the perception system to start matching the observed objects with the stored landmarks. The matching may

be used to update the position of the vehicle by combining the current position estimate and the position estimated from landmark matching [11], or to take some other action defined in the mission [11]. This first system demonstrated the use of landmarks extracted from range images for map-based navigation. This system used a simple representation of the objects, their *(x,y)* location, and therefore could handle only relatively simple objects such as trees, mailboxes, etc. This chapter addresses the next step, that is to store a more complete description of the objects, and to use those models for landmark recognition, so that the system can handle a larger set of objects. The scenario and the infrastructure of the system remain the same, but it will be able to handle general environments. The next two sections describe the type of models and the techniques used for landmark recognition in this scenario, respectively.

2.1.2 Sensing

In this work, object models are built using the Erim laser range finder [5]. The sensor acquires 64x256 range images at a rate of 2 Hz. Its range resolution is 3 in from 0 to 64 ft. In addition to range, the sensor measures the intensity, generating what is sometimes called the "reflectance" image. Pixels in the range image may converted to points in 3-D space by converting (ρ,θ,ϕ), ρ is the range, θ the horizontal scanning angle, and ϕ the vertical scanning angle, to Cartesian coordinates *(x,y,z)* in some arbitrary reference frame fixed with respect to the sensor. In the remainder of this chapter, there is no distinction between the two representations in that a pixel in the range image is equivalent to a point in space. all the 3-D coordinates are assumed to be defined in a standard reference frame attached to the vehicle. Also, the sensor is assumed to be fixed with respect to the vehicle. Coordinates that are described as being "with respect to the vehicle", "with respect to the sensor", or "with respect to the current vehicle position" are expressed with respect to this standard reference frame.

2.2 Building Object Models

Many object representations are possible, from parametric patches such as planes and quadrics, to complex parametric shapes such as superquadrics. All those representations approximate objects by a limited set of parametric shapes. Expanding the class of allowable shapes typically requires the use of a larger number of parameters, which yields to representations that are computationally expensive and unstable. An interesting attempt to circumvent this limitation was introduced in the TraX system in which multiple shape representations are used. Possible representations include 2-D blobs, 3-D blobs, superquadrics, generalized cylinders. The appropriate representation is selected based on the amount of data available for a given object. The system switches from a coarse representation to a more detailed one whenever enough data is accumulated from consecutive images. We also use this idea of representation refinement but, instead of using parametric shapes, we represent objects by discrete surfaces that can have arbitrary shapes. Specifically, an object is represented by a discrete mesh of nodes connected by links. The surfaces are "free-form" in that they can theoretically represent any closed surface. The next three sections describe the model building algorithms and implementation in detail. First, the basic model fitting algorithm is described in Section 2.2.1. Then, details of the actual implementation are given in Section 2.2.2. The extension of the algorithm to building models from multiple observations is discussed in Section 2.2.3. Finally, performance and systems issues are discussed in Section 2.2.4. Thorough those sections, the emphasis is on the specifics of the use of free-form surface models for building landmark models for a mobile robot. In particular, Section 2.2.2. describes the implementation issues that have to be addressed in order to tailor the general approach to this application.

2.2.1 Surface Models

Given a set of features and data points, a surface model is built by deforming a discrete surface until it satisfies the best compromise between three criteria: the surface should fit the data closely, it should agree with the features in the cluster, and it should be smooth except at a small number of discrete locations (e.g., corners). This compromise is achieved by representing the influence of features, data points, and surface smoothness by a set of forces acting on the nodes of the mesh. Forces generated by features use a spring model, i.e., proportional to distance between node and feature, so that features have an effect only when the model is far from the features. Forces generated by the data points follow a gravity model, i.e., inversely proportional to the square of the distance between node and data points, so that data points affect model shape only when it is close to the data. Additional internal forces are included to ensure overall smoothness of the resulting model. Those forces are independent of feature and data. Given those forces, the model behaves as a mechanical system composed of a set of nodes with nominal masses. The mechanical analogy gives a relation between the motion of each node and the set of forces applied to the node. The shape of the model is computed iteratively by moving each node at each time step according to the mechanical model. The final shape is obtained after a maximum number of iterations is reached, or after the shape does not change significantly. The model is initialized as sphere placed near the center of the object. This approach to model fitting has many desirable properties. In particular, this definition of feature and data forces leads to a natural model fitting sequence: Features define the overall shape during the initial iterations, while the model is still far from the data, then data controls the local shape as the iterations proceed and the model comes closer to the data. Another important feature is that the algorithm uses directly three-dimensional data that may be expressed relative to any arbitrary reference frame. In particular, the algorithm is not dependent on the existence of a 2-D reference image coordinate system, or on a 2-1/2D surface model of the form $z = f(x,y)$. This becomes an important consideration when data from multiple images is used, in which case there is no natural mapping between 3-D data points and 2-D image points. Deformable surfaces have been used in the past to build models of curved object from range or intensity image data [8][12]. A complete presentation of the theory and implementation of deformable surfaces on which this chapter is based can be found in [3].

2.2.2 Implementation Issues

Several implementation issues have to be solved in order to use such a technique in this application. First, features have to be extracted from the range and reflectance images to control the model fitting. Second, the position and radius of the sphere used to initialize the surface must be computed from image data. Such a surface should be initialized "near" every object in the scene. Third, only part of the surface model is reliable since only part of the object is visible. It is therefore necessary to quantify the reliability of each node on the surface model. Finally, model fitting as described in the previous section may be very expensive computationally because of the large number of points and features. Solutions to each of those problems are discussed in the remainder of this section. The model fitting algorithm is illustrated by computing a model from the range image shown in Figure 2.1. This is a relatively simple case since there is a single isolated object in the scene. A more complex example involving multiple objects is discussed in the next section.

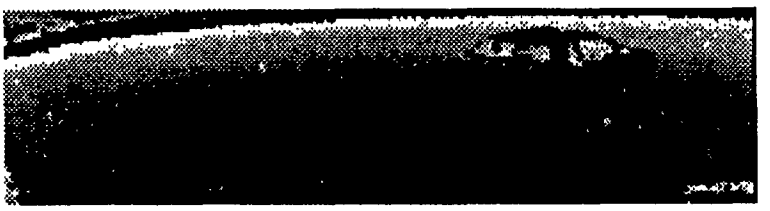

Figure 2.1: Range Image

The features are currently edges in the range and reflectance images. Edges in range image are extracted using a

Canny edge detector modified to take into account the typical pattern of pixel values in a range image. Specifically, the variation of range between adjacent pixels is greater at the top of the image than at the bottom. Therefore, the sensitivity of the edge detector varies from top to bottom of the image. Edges in the reflectance image may be due to surface markings or to shape changes. They are also extracted using a Canny edge detector. The edges are represented by line segments. It is important to note that a complete set of edges is not needed for the model fitting to work. Only the major features of the object are needed so that the model can converge to the right shape. As a result, conservative thresholds are used to extract edges in order to retain only the major discontinuities. In addition, a detailed description of the graph of features is not needed, the list of line segments is sufficient. Figure 2.2 (a) show the features extracted from the image of Figure 2.1.

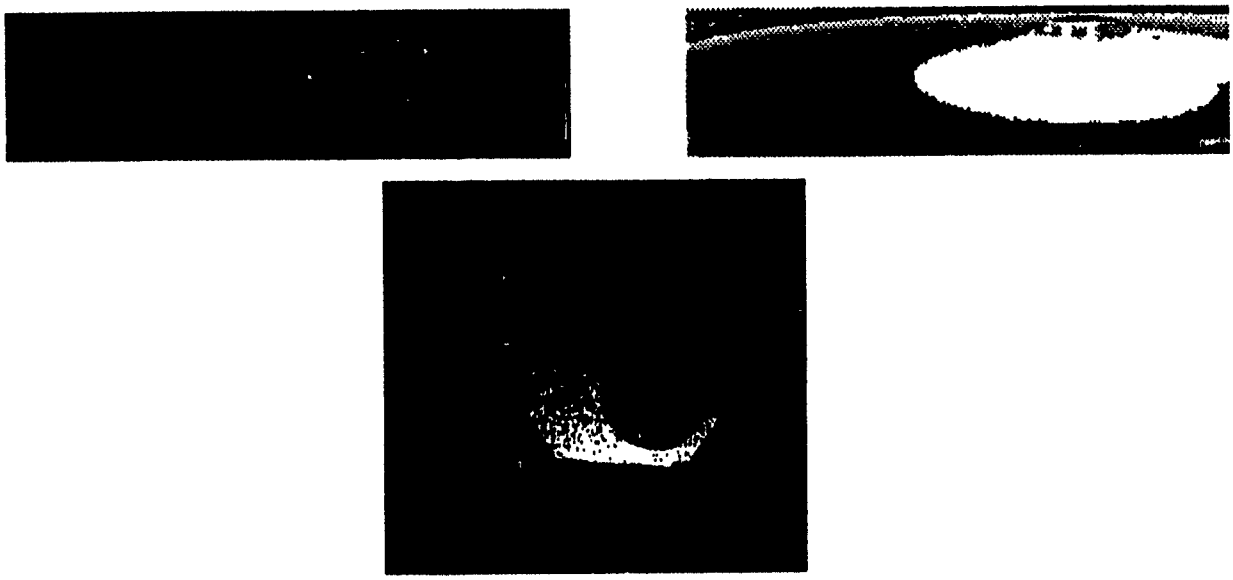

Figure 2.2: (a) Features Extracted from the Image of Figure 2.1; (b) Feature and Data Cluster; (c) Overhead View

To initialize the model fitting, sets of features and data points that correspond to individual objects must be extracted from the image. This is essentially a segmentation problem in that the range image must be segmented into regions such that each region corresponds to one object. In practice, it may be hard to reliably compute an exact segmentation. To avoid the segmentation problem, nearby features are grouped into clusters and each feature cluster is assumed to correspond to a single object. To facilitate the clustering operation, regions that correspond to slanted surfaces are used as well as edges. The regions are extracted by grouping pixels with similar surface normals into connected regions. As in the case of edge features, an accurate and complete region segmentation is not needed as long as the largest regions composing each object are found. The regions provide additional information on the location of potential objects since those surface are normally found on objects. They are used to facilitate the detection of feature clusters but they are not used in the actual model fitting. A sphere of radius R_s is initialized at the center of each feature cluster and is used to start the model fitting. The data points used in the model fitting are those within a fixed radius R_d of the center of the cluster. The geometry of model fitting initialization is summarized in Figure 2.3. The radii R_s and R_d are nominal values determined from the average size of the objects expected in the environment. In the examples presented in this chapter, Rs is one meter, and Rd is three meters. Those values need not be very accurate as long as all the data points are included in the model fitting for a typical object and as long as the initial sphere lies within the object. Here, the only assumption is that the average size of typical objects is known in advance. Although somewhat restrictive, this is a reasonable assumption for the current application. This technique for initial object identification may generate initial clusters that do not correspond to actual objects, or it may merge two objects into a single cluster if they are close enough. Those errors are corrected by merging multiple

observations as described below. This approach to finding potential objects of interest in a range/reflectance alleviates the need for an accurate segmentation by relying on a few, easy to find, features. Figure 2.2 (b) and (c) show the region that is used for fitting a model to the object of Figure 2.1. In Figure 2.2(b), the white pixels are the data points used in the model fitting. Figure 2.2 (c) is an overhead view of the same scene with the grey points being the data points used in the fitting, along with the features of Figure 2.2 (a).

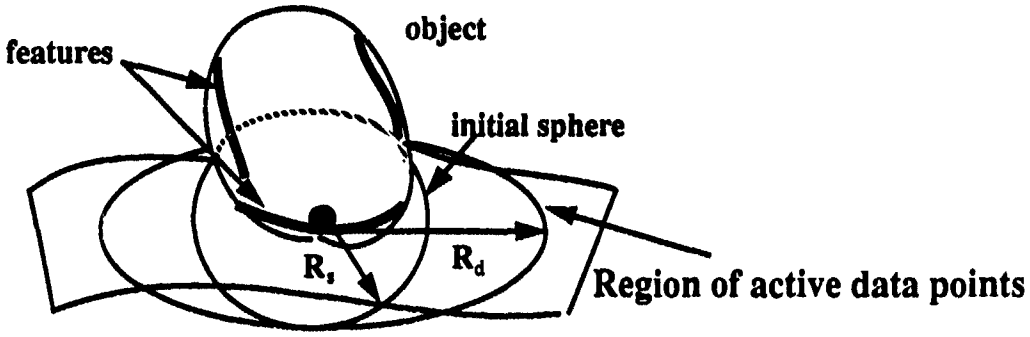

Figure 2.3: Initializing Model Fitting from Feature Clusters

Given a cluster and the initial sphere, the model fitting proceeds as described in Section 2.2.1. The force generated by an edge segment at a node of the model is computed by integrating the forces generated by the points of the segments over the entire segment. The 3-D coordinates of the end- points of the segment are used in this computation. Similarly, the 3-D coordinates of the data points are used to compute the data force at a node of the model surface. This involves finding the data point closest to the node, computing the distance, and the corresponding force. The coordinates of both edge segments and data points may be expressed in any arbitrary reference frame. In the results presented in this chapter, the model surface is based on 500-point tessellation. This number of nodes is sufficient for this set of experiments, although additional work is needed to determine the best mesh resolution for this application. The number of iterations is limited to 200.

The model fitting may be quite expensive because the distance between each node and the data points and between each node and the features have to be computed at each iteration in order to evaluate the external forces. To reduce the computation time, I use the fact that the distances do not change significantly from one iteration to the next if the node moves by a very small amount. In particular, the forces need not be recomputed if the position of a node differs from its previous position by an amount that is small compared to the resolution of the sensor. In practice, the forces, and thus the distances between node, data, and features, are recomputed only if the node has moved by more than 1 cm since the previous iteration. This reduces the computation time drastically towards the end of the iterations since most nodes are very close to their final positions. This test has little effect at the beginning of the iterations since the surface tends to move faster subject to the influence of the features. During this phase, however, most nodes are too far from the data points for the data forces to have any influence.

The next issue is that only part of the object is visible, even after merging multiple images as described in the next Section. As a result, parts of the model correspond to region where no data is available. Clearly, those parts are less reliable since they are smooth interpolations between parts of the model where data is available instead of being good approximations of the object. Therefore, model nodes in those regions should be given a smaller confidence than in other regions. This is computed by finding the data point from the original data set that is the closest to each node. If such a data point exists and its distance is smaller than a threshold, the node is considered reliable, otherwise it is considered unreliable and a lower weight will be used for this node in the landmark recognition algorithm.

Finding the distance between data points and model nodes can also be time consuming. The brute force approach would consist in traversing the list of all data points for every node and find the closest ones which is obviously unacceptable. A more efficient approach is based on the observation that the data point closest to a node should be close to the line L defined by the node and its surface normal. Therefore, only the set data points that are close to this line is searched for the closest point. To minimize the amount of search, all the data points are first projected on a 2-D discrete grid, then, for each model node, the line L is also projected. Finally, only the data points whose projection lies within a cone around the line are taken into consideration (Figure 2.4). The projection of the data set onto the grid has to be computed only once because the data is static and does change during the model fitting. In this application, there is a natural plane for the grid, the ground plane on which the vehicle travels. The resolution should be chosen so that the grid cells are small enough so that only the data within the cone of interest are searched, and large enough so that the grid does not contain too many empty cells which would slow down the search. A cell size of 20 cm realizes a good compromise in the current implementation. This implementation reduces the set of data points to a small subset which makes the computation of the closest data point efficient. Instead of projecting the data set onto a 2-D plane, it could be stored as a three-dimensional array. Theoretically, this would give better performance since only the data points that are inside the 3-D cone around L are taken into consideration, whereas points that are close in 2-D but far in 3-D may be taken into consideration in the current approach. In practice, however, a 3-D grid would be mostly empty and most of the time would be spent exploring empty space inside the cone of interest yielding worst performance than using the 2-D projection.

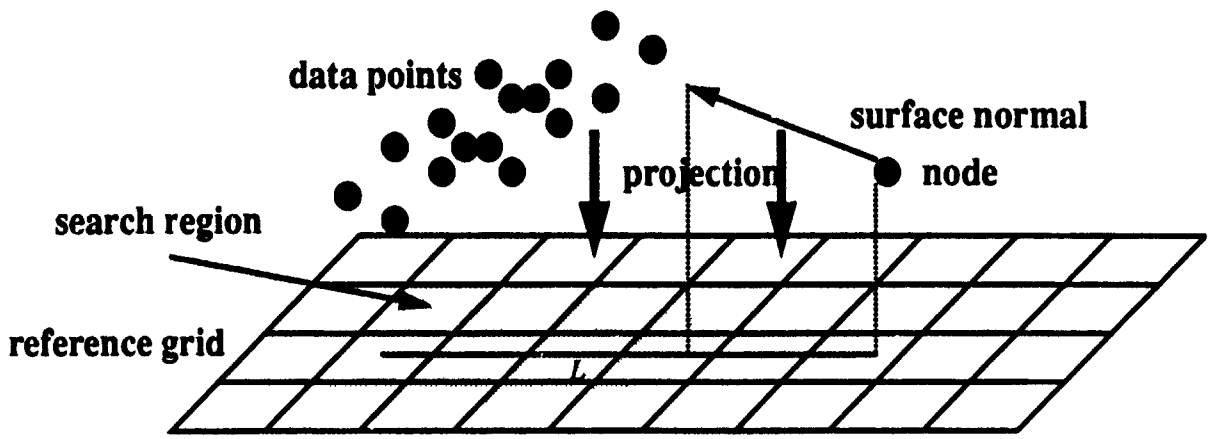

Figure 2.4: Computation of Closest Data Point

2.2.3 Refining Surface Models by Merging Observations

Using data from multiple images to build a model is necessary for several reasons. First, as pointed out in the previous section, the feature cluster approach to extracting objects from images may make occasional errors. Those errors can be corrected only by checking the consistency of the feature clusters across images taken at different locations. Second, only a partial view of an object is obtained from a given viewpoint, thus yielding a partial model. A more complete model may be obtained by merging data acquired from other locations around the object. Finally, as pointed out in [2], an initial model can and should be refined by accumulating data to yield the most accurate model. In this application, multiple observations are obtained by acquiring range images from vehicle positions separated by small distances, typically 50 cm. The requirement of small displacement is necessary to ensure that an object is visible in a large enough number of images, and to ensure that the estimate of the displacements between vehicle positions are accurate enough. The merging of observations is a three-step process: identify common clusters between images, remove incorrect clusters, and merge data and features from matched clusters.

Given a current set of clusters, corresponding clusters in the next image are searched to find candidates for matches. The set of possible matches is traversed to find the best set of matches between the two sets of clusters. Common clusters are matched by predicting where an existing cluster should appear in the next image. In this application, this can be done by using the estimate of vehicle displacement between the position for the new image and the reference position. This estimate is quite accurate for small displacements of the vehicle from image to image. As a result, there are typically very few possible matches, and most often only one, for each cluster, thus reducing the search from potentially combinatorial to close to linear in most cases. Incorrect clusters are removed by maintaining a confidence number defined as the ratio of the number of time a cluster is matched versus the number of time it is predicted to appear in the images. The confidence is low if the cluster does not correspond to an actual object and therefore appears in only one, or a few, of the images of a sequence. Therefore, clusters with low confidence are removed while clusters with high confidence are retained.

For each cluster, the features from all the images in which it appears are grouped into a single list. Similarly, all the data points from all the images in which the cluster appears are grouped into a single list. Once this matching and merging of clusters is completed, a sphere is initialized at the center of each cluster and used as a starting point to the model fitting as described above. Figure 2.5 (left) shows a sequence of range images taken in parking lot, the objects on the left are parked cars, Figure 2.5 (right) shows how the clusters corresponding to the objects are tracked between images. In this display, the extremities of the black and white line segments are at the centers of the clusters and join matching clusters. Three sets of clusters are correctly merged into three objects on the right side of the images. An erroneous cluster is detected on the left side but is discarded since it is not matched consistently in this sequence. This example shows that extracting, matching, and merging clusters of features yields a good initial list of objects from the range image even in the absence of actual segmentation of the image.

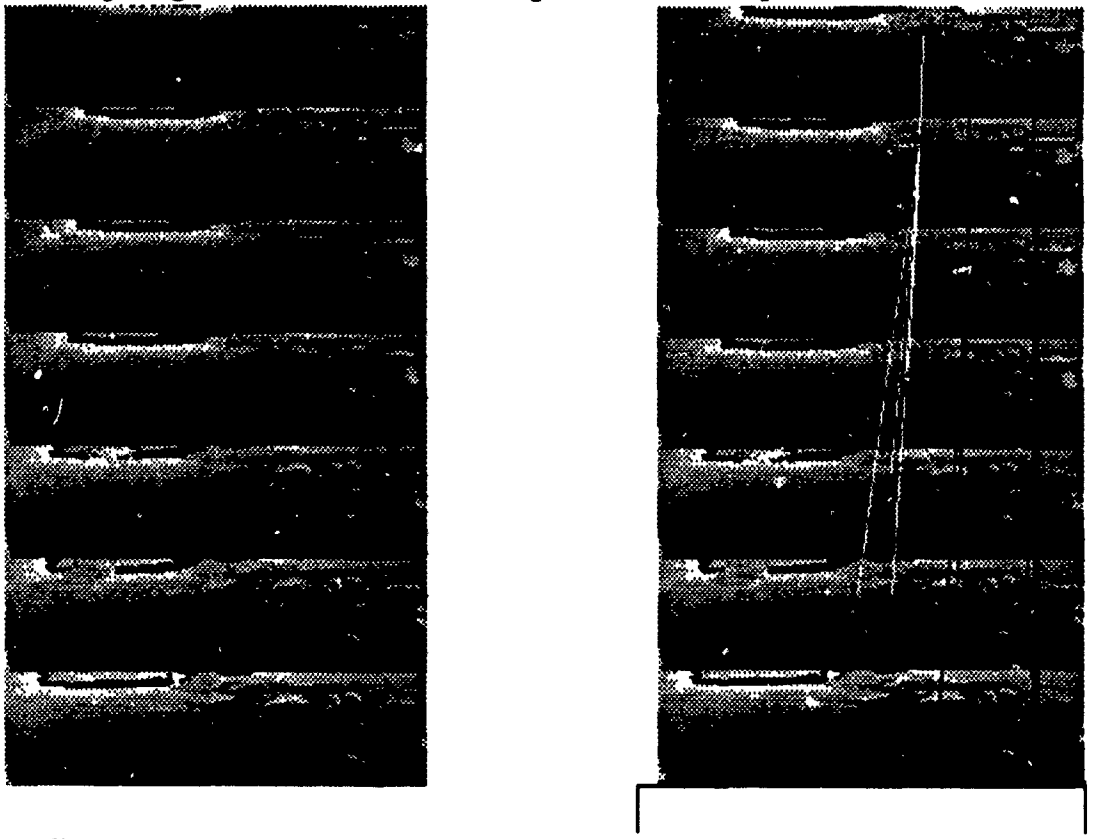

Figure 2.5: Sequence of range image (left); Tracking of objects between images (right)

One implementation issue is that simply grouping the features from several images in one list is very inefficient since several slightly different copies of a feature may be present in the list. In addition, this would effectively give a

higher weight to duplicated features, thus introducing a bias toward this feature in the deformation process used in model fitting. The obvious solution is to identify common features between observations within each cluster. Since all the coordinates of all the features are expressed in the same coordinate frame, edge segments corresponding to the same physical feature should be close to each other in this reference frame. A natural way to merge redundant features is therefore to search the set of overlapping features to find groups of segments that are nearly collinear and that have large overlap with each other. Segments within a group are merged into a single segment by first computing the least-squares line fit to all the vertices and by projecting the vertices onto this line. The two extrema of the projections along with the line describe the resulting segment (Figure 2.6). This algorithm is based on heuristics for defining the "best" combination of features, which is sufficient for the current application. However, more rigorous algorithms based on optimal estimation should be used in the future.

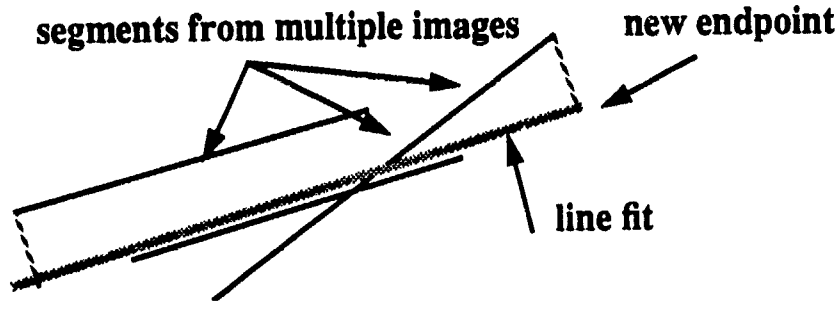

Figure 2.6: Merging Line Segments

A similar issue is that merging the sets of data points from several images into one list may lead to grossly oversampled surfaces. For example, a surface patch that has a thousand data points measured on it would end up with ten times that number if it is fully visible in ten successive images. Clearly, such a large amount of data is unnecessary. It slows down the model fitting drastically, and it does not improve the resulting model. It is therefore important to have a strategy to add data from new observations only when it might improve the model. One possible strategy is to add a data point from a new observation only if the density of existing data points in its vicinity is small enough. The threshold on data density is relative to the resolution of the sensor, in this case three inches, because adding points in a region where the average distance between data points is much smaller than sensor resolution does not add any information. Although the results presented in this chapter were obtained using this strategy, it is not optimal because it would be better to keep the most recent measurements and discard the old ones if the density becomes high enough, or better yet to combine data points using an optimal estimation technique based on the uncertainty on the measurements.

As an example, Figure 2.7 shows the set of models computed from the image sequence of Figure 2.5. The display shows an overhead view of the set of data points and of the tessellation associated with each object. The line segments correspond to features from the images. Only the data in the right part of the images in displayed. Since only part of each object is visible, only the model nodes that are close to the data are taken into consideration later on in the matching.

This is a "batch" approach to merging observations in that all the images in a sequence are processed first, and then the model fitting is applied to clusters that contain data and features from all the images. A recursive approach would be more natural: Each time a new image is available, the current object model for each cluster is modified according to the features and data from the new image. The recursive approach is a natural implementation of the idea of model refinement which is more efficient than the batch approach since only a few additional iterations of model fitting are needed each time a new image is taken. However, it is not clear that the gain is significant since redundant features and data cannot be eliminated as easily using a recursive approach. Also, some of the

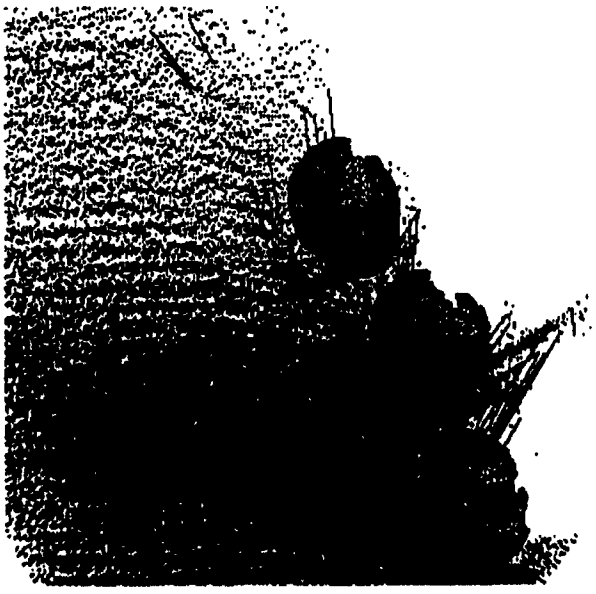

Figure 2.7: Models Built from the Sequence of Figure 2.5

optimizations described in Section 2.2. require that all the data be available at the beginning of the model fitting. The current approach demonstrates the use of multiple observations and the model building capabilities but more work is needed to find the optimal strategy for combining multiple observations and model fitting.

2.2.4 Performance and Systems Issues

Using free-form discrete surface has several advantages. First, it is very general since it does not rely on a particular set of geometric primitives. Second, a given model can be refined in a natural way by simply adding new data and iterating the surface fitting process. Third, it does not require an exact segmentation object/background as an input, thus being able to use a crude segmentations as input. In addition, it does not take into account spurious features and data that may be included in a cluster. The main drawback of this approach is that the surface model provides a good approximation of the overall shape of an object but may not yield as good a local approximation as other techniques. For example, sharp surface discontinuities such as corners may be recovered best by local surface analysis, whereas the method described here will tend to smooth those features.

Another issue is the computation time required by the model fitting algorithms. Building a model of a typical object from a sequence of ten images may take several minutes on a Sun4 workstation. This includes converting range pixels to 3-D coordinates, extracting features, grouping feature into clusters, merging clusters from multiple images and doing the actual iterative model fitting. As a result, this technique can be used in a scenario in which a sequence of images is first collected and then processed off-line to produce the object models, but it cannot be used to generate models in real time as the vehicle travels, even at low speed. Currently, this is not a major limitation since most scenarios can accommodate off-line model building.

2.3 Finding Landmarks in Range Images

In the scenario introduced in Section 2.1.1, the object models stored in the map are matched with observations to correct vehicle position and to identify locations at which the vehicle must take specific action. This problem can be stated as a pose determination problem: Find the pose of a model that is most consistent with the data in a range image taken at the current vehicle position. The geometry of the problem is illustrated in Figure 2.8: A model represented by a discrete surface as described in Section 2. is predicted by the navigation system to be within the

field of view of the vehicle at its current location. The problem is to find the pose of the landmark with respect to the vehicle coordinate system defined by the six parameters $P = (x,y,z,\theta,\phi,\psi)$. Knowing P, the vehicle pose with respect to the map coordinate can be easily derived. If several models are predicted at once, the algorithm must be able to compute the correct mapping between image regions and landmarks. Unlike model building which is an off-line activity, landmark finding must be executed on-line as the vehicle is traveling. This implies that computational efficiency is critical in landmark finding. This is a hard problem in general but the navigation scenario of Section 2.1.1. introduces constraints that make pose determination possible. In this Section, I describe the approach to pose determination and discuss some implementation issues. Section 2.3.1 gives an overview of the algorithm in the context of the map-based navigation scenario. The algorithm is divided into two parts: initial pose estimation and pose refinement which are discussed in sections 2.3.2 and 2.3.3. Performance and possible extensions of the algorithm are discussed in Section 2.3.4.

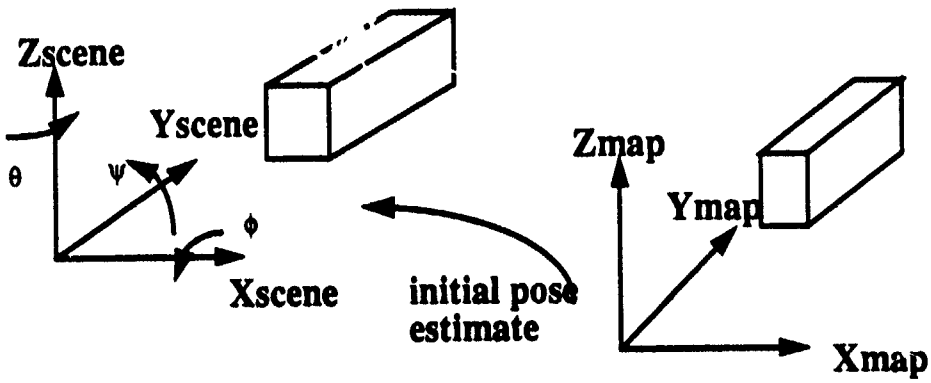

Figure 2.8: Geometry of the Pose Determination Problem

2.3.1 Overview

This recognition problem is very hard in general if there is no apriori information. In particular, it is very hard if there is no information on the expected pose of the model in the image. Fortunately, the navigation scenario introduces strong constraints on the problem that render the landmark recognition problem manageable. There are basically three constraints that can be exploited. First, the objects are known to be on the same terrain on which the vehicle is traveling. Second, the position and orientation of the vehicle with respect to the reference frame in which the map is represented is known within some small uncertainty. Third, the objects are static and their locations in the map is assumed to remain constant. The first constraint implies that the elevation z, and the angles ϕ and ψ, of the object with respect to the vehicle are very close to their values in the map. The second constraint implies that the x,y location and q orientation of the model with respect to the vehicle can be predicted within a small uncertainty. This is a reasonable assumption since the vehicle pose can always be estimated from other sources, such as dead reckoning and road tracking, for example. The third constraint guarantees that there is a rigid transformation between object in vehicle reference frame and model in map reference frame. As a result of those three constraints, only a small subset of the pose space has to be searched in order to find the best model pose. The size of pose space is defined by the expected variation in terrain for the z, ϕ, and ψ degrees of freedom, and by the expected maximum uncertainty in vehicle pose for the x, y, and θ degrees of freedom. The numbers currently used are plus or minus 5 degrees for ϕ and ψ, plus or minus 1 meter for the z component, plus or minus 3 meters for the x and y components, and plus or minus 20 degrees for the θ component. Those numbers are overestimates of the expected uncertainty on vehicle pose that were chosen to demonstrate the system. A detailed analysis of the actual uncertainty in the current system is described in [10]. In the future, the actual uncertainty on vehicle pose should be used directly instead of those arbitrary values to make the system more efficient.

Having defined the possible poses of the model with respect to the vehicle, the next step is to find the best model pose within this space by matching the model representation with the image data. A natural way of doing the matching would be to extract object models from the image as described above, and compare them with the stored model. Another approach is to directly compare the stored model with the image data directly. Although the first approach is closer to the traditional object recognition approach, in which the same representations are used for observed and stored models, it is more computationally expensive because of the time required to extract and build models from the image. Furthermore, the pose constraints make the second approach feasible even though it would be impractical in the general case. Another advantage is that does not require any preprocessing of the image except for some initial filtering. In particular, it does not require an exact segmentation of the scene. In this approach, the pose determination is a two-stage process. First, the pose space is discretized and a measure of similarity is evaluated for each possible pose P_i in the discretized pose space. The pose P_i^{min} that corresponds to maximum similarity is retained. This first step gives a coarse approximation of model pose. In the second step, the minimum of the similarity measure is found through a gradient descent in pose space, taking P_i^{min} as a starting point.

Similar approaches to pose determination have been used in other perception systems for navigation. As an example of the initial pose determination step, in [7] landmark pose is determined by comparing the predicted appearance of a superquadrics model surface with a range image of a scene. As an example of the pose refinement step, a gradient descent technique is used in [6] to minimize the distance between a stored terrain map and the terrain map observed by a laser range finder at the current vehicle position. Although based on different models and slightly different scenario, those two systems contain the two major building blocks of our approach: initial pose determination through search of pose space, and gradient descent through estimation of the derivatives of a similarity measure with respect to pose parameters.

2.3.2 Initial Pose Determination

There are two components that affect the performance of this algorithm: the resolution of the discretized pose space, and the similarity measure. The resolution of the pose space should be coarse enough so that not too many poses are evaluated, but it should also be fine enough so that P_i^{min} is close enough to the actual minimum for the second step to converge properly. The resolution depends also on the average size of the objects and on the resolution of the sensor. For the objects used in the currant experiments, resolutions of 0.5 m for the translational degrees of freedom, and 5o for the rotational degrees of freedom realize a good compromise. This involves computing the similarity measure at about 1800 different poses in the worst case. The similarity measure is defined as the sum of mean square distances between each node of the model and the corresponding point from the image weighted by the surface area represented by that node. The sum is taken over the set of nodes that is predicted to be visible in the image for a given pose. There two problems with this initial definition of the similarity measure. First, if a few image points are far from the surface the similarity measure becomes very high even though the pose may be correct. This can happen because of occasional erroneous range measurements, or, more commonly, because part of the predicted model intersects the background in the image. This problem is solved by not including distances that are greater than a threshold in the summation. The threshold is again related to the expected size of the objects, or, more precisely, to the minimum distance between object point and background at an occluding edge. A pose is retained for further consideration if more than 50% of the expected visible area of the model is included in the summation according to the threshold. The complete algorithm for initial pose determination is illustrated in Figure 2.9.

The 50% threshold is used to reduce the computation time of the similarity measure. More precisely, the computation of the similarity is stopped as soon as the percentage of surface area that remains to be evaluated plus the percentage that has already been included in the summation is lower than 50%. This stopping condition means that even if the computation were carried through, it would be impossible to include the minimum 50% of visible

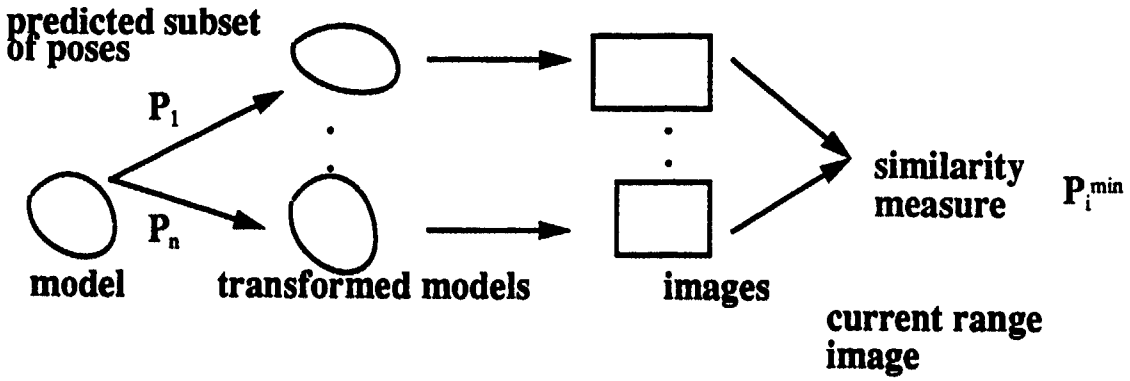

Figure 2.9: Initial Pose Determination

area, and therefore the pose would be rejected. This optimization of similarity computation speeds up the search of pose space by a factor of two on average.

The computation of similarity for all poses would still be very expensive if model nodes had to be converted to pixel positions in image for every possible pose. In the actual implementation, the positions of the model nodes in the range image are computed off-line for every pose in the discretized pose space. They are computed only once and stored along with the model. To facilitate the computation of similarity, the expected model appearance for a given pose is stored as an image, that is an array of points registered with the range image, by interpolating between nodes. Similarity can then be evaluated by adding up the distances between individual points in the range image and points in the predicted image of the model. Precomputing and storing the model appearance for all the poses is clearly an improvement in terms of computation time but it may require a large amount of storage space. In practice, however, a typical model requires a thousand points per pose on average for a total size of two to three Megabytes on average. This model size is acceptable in the navigation scenario since only a small number of models may be active and loaded in the system at a given time.

2.3.3 Pose Refinement

The initial pose P_i^{min} is only a coarse approximation of the best pose since its estimation is limited by the resolution of the pose space. A natural way of refining the pose estimate is to use a gradient descent technique to optimize similarity, taking P_i^{min} as a starting value. Since both data and model are based on a discrete representation, the gradient must be estimated numerically. This is done by computing the difference between the similarity measure at the current pose and similarity at poses obtained by varying the parameters by a small amount. Those differences are estimates of the derivatives of similarity with respect to pose parameters. The pose is updated by moving in the direction of the gradient by a small amount. The steps used for computing the gradient and for updating the pose are 10 cm and 0.5 degree in translation and rotation, respectively. Those two values also define the accuracy of the resulting pose. Those numbers are larger than in other recognition systems but they reflect the resolution of the sensor and based on estimates of the best accuracy that can be reasonably expected from this sensor.

A known problem with this type of techniques is that there is a cross-talk between the translational and rotational parts of the pose parameters. Specifically, a small $\Delta\theta$ may have the same effect on the similarity measure as a small variation in translation Δx. To minimize this effect, (x,y,z) and (θ,ϕ,ψ) are updated separately at alternating iterations. Also, this approach could lead to local extrema in general. In this case, the starting pose P_i^{min} is close enough to the best pose that the algorithm converges rapidly toward the optimum. The iterations stop when the similarity does not improve significantly by changing the pose. In practice, only two or three iterations are necessary

to find the best pose.

2.3.4 Performance and Extensions

The entire pose determination procedure takes between 100 and 500 ms on a Sparc2 workstation depending on the model. This computation time makes it possible to use this technique to accurately locate landmarks in the environment while the vehicle is traveling in continuous motion at moderate speeds. The basic operations used in pose determination may be easily distributed over multiple processors since most of them are point-by-point operations. This would yield real-time operation of the system. Figure 2.10 shows where one of the models of Figure 2.7 is found in a range image. The top image shows the superimposition of the outline of the visible part of the model, shown as a black contour. The visible part is defined as the portion of the model that is used to evaluate the similarity at this pose. The bottom image show only the predicted appearance of the model. Only the part that is close enough to the data, that is the part that contributes to the similarity measure, is shown. In this example, an artificial error of one meter in translation was introduced in the initial estimate of pose, which is corrected by the pose determination algorithm.

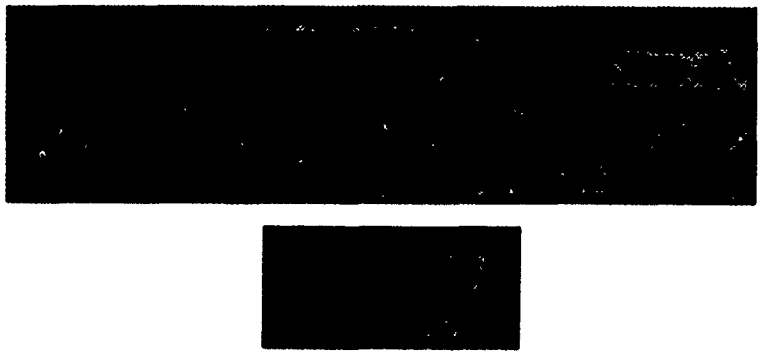

Figure 2.10: Pose Determination for a Single Object

The pose determination described so far assumes that a single model is to be found in the image. In practice, however, several landmarks may be predicted to appear in the field of view of the sensor leading to ambiguous interpretations of the scene. This situation is addressed by computing P_i^{min} for, each of the predicted models, and verifying that the resulting set of poses is consistent with the relative positions of the models in the map. Figure 2.11 shows the identification of two models in a range image. The format of the display is the same as in Figure 2.10 except that the bottom image shows the predicted appearance from both models. An additional problem with multiple model is that the map objects may occlude each other if they are close enough to each other. As mentioned before, the amount of occlusion can be predicted and used to compute a more accurate similarity measure, although this is not yet implemented.

2.4 Conclusion

Modeling objects based on free-form surfaces is a promising approach to modeling and identifying landmarks for map-based navigation. It makes few assumptions about the shapes of the objects, it can model refinement based on merging multiple images, and the resulting models can be identified in range images using the algorithms of Section 2.3. However, a number of issues remain to be addressed before this becomes part of a complete navigation system. Most importantly, the current implementation is based on assumptions that could be relaxed. For example, the average size of the objects is assumed to be known and is used to compute cluster and initial surface radii. This assumption is acceptable when only few objects are expected in the environment. However, to be able to deal with richer environments, the algorithms should be able to estimate those radii from the feature cluster itself. Another

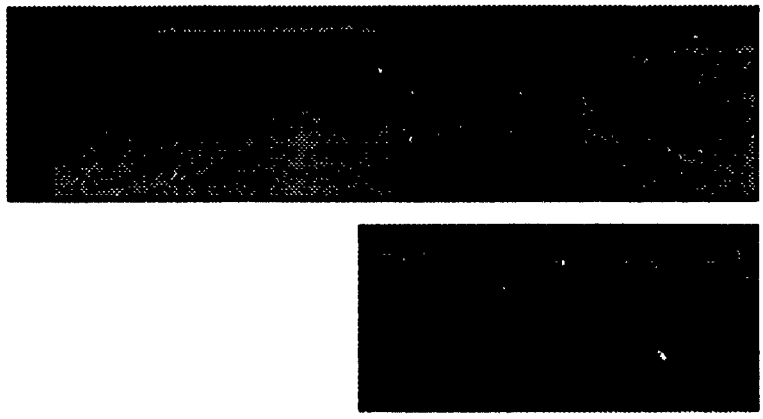

Figure 2.11: Pose Determination for Two Objects

improvement is that the models should include more explicit information about their expected accuracy. Currently, they include a measure of confidence at each node based on how far the node is from the original data. This measure should be defined more carefully and should take into account data uncertainty. In addition, it should be taken into account explicitly in the landmark finding algorithm. Currently, nodes that have a low confidence are simply discarded. The implementation and the experiments have focused on single object identification without representing the interaction between objects form the map. In particular, the expected occlusions between objects given a pose should be explicitly computed and used in the landmark finding algorithm. Finally, the computation time required for finding landmarks in images must be reduced so that landmarks may be identified while the vehicle travels in continuous motion at normal speeds.

2.5 References

[1] P. Besl and R. Jain, "Segmentation Through Symbolic Surface Descriptions", Proc. CVPR Miami, pp 77-85, 1986.

[2] B. Bolles and A. F. Bobick, "Representation Space: An Approach to the Integration of Visual Information", Proc. Image Understanding Workshop, 1989.

[3] H. Delingette, M. Hebert, K. Ikeuchi, "Shape Representation and Image Segmentation Using Deformable Surfaces", Proc. Computer Vision and Pattern Recognition, June 1991.

[4] M. Hebert, "Building Object and Terrain Representations for an Autonomous Vehicle", Proc. American Control Conference, June 1991.

[5] M. Hebert, E. Krotkov, "Imaging Laser Radars", Proc. IROS Workshop, Osaka, November 1991.

[6] I. Kweon, "Modeling Rugged Terrain with Multiple Sensors", PhD. Thesis, The Robotics Institute, Carnegie Mellon University, July 1990.

[7] A. Pentland, R. Bolles, "Learning and Recognition in Natural Environments", in Robotics Science, Ed. M. Brady, MIT Press, 1989.

[8] D. Terzopoulos, D. Metaxas, "Dynamic 3D Models with Local and Global Deformations: Deformable Superquadrics", Proc. ICCV, 606-615, 1990.

[9] C. E. Thorpe, "Vision and Navigation, The Carnegie Mellon Navlab", Kluwer Academic Publishers, 1990.

[10] C. E. Thorpe, O. Amidi, J. Gowdy, M. Hebert, "Integrating Position Measurement and Image Understanding for Autonomous Vehicle Navigation", Second International Workshop on High Precision Navigation, University of Stuttgart, Stuttgart, Germany, November 1991.

[11] C. E. Thorpe, J. Gowdy, "Annotated Maps for Autonomous Land Vehicles", Proc. Image Understanding Workshop, 1990.

[12] A. Witkin, M. Kass, D. Terzopoulos, "Physically Based Modeling for Vision and Graphics", Int. Journ. of Computer Vision, pp321-331, 1988.

3. Representation and Recovery of Road Geometry in YARF

3.1 Introduction

Recovery of road structure from segmentation data poses two issues which must be addressed in designing a road following system: the nature of the representation of road structure and the nature of the process which determines the model parameters given a particular set of segmentation data.[1] Selection of an appropriate road representation and data fitting scheme requires balancing a number of conflicting criteria:

- The accuracy with which the class of models selected reflects the actual structure of the road;
- The computational cost of extracting the model parameters from segmentation results; and
- The robustness and stability of the fitting process in the presence of noise in the segmentation.

YARF adopts a representation scheme in which the ground is assumed to be locally flat, and the road is modelled as a one dimensional set of features swept perpendicular to a spine curve. The spine curve is approximated locally as a circular arc for computational efficiency. Examination of alternative methods of representation in use suggests that this type of road model is the best currently available for balancing the above criteria.

YARF incorporates two methods for extracting the spine arc parameters given a set of feature positions on the ground plane: standard least squares fitting and least median of squares fitting. Least median squares is a robust estimation technique [12] which attempts to eliminate the influence of contaminating data points on the estimate of the model parameters. Such a technique is useful in cases where false positive responses from segmentation algorithms result in outlying data points which would otherwise corrupt the fit of the model parameters.

This chapter begins with an examination of the various road representation schemes and parameter recovery methods that have been used in previous systems. We argue that low order parametric models are the best representational scheme currently available based on a comparison of existing systems. In particular, representing the road as a circular arc has proven very effective.

We then present an analysis of the errors introduced in linearizing the circular arc model and describe how these errors are dependant on the coordinate system chosen for the data fit. Simulation results are presented to show that the magnitude of the errors introduced by linearizing the circular arc model are small in the range of curvatures of interest when the data is rotated into a "natural" coordinate system before fitting.

The chapter closes with a description of Least Median of Squares fitting. Examples are shown to illustrate the need for outlier detection for road following and to show the ability of LMS to eliminate discordant observations which would otherwise corrupt the estimate of road shape.

3.2 Techniques for recovery of road model parameters and methods of road representation

3.2.1 Methods for recovering model parameters

Three main methods have been used to recover road model parameters given image segmentation data: boundary backprojection, voting in the model parameter space, and statistical fitting techniques.

In boundary backprojection, features detected by the segmentation are backprojected onto the (assumed) ground

[1]This chapter is a version of a chapter from Karl Kluge's thesis, "YARF: A System for Adaptive Navigation of Structured City Roads"

plane, and consistency constraints are applied to determine which features are part of the road. This is the method used in the VITS [14], FMC [7], and U. Bristol [13] systems. Algorithms which recover three dimensional road structure using assumptions of constant road width and zero road bank [3] [4] backproject feature points using assumed image projection geometry. The backprojection process doesn't enforce any higher level constraints on relative feature location, and as a result errors in the image segmentation can produce arbitrary errors in the recovered road shape.

In parameter space voting techniques, detected feature locations vote for all possible roads they are consistent with. This method is used in the SCARF [2], ALVINN [11], and U. Michigan [8] [10] algorithms, and in some of the LANELOK [5] [6] algorithms. The main advantage of these techniques is their robustness in the face of large amounts of noise in the segmentation results. The main disadvantage is the difficulty of using voting for models which have more than two or three parameters, resulting in large multidimensional Hough spaces. Also, peak detection in the accumulator space can be difficult.

In statistical fitting procedures, road model parameters are fit using the observed data points and the equations of the road model. Standard techniques such as least squares or robust techniques which are less sensitive to outlying data observations can be used, VaMoRs [9], YARF, and other of the LANELOK algorithms use this type of technique. Of the available techniques for model parameter recovery, statistical fitting methods have a number of advantages. They are computationally efficient and they have a vast literature of theory, techniques, and tools associated with them.

3.2.2 Methods for modeling road structure

A variety of schemes has been proposed for representing roads. In order of increasing number of parameters in the model, they are: by steering direction; by linear road segments; by circular arc road segments; by flat road segments with locally parallel edges; and by three dimensional roads constrained to have constant width and no banking.

The simplest road representation is to summarize the segmentation data by a steering direction, independent of the actual road geometry. This is the approach taken in the ALVINN neural net road follower. In principle, ALVINN could learn appropriate steering commands for roads which change slope, bank, etc. In practice, to expand the range of training images, images are backprojected onto a flat ground plane and reprojected from different points of view. In order to generate synthetic training data from images with significant variations in ground slope ALVINN would have to recover the road geometry explicitly, in which case the system could drive without the neural net. This may prove to be a limiting factor on hilly roads.

The next simplest road representation is to model the road as linear on a locally flat ground plane (or equivalently, as a triangle in the image plane). The road has three parameters, the road width and two parameters describing the orientation and offset of the vehicle with respect to the centerline of the road. LANELOK and SCARF take this approach. Tests with YARF fitting a linear road model to detected feature points suggest that the steering behavior observed is similar to that produced by modeling the road centerline as a circular arc, the main deficiency of a linear road model being inaccuracy in predicted feature locations on roads with noticeable curvature. The main limit of this type of scheme is the need to move a sufficiently small distance between fits so that the straight path being driven along does not diverge too much from the actual road.

Modeling the road as a cross-section swept along a circular arc explicitly models road curvature but retains the flat earth assumption used in linear models. VaMoRs, YARF, and the U. Bristol system use this approach. The equations describing feature locations can be linearized to allow closed form least squares solutions for the road heading, offset, and curvature, as well as the relative feature offsets.

A more general model of road geometry retains the flat earth assumption, but requires only that road edges be locally parallel, allowing the road to bend arbitrarily. This can be done by projection onto the ground plane (VITS and the FMC system), or in the image plane (work at U. Michigan cited above). The lack of higher order constraint on the road shape can lead to serious errors in the recovered road shape when there are errors in the results of the underlying image segmentation techniques.

Several algorithms have been developed to recover three dimensional variations in road shape under the assumption that the road does not bank [3] [4]. These current algorithms use information from a left and right road edge, which precludes integrating information from multiple road markings. Evaluation of an early zero-bank algorithm by the VITS group as part of the ALV project suggested that such algorithms may be very sensitive to errors in feature location by the segmentation processes. This is due to the assumption of constant road width, which leads to errors in road edge location being interpreted as the result of changes in the terrain shape.

Circular arc models would appear to be the technique of choices in the absence of algorithms for the recovery of three dimensional road structure which are robust in the presence of noise in the segmentation data. They have a small number of parameters, they impose reasonable constraints on the overall road shape, and statistical methods can be used for estimating the shape parameters, with all the statistical theory and tools that use of such methods allows the system to apply to the problem.

Figure 3.1 summarizes the position of existing road following systems in the space of road representation schemes and parameter recovery mechanisms.

	statistical fit	Hough space	backproject
steering direction		ALVINN	
linear centerline	LANELOK	SCARF	
arc centerline	VaMoRs, YARF		U. Bristol
parallel edges			VITS, FMC
vanishing point		U. of M, SHIVA	
zero bank			U. Md., et al.

Figure 3.1: Road representations and parameter recovery techniques used in various systems.

3.3 Road model and parameter fitting used in YARF

YARF models the road as a one-dimensional feature cross-section swept on a flat ground plane perpendicular to a spine curve (hereafter referred to as a generalized stripe model). Such a model lends itself to parameter estimation using statistical fitting techniques and seems to work reasonably well even in the presence of mild variations in ground plane orientation (gentle hills, for instance). Figure 3.2 shows an image of a two lane divided road. Feature points have been detected along both white lines and the double yellow line in the center. Figure 3.3 shows the recovered road shape on the ground plane.

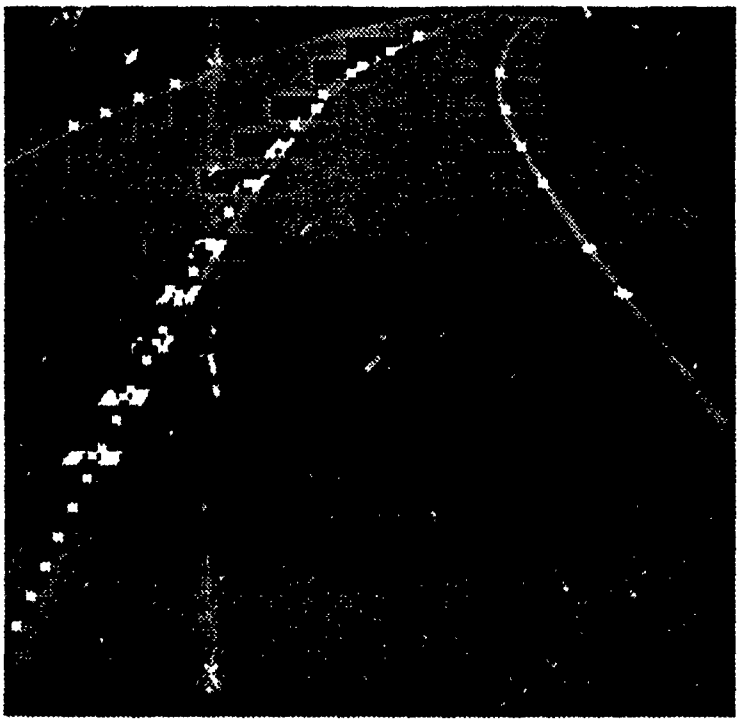

Figure 3.2: Road image with trackers on lane markings

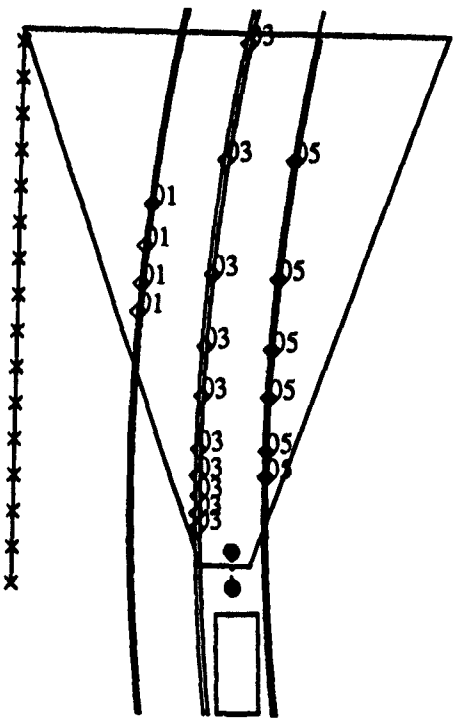

Figure 3.3: Reconstructed road model

YARF assumes that the spine curve can be approximated by a circular arc. In order to have a system which is linear in its parameters a parabolic approximation is made to a circular arc. This parabola represents the binomial series expansion of the circular arc equation. The term representing the displacement of a detected feature point from the spine is also linearized. The final linear model that results from these approximations is $x = 0.5 \times curvature \times y^2 + heading \times y + spinetrans - offset$, where (x,y) is the position on the ground plane of a

detected feature point, *offset* is the offset of the feature from the road spine, *curvature* is the curvature of the spine arc, *heading* is related to the tangent of the spine arc at the x-intercept, and *spinetrans* is the x-intercept of the spine arc.

Given a set of data points lying on different features is the road model, standard statistical fitting techniques can be used to recover the spine arc parameters of *curvature*, *heading*, and *spinetrans*. YARF uses either standard least squares fitting or least median of squares fitting. The next section discuss the errors introduced by making the approximations used to derive a linear system, giving an analysis of the magnitude of the errors introduced. After that fitting techniques are discussed, with an explanation of least median of squares fitting and why it is preferable in some cases to standard least squares.

3.4 Errors introduced by linear approximations in YARF

There are two sources of error introduced by the linearizations. The first arises from the approximation of a circular arc by a parabola. The second arises from translating points parallel to the x-axis to move them onto the spine. These sources of error are discussed below.

3.4.1 Approximating a circular arc by a parabola

Consider the equation of a half circle centered at the origin, $x=\sqrt{r^2-y^2}$. This can be expressed as a series, $x=c_0+c_1\times y+c_2\times y^2+....$ Performing the binomial series expansion to solve for the coefficients results in the solution $c_0=r$, $c_1=0$, $c_2=-0.5\times r^{-1}$, and in general $c_n=(c_{n-2}\times(n-3))/(n\times r^2)$. Ignoring terms beyond y^2 yields the parabola $x=r+0.5\times y^2\times r^{-1}$. Introducing translation in x simply changes the interpretation of the constant term of the series from $c_0=r$ to $c_0=r+x_{center}$. Translation in y makes the coefficient of the y term in the series nonzero by substituting $y'=y-y_{center}$ into the parabola equation above.

The y value about which the series approximation of the spine arc is implicitly being expanded is the axis of the parabola. The further from that axis data points lie, the greater the divergence between the estimated arc parameters and the actual arc parameters. Since the fit constrains the axis of the parabola to be parallel to the x axis, rotating the data so that the x axis passes through the mean y value of the data points reduces the fraction of the arc circumference spanned by the fit, and increases the accuracy of the estimate of the spine arc parameters

3.4.2 Translating data points perpendicular to the Y-axis rather than perpendicular to the arc

Data points from features offset from the spine have to be translated to lie on the spine in order to fit the spine parameters. The translation is made parallel to the x axis rather than perpendicular to the (unknown) spine arc in order to keep the problem linear (see Figure 3.4). The error introduced by this approximation is $error=(x-x_{center})-offset+\sqrt{(x-x_{center})^2-offset^2-(2\times offset\times radius)}$

The magnitude of this error is also dependant on the coordinate system chosen for the fit. Again, rotating the data so that the x axis is roughly perpendicular to the predicted road at the mean y value of the data spreads the error more evenly among the points and reduces the size of the error for the points with larger y values.

3.4.3 Evaluation of error introduced by linear approximations to circular arc model: Simulation results

Simulations were performed in order to provide quantitative estimates of the errors introduced by the linearizations described above, and to show the importance of fitting the data in a "natural" coordinate system in which the x axis is perpendicular to the road at the mean y value of the data points. We call such rotation of the data

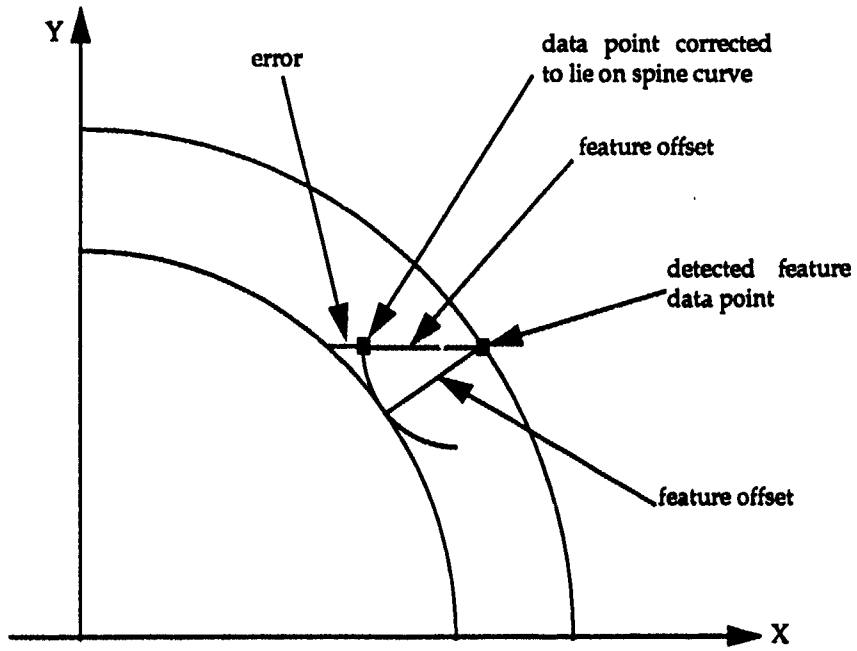

Figure 3.4: Error introduced by translating points to road spine parallel to the X axis

before model fitting *virtual panning*. The camera and road geometry models from an actual Navlab run were used to generate synthetic road images of specified curvature, and YARF was run on the synthetic images to gather data on the difference between the estimated road shape and the actual road shape.

The simulated vehicle drove 2 meters between images, keeping centered in the lane with the rear axle perpendicular to the spine curve. The simulator was set up to use the same road and camera models to generate the images and to backproject and fit the data, and the image data is idealized. This eliminates sources of error other than the approximations described above. After allowing the simulation to run for 10 frames to allow the system to settle into a steady state, the fits from the eleventh to twentieth frames were averaged and compared to the known model.

The error measure chosen was distance from the true lane center to the estimated lane center at a given distance along the estimated lane center arc. The error was plotted for distances along the estimated lane center starting at the rear axle of the vehicle and extending out to 40 meters. The front end of the vehicle is about 3.5 meters in front of the rear axle.

Figure 3.5 shows the results for the first set of simulations, in which the parameter fits were done in the vehicle coordinate frame. Note that in all cases the error in the range of 5 to 15 meters from the rear axle is very small. The asymmetry of the results is due to the pan of the camera and the offset of the camera from the center line of the vehicle.

Figure 3.6 shows the results for the second set of simulations In this set of simulations the data was rotated so that the x axis was perpendicular to the predicted road at the mean y data value. The vertical scale of these plots is not the same as in Figure 3.5 in order to improve readability. Notice that the magnitude of the error is kept under 80 cm. at all distances out to 40 meters along the estimated lane center, and for all radii of curvature down to +/- 30 meters. This shows the improvement in fit accuracy achieved by rotating the data into a "natural" coordinate system.

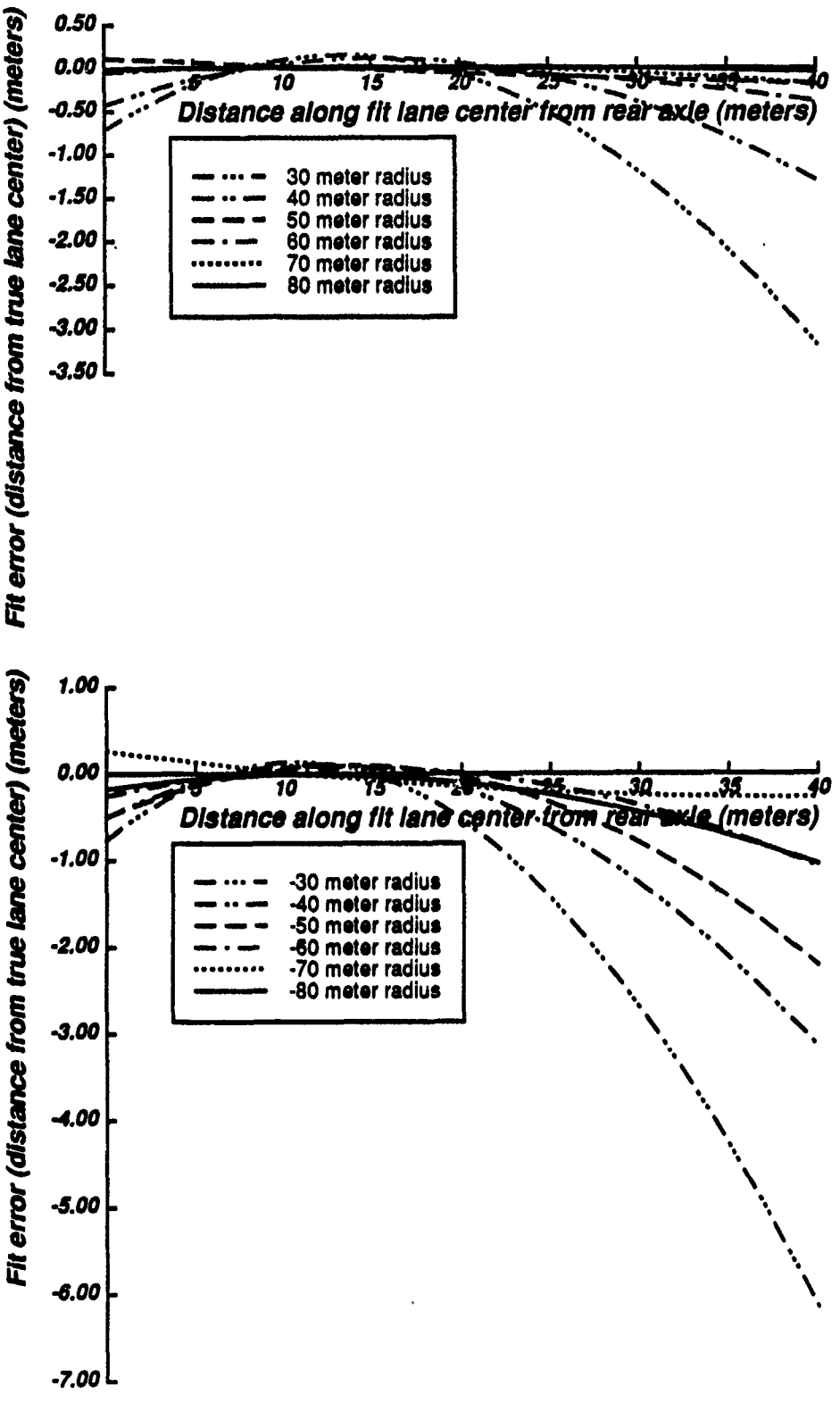

Figure 3.5: Fit error, fits done in vehicle coordinate system

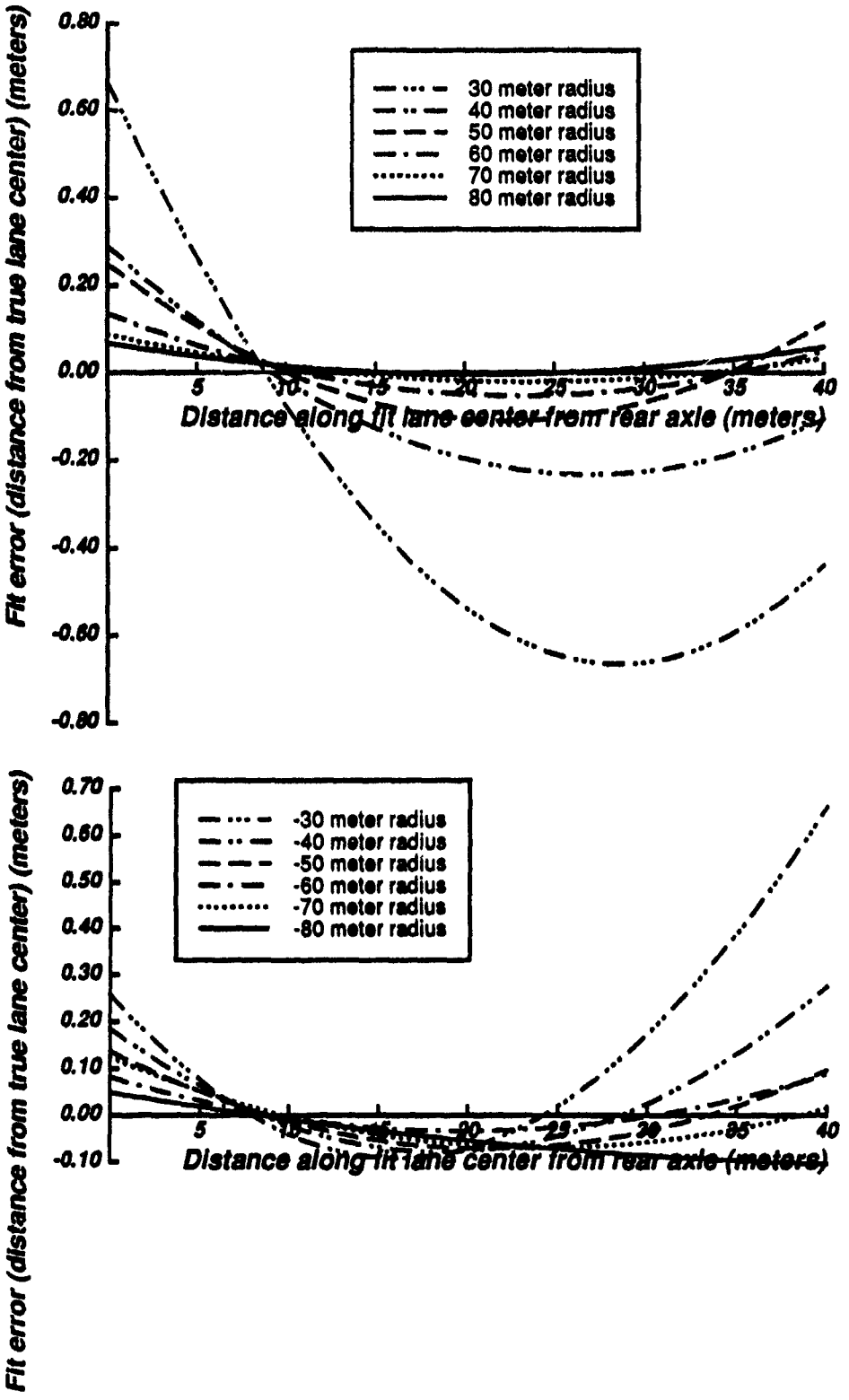

Figure 3.6: Fit error, virtual panning of data before fit

3.5 Parameter estimation by Least Median of Squares fitting

3.5.1 Robust estimation: terminology and the LMS algorithm

Data can be contaminated by observations which do not come from the process whose parameters are being estimated. Such observations are called *outliers*. Their presence in a data set can result in parameter fits that are grossly incorrect when standard least squares techniques are used as estimators. Outliers pose a particular problem for the YARF system. They will arise when there is a false positive response from a tracker. Because the tracker windows are placed at the predicted road position, they will not be random and may pull the fit incorrectly towards the prediction and away from the actual road.

There are two approaches to making estimation insensitive to outliers. The first, *outlier detection*, attempts to identify the contaminating data points and eliminate them before performing a standard least squares fit to the remaining data. A good survey of techniques for outlier detection can be found in [1]. The second approach, *robust estimation*, attempts to design estimators which are less sensitive to the presence of outliers than standard least squares estimation.

An increasingly popular robust estimation techniques is called *Least Median of Squares* (or LMS) estimation [12]. Consider the linear system $y_i = \beta x_i + c$, where β is the vector of parameters to be estimated, and c is a noise term. Standard least squares finds the estimate β' which minimizes $\sum r_i^2$, where r_i is the residual $r_i = \beta' x_i - y_i$. Least Median of Squares tries to find the estimate β' which minimizes $median(r_i^2)$. To give a simple geometric intuition for what the LMS estimate is, picture the two dimensional linear case. The LMS estimate is the line such that a band centered on the line which contains half the data points has the minimum height in y (the dependent variable) (see Figure 3.7).

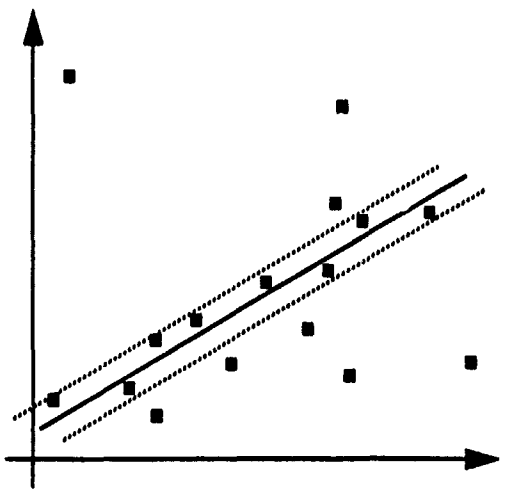

Figure 3.7: Example LMS fit

The computation of the LMS estimate is straightforward, and is similar to Bolles' RANSAC algorithm. Random subsets of the data are chosen. The standard least squares estimate of the parameters is made for each subset, and the median squared residual for that estimate is computed. The estimate which produced the lowest median squared residual is selected as the final estimate.

The *breakdown point* of an estimator is the smallest fraction of the data that need to be outliers in order for the parameter estimates to be arbitrarily bad. In the case of standard least squares, the breakdown point is asymptotically zero, since a single outlying observation can cause pull the fit arbitrarily far from the correct result. The breakdown

point of LMS estimation is 50%, the maximum achievable.

The *relative efficiency* of an estimator is the ratio of the lowest achievable variance for the estimated parameters (given by the Cramer-Rao bound) and the variance achieved by the given estimator. In the case of LMS estimation the relative efficiency is $2/\pi = 0.637$. In practice, the variance in the parameter estimates can be reduced by using the value of the median squared residual to estimate the variance of the noise in the data, eliminating data points more than three standard deviations away from the initial LMS fit, and refitting the remaining data points using standard least squares.

Two phenomena complicate the task of identifying outlying observations. The first, *masking*, occurs when there are multiple ouliers in the data which jointly influence the fit in such a way that their residuals do not look unusual. The second, *swamping*, occurs when outliers influence the fit in such a way that valid data points have suspiciously large residuals which make them appear to be outliers. Selecting a robust estimation technique which shows low sensitivity to masking is important in the YARF domain because outliers will occur near the predicted road location, and will therefore tend to influence the fit in a consistent way. LMS estimation shows little sensitivity to masking, another factor in its favor.

3.5.2 Examples showing the effects of contaminants on road shape estimation

Contaminating data points can arise from a number of sources. False positive responses from the low level image segmentation techniques are the most obvious source, but changes in road appearance present another source. Figure 3.8 shows an example of this. In this experiment a human drove Navlab II on a local highway at a speed of 45 miles per hour while YARF attempted to track the lane. Three successive fit results are shown from left to right. At the top of the first frame the right white stripe begins to curve off to the right for the exit ramp. The road is actually straight, but the fit curves off slightly. This error results in incorrect predictions for the feature locations in the middle frame. The white stripe on the right is located as it veers off on the exit ramp, but the white stripe on the left has been lost (the asterisks represent the predicted feature locations where the tracker returned failure). In the third frame on the right YARF is now tracking the exit lane while the vehicle continues in its lane, resulting in the left edge of the reconstructed lane passing through the vehicle. While the data in this example is not dense enough for LMS to detect the error, it shows the way in which the contaminants can be highly structured.

The second example (Figure 3.9) shows a case in which the outliers are the result of errors in the segmentation. The lane being followed has a double yellow line on the left side and a single solid white line on the right side. Due to error in the predicted road location some of the trackers for the double yellow line are off the road on grass and return false feature locations. The road actually curves off to the right, explaining the tendency of the points from the left lane edge to fall to the right of the fit in the middle of the diagram, and the failure of the white stripe tracker to locate the right lane edge in that same area (the points marked with asterisks). The LMS fit on the right shows the correct road fit, with the erroneous feature points at top far off to the left of the lane.

3.6 Conclusion

In this chapter we have explained the motivation behind YARF's selection of road representation and model fitting algorithms. We have shown how an analysis of the errors introduced by linearizing the circular arc road model leads to the idea of performing virtual panning on the data to reduce the errors in the model parameter estimates, and presented quantitative results from simulation runs to show the improvement from virtual panning. Also, we have explained the motivation for using least median squares estimation to avoid errors caused by outlying data points

Future work would involve an attempt to characterize the errors induced in the parameter estimates in cases where

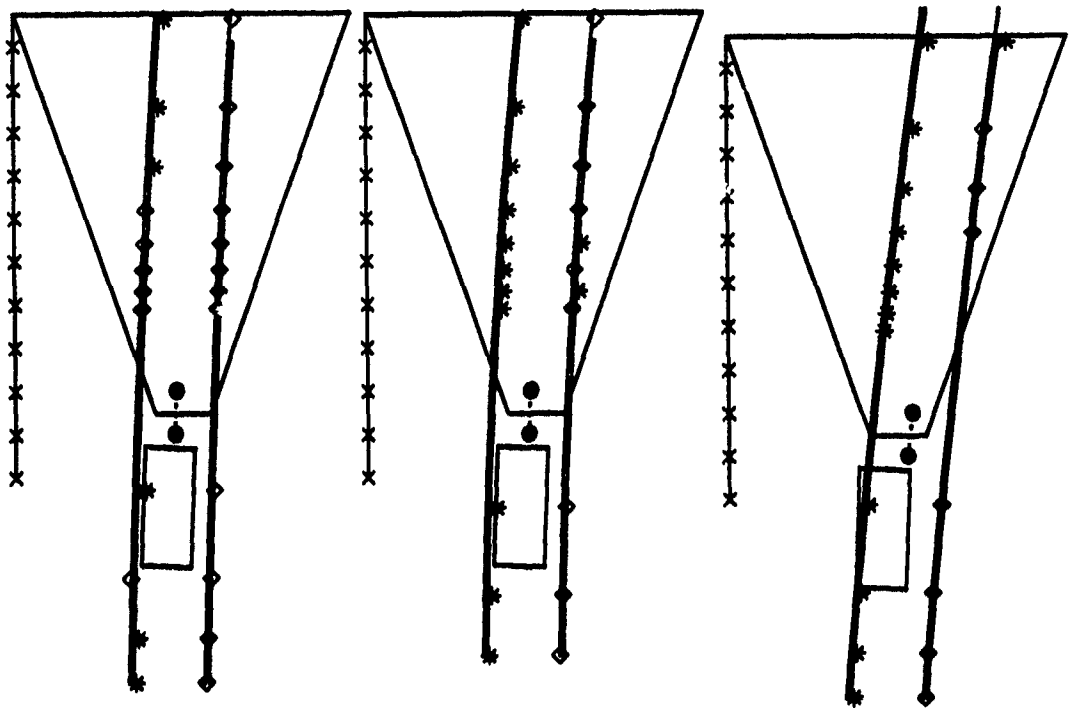

Figure 3.8: Led astray by the exit ramp

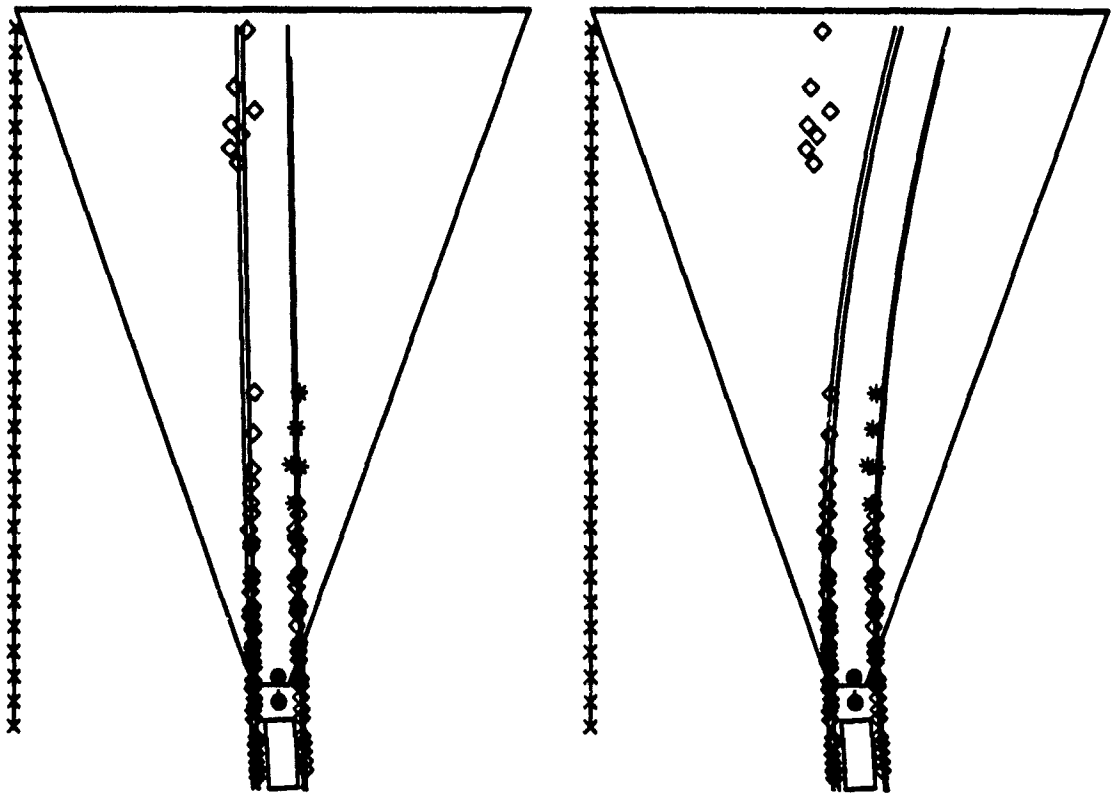

Figure 3.9: Comparison of least squares fit (left) and least median squares fit (right) of data with outliers

the flat ground plane assumption doesn't hold. Also there is a need for the development of algorithms which can recover three dimensional road structure with less sensitivity to noise than current algorithms, and which can incorporate information from road features other than the edges of the lane being followed.

References

[1] Beckman, R. J., and Cook, R. D.
Outlier.....s.
Technometrics 25(2):119-149, May, 1983.

[2] Crisman, Jill.
Color Vision for the Detection of Unstructured Roads and Intersections.
PhD thesis, Carnegie-Mellon University, 1990.

[3] DeMenthon, Daniel, and Davis, Larry.
Reconstruction of a Road by Local Image Matches and Global 3D Optimization.
In *Proceedings 1990 IEEE International Conference on Robotics and Automation.* May, 1990.

[4] Kanatani, Kenichi, and Watanabe, Kazunari.
Reconstruction of 3-D Road Geometry from Images for Autonomous Land Vehicles.
IEEE Transactions on Robotics and Automation 6(1):127-132, February, 1990.

[5] Kenue, Surender K.
LANELOK: Detection of Lane boundaries and Vehicle Tracking Using Image-Processing Techniques -- Part I: Hough-Transform, Region Tracing and Correlation Algorithms.
In *SPIE Mobile Robots IV.* 1989.

[6] Kenue, Surender K.
LANELOK: Detection of Lane boundaries and Vehicle Tracking Using Image-Processing Techniques -- Part II: Template Matching Algorithms.
In *SPIE Mobile Robots IV.* 1989.

[7] Kuan, Darwin; Phipps, Gary; and Hsueh, A.-Chuan.
Autonomous Land Vehicle Road Following.
In *Proceedings First International Conference on Computer Vision.* June, 1987.

[8] Liou, Shih-Ping, and Jain, Ramesh.
Road Following Using Vanishing Points.
Computer Vision, Graphics, and Image Processing 39:116-130, 1987.

[9] Mysliwetz, Birger D., and Dickmanns, E. D.
Distributed Scene Analysis for Autonomous Road Vehicle Guidance.
In *Proceedings SPIE Conference on Mobile Robots.* November, 1987.

[10] Polk, Amy, and Jain, Ramesh.
A Parallel Architecture for Curvature-Based Road Scene Classification.
In *Roundtable Discussion on Vision-Based Vehicle Guidance '90 (in conjunction with IROS).* July, 1990.

[11] Pomerleau, Dean A.
Neural Network Based Autonomous Navigation.
Vision and Navigation: The Carnegie Mellon Navlab.
In Charles E. Thorpe,
Kluwer Academic Publishers, 1990, Chapter 5.

[12] Rousseeuw, Peter J. and Leroy, Annick M.
Robust Regression and Outlier Detection.
John Wiley & Sons, Inc., 1987.

[13] Schaaser, L. T., and Thomas, B. T.
Finding Road Lane Boundaries for Vision Guided Vehicle Navigation.
In *Roundtable Discussion on Vision-Based Vehicle Guidance '90 (in conjunction with IROS).* July, 1990.

[14] Turk, Matthew A.; Morgenthaler, David G.; Gremban, Keith D.; and Marra, Martin.
VITS -- A Vision System for Autonomous Land Vehicle Navigation.
IEEE Transactions on Pattern Analysis and Machine Intelligence 10(3), May, 1988.

4. A Computational Model of Driving for Autonomous Vehicles

4.1 Introduction

Driving models are needed by many researchers.[1] Intelligent vehicle designers need them to make driver aids that work in dynamic traffic situations. Robot vehicle builders need them to drive vehicles autonomously in traffic. Traffic engineers need them to improve the safety of highways. To be most useful, a driving model must be *detailed* and *complete*. A *detailed* model must state specifically what decisions must be made, what information is needed, and how it will be used. Such models are called computational because they tell exactly what computations the driving system must carry out. A *complete* driving model must address all aspects of driving. In the course of our research in robotics, we have developed a computational model that addresses a level of driving which has not been previously addressed. We have implemented this model in a system called Ulysses.

The driving task has been characterized as having three levels: strategic, tactical and operational [27]. These levels are illustrated in Table 4.1. The highest level is the *strategic* level, which develops behavioral goals for the

Level	Characteristic	Example	Existing model
Strategic	Static; abstract	Planning a route; Estimating time for trip	Planning programs (Artificial Intelligence)
Tactical	Dynamic; physical	Determining Right of Way; Passing another car	Human driving models
Operational	Feedback control	Tracking a lane; Following a car	Robot control systems

Table 4.1: Characteristics of three levels of driving.

vehicle. These goals may be based on route selection and driving time calculations, for example. The strategic goals are achieved by activities at the middle, *tactical*, level, which involves choosing vehicle maneuvers within the dynamic world of traffic and traffic control devices (TCD's). The maneuvers selected at the tactical level are carried out by the *operational* level of speed and steering control.

Substantial progress has been made in automating various parts of the driving task, particularly at the strategic and operational levels, but no system has yet implemented the tactical level. At the strategic level, planning programs in the Artificial Intelligence community are quite good at planning errands, finding routes, and performing other abstract tasks. However, they do not solve the problems of vehicle maneuver selection because they are not designed to work in a dynamic domain and without complete knowledge of the problem. At the operational level, several robot projects have demonstrated the ability to drive a vehicle on roads that are essentially devoid of traffic and TCD's. These systems can track lanes, but have no real knowledge of driving laws and general vehicle behavior. Thus, they too avoid the problems of maneuver selection that form the tactical level of driving.

Traffic engineers and psychologists have long studied the driving task, including tactical driving, and have

[1] An earlier version of this report appeared as technical report CMU-CS-91-122, authored by Douglas Reece and Steven Shafer

developed many good theories and insights about how people drive. Unfortunately, these models of human driving do not explain exactly what and how information is processed—what features of the world must be observed, what driving knowledge is needed and how it should be encoded, and how knowledge is applied to produce actions. A model must answer these questions before it can be used to compute what actions a robot should take.

Our driving program, Ulysses, is a computational model of tactical driving. The program encodes knowledge of speed limits, headways, turn restrictions, and TCD's as constraints on acceleration and lane choice. The constraints are derived from a general desire to avoid collisions and a strategic driving goal of obeying traffic laws. Ulysses evaluates the current traffic situation by deliberately looking for important traffic objects. The observations, combined with the driving knowledge and a strategic route plan, determine what accelerations and lane changes are permitted in this situation. The program then selects the one action that allows the robot to go as fast as possible. While this model has limitations, it drives competently in many situations. Since it is a computational model, Ulysses shows exactly what information a driver needs at each moment as driving decisions are made. Furthermore, the program can be tested objectively on a real vehicle.

Our eventual goal is to use Ulysses to drive a real vehicle. At this time, however, the model has only been implemented in computer simulation. We have constructed a microscopic traffic simulator called PHAROS (for Public Highway and ROad Simulator) [30] for our driving research. PHAROS represents the street environment in detail, including the shape and location of roads, intersections, lines, markings, signs, and signals. The cars in PHAROS are driven using a simplified version of the driving model. The simulator generates an animated display of traffic that can be used to observe driving behavior. PHAROS performs the perception and control functions for Ulysses so that Ulysses can drive a robot through a road network in simulation.

This chapter describes our driving model for robots in detail. The next section reviews existing driving models, including both robot driving systems and human driving models. We then present Ulysses, and describe the important features of PHAROS. The chapter concludes with a discussion of possible extensions to the model and other future research.

4.2 Related Work

4.2.1 Robots and Planners

Computers have been used to automate several aspects of the driving task. Various research groups have been investigating vehicle steering and speed control for at least 30 years [5, 13, 15, 24, 28, 34]. This work generally assumes that special guides are placed in the roads, so the vehicles are not completely autonomous. In the 1980's, robots began driving on roads autonomously [9, 20, 22, 29, 36, 37, 38, 39, 42]. The different robots have strengths in different areas; some are fast (60 mph), while others are very reliable in difficult lighting or terrain conditions. Autonomous vehicles can also follow other vehicles, with or without a special guide device on the lead vehicle [4, 7, 14, 19, 21, 36].

These existing robot systems address only the operational level. Consider the driver approaching the intersection in Figure 4.1 from the bottom. A robot with current operational capabilities could track the lane to the intersection, find a path across the intersection, and then start following a new lane. The robot could also perhaps detect the car on the right and stop or swerve if a collision were imminent. However, in this situation a driver is required to interpret the intersection configuration and signs and decide whether it should pass in front of the other car. Current robot driving programs cannot perform this tactical task. Nevertheless, it is the success of automonous vehicles at the operational level that motivates us to study the tactical level.

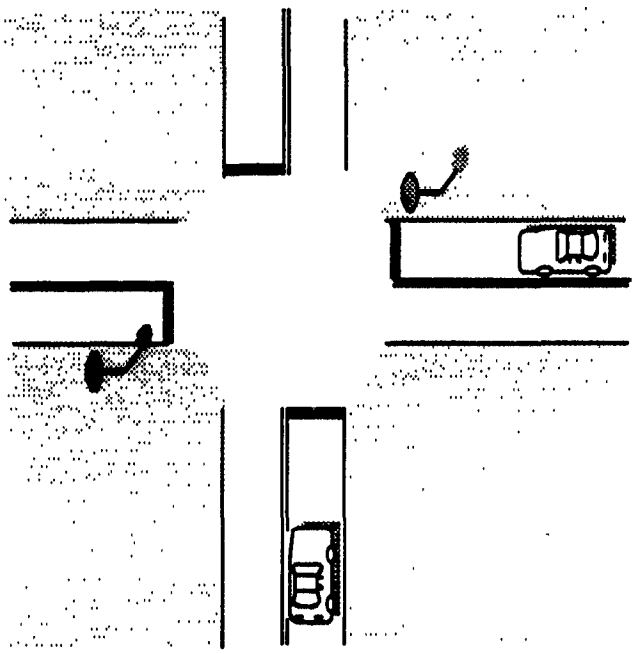

Figure 4.1: Example of tactical driving task: driver approaching crossroad.

Computers have also been used to automate strategic driving functions. Map-based navigation systems have advanced from research projects to commercial products in the last decade [3, 11, 18, 32, 35, 41]. Artificial Intelligence programs have been applied to many abstract problems, including the planning of driving errands [17]. These planners work on static problems using information conveniently encoded in a database ahead of time. Let us consider again the driver of Figure 4.1. A strategic planner may have already determined that this driver is going to a pizza store, and that he must turn left at this intersection, and that he should drive quickly because he is hungry. However, the planner (probably) does not know ahead of time what TCD's are present at this intersection, and certainly cannot predict the arrival of cross traffic. Since the situation is unknown ahead of time, the driver must get data by *looking* for signs and cars when he gets to the intersection. This data must be interpreted to form abstract concepts such as "the other car is stopping." In general, the world is uncertain and dynamic at this level, and the driver must continually use perception to assess the situation. Strategic planners are not designed to deal with these tactical problems.

4.2.2 Human Driving Models

Psychologists, traffic engineers and automotive engineers have studied human driving a great deal. Their goal is to make cars and roads safer and more efficient for people. The result of this work is a multitude of driving models spanning all levels of driving. Michon identified seven types of models [27]: task analysis, information flow control, motivational, cognitive process, control, trait, and mechanistic. Each has different characteristics and addressed different aspects of driving.

Task analysis models. A task analysis model lists all of the tasks and subtasks involved in driving. The paragon of these models is McKnight and Adam's analysis [26]. Their work provides an exhaustive breakdown of all activities on the tactical and operational levels. We have found this listing very useful for determining whether our model performs all of the necessary subtasks in various situations. However, a list of tasks alone is not sufficient for describing a driving model. This is because a task list does not address the dynamic relations between tasks. The

list does not specify how the driver chooses a task in a given situation, or whether one task can interrupt another, or how two tasks might be performed simultaneously (especially if they require conflicting actions). The McKnight work also leaves situation interpretation vague. For example, two tasks require a driver to "observe pedestrians and playing children" and "ignore activity on the sidewalk that has no impact on driving." However, there are no computational details about how to discriminate between these situations.

Information flow control models. Information flow control models are computer simulations of driving behavior. Early computer models of drivers were essentially implementations of task analysis models [27]. As such, they have the same weaknesses as the task analysis models. More recent microscopic traffic simulators such as SIMRO [6], TEXAS [16], and NETSIM [12, 43] do not have these weaknesses because they perform multiple tasks simultaneously. They also have the ability to start and stop tasks at any time in response to traffic. For example, NETSIM evaluates the traffic situation frequently (every second) and makes a fresh selection of appropriate subtasks. NETSIM is not intended to be an accurate description of human cognitive processing, but it produces reasonable driver behavior in many situations. NETSIM is a direct ancestor of our system, PHAROS, which we describe later in this chapter.

NETSIM cannot be used as a complete driver model because it lacks several necessary components. There are gaps in its behavior; for example, cars are discharged from intersection queues into downstream streets without having to accelerate and drive normally to and through the intersection. Neither does NETSIM contain knowledge of how to interpret traffic conditions from observable objects. We also found unmodified NETSIM inadequate as a simulator testbed for robotics research because it cannot represent physical information such as road geometry, accurate vehicle location, or the location and appearance of TCD's.

Motivational models. Motivational models are theories of human cognitive activity during driving. Van der Molen and Botticher recently reviewed several of these models [40]. The models generally describe mental states such as "intentions," "expectancy," "perceived risk," "target level of risk," "need to hurry" or "distractions." These states are combined with perceptions in various ways to produce actions. Since motivational models attempt to describe the general thought processes required for driving, one would hope that they would form a basis for a vehicle driving program. However, the models do not concretely show how to represent driving knowledge, how to perceive traffic situations, or how to process information to obtain actions. Van der Molen and Botticher attempted to compare the operations of various models objectively on the same task [33, 40], but the models could be implemented only in the minds of the model designers. Some researchers are addressing this problem by describing *cognitive process models* of driving (for example, Aasman [1]). These models are specified in an appropriate symbolic programming language such as Soar [23].

The remaining types of models have limited relevance to tactical driving. *Control models* attempt to describe the driver and vehicle as a feedback control system (e.g., [31]). These models are mainly useful for lane keeping and other operational tasks. *Trait models* show correlations between driver characteristics and driving actions. For example, drivers with faster reaction times may have a lower accident rate. This correlation does not describe the mechanism by which the two factors are related. Finally, *mechanistic models* describe the behavior of traffic as an aggregate whole. These models express the movement of traffic on a road mathematically as a flow of fluid [10]. This type of model cannot be used to specify the actions of individual drivers.

4.2.3 Ulysses

In this chapter we present a new computational model of driving called Ulysses. It is computational because it explains how to compute driving actions from sensed data. Ulysses encodes knowledge for performing a variety of tactical driving tasks, including maneuvering in traffic on multilane highways and negotiating intersections. Like

the information flow control models, Ulysses performs all appropriate tasks simultaneously. Ulysses goes beyond models such as NETSIM because it describes how to drive in the transitions between states (e.g. between free flow and enqueued). Unlike existing models, Ulysses makes decisions based on observable phenomena. The perceptual part of driving is therefore described in terms of looking in specific areas for specific objects. This explicit situation assessment is much more concrete than the "risk perception" in the motivational models. Ulysses operationalizes concepts such as "risk avoidance" in these models with specific constraints on lane selection and speed. Since Ulysses is implemented as a computer program (in the language Allegro CommonLisp), it can be analyzed and tested objectively. It can be used in various driving situations to study the perceptual and information processing requirements of the task. And ultimately, Ulysses can be used to compute actions for an actual vehicle driving in traffic.

4.3 The Ulysses Driving Model

We have implemented a computational driving model in a program called Ulysses. Ulysses defines a complete system for driving — what a driver must look for, how situations are evaluated, what practical knowledge is needed, and how this knowledge is encoded and applied. Figure 4.2 is a schematic of the entire driver model. Only the tactical level is implemented in detail in Ulysses. The model treats the operational and strategic levels abstractly since the details have already been addressed by other work. These levels are discussed at the end of the section.

Figure 4.2 shows that at the tactical level, Ulysses performs several perception and decision functions. Ulysses uses the route plan created at the strategic level as a guide in scanning the road ahead along the intended route. The portion of the strategic route plan that is actually visible to the robot is called the *corridor* in our model. Ulysses identifies the corridor at the tactical level so it knows which signs, signals and other cars are important. The corridor is built up incrementally as the Ulysses finds intersections and chooses which direction to look further. As the corridor is found, implicit goals to drive lawfully and safely cause constraints to be generated. The constraints are triggered by the presence of various traffic objects. Ulysses must look for all objects that could trigger a constraint. After all constraints have been applied, Ulysses chooses an acceleration and lane-changing action from the available choices. This selection is based on the implicit goals of driving quickly and courteously. State variables are used to record decisions such as accepting gaps in traffic that affect actions for a period of time. Table 4.2 summarizes the state variables used in Ulysses; these will be explained later in this section.

In order to be able to respond quickly to unpredictable events, Ulysses frequently repeats its visual search and evaluation of the current situation. The decision cycles have a period of 100ms. This rapid polling simulates the responsiveness of perceptual interrupts. However, the polling scheme allows constraint evaluations to activate perception rather than the other way around. Ulysses uses this demand-driven perception at the tactical level to provide a mechanism for focusing its perceptual attention. Focusing perception is important for robots because machine perception is very difficult; it would be impossible to perceive and analyze everything in the field of view in 100 ms.

In the remainder of this section we explain the specific driving knowledge in Ulysses by describing a series of scenarios of increasing complexity. The scenarios include a simple highway with only one lane, intersections with various traffic control devices, and finally multi-lane roads. The section concludes with a discussion of perception, strategic plans and operational control.

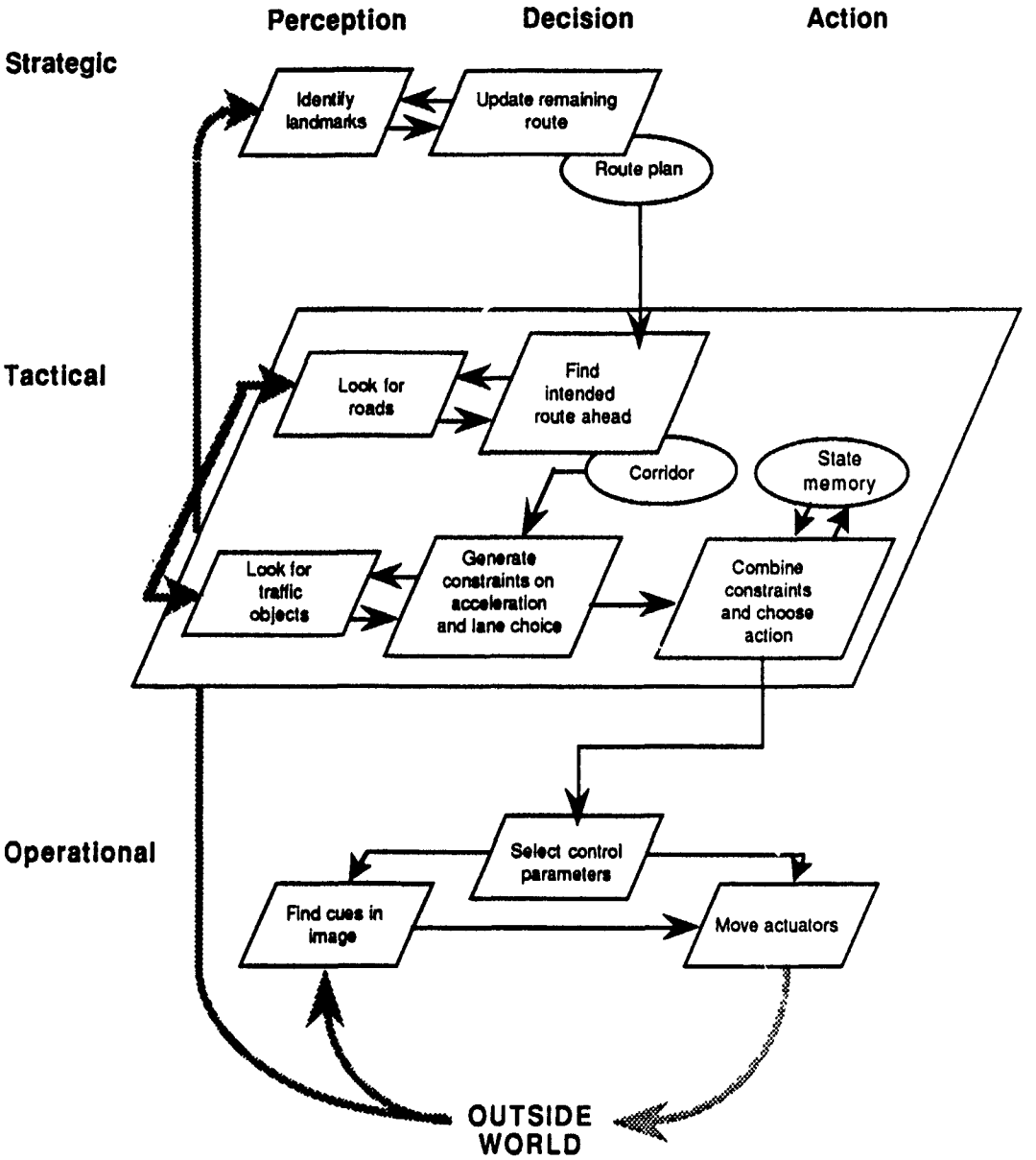

Figure 4.2: Schematic of the Ulysses driver model

4.3.1 Tactical Driving Knowledge

4.3.1.1 A Two-Lane Highway

Figure 4.3 depicts a simple highway driving situation. In this scenario no lane-changing actions are necessary, but there are several constraints on speed.

The first two constraints are derived from general safety goals—i.e., self-preservation. The speed of the vehicle must be low enough to allow it to come to a stop before the end of the road is reached; the speed on a curve must keep the vehicle's lateral acceleration below the limit imposed by friction between the tires and road surface.

State Variable	Values
Speed Limit	<current speed limit>
In intersection	Street, Intersection
Wait	Normal, Wait for gap, Wait for merge gap, Accept
Lane Position	Follow lane, Init-left (-right), Changing-left (-right)

Table 4.2: Ulysses state variables.

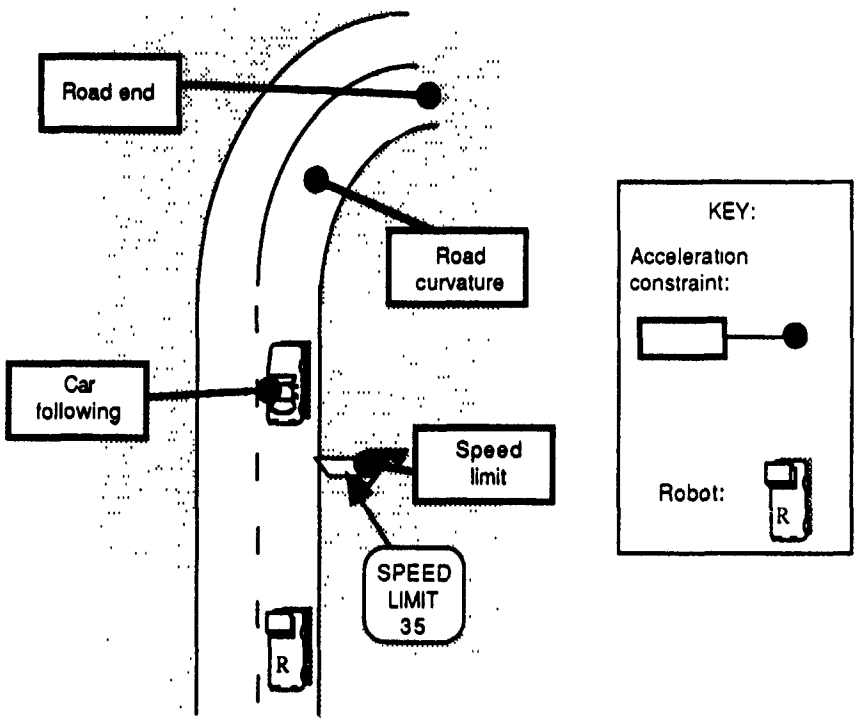

Figure 4.3: The two-lane highway scenario.

Although it is possible that these constraints can be met by the operational level systems of the robot, the prediction of future speed constraints from observations of distant conditions is in general a tactical activity. This is especially true if future conditions are detected not by tracking road features but by reading warning signs. Ulysses generates the road end and road curvature constraints by examining the corridor. The robot must be stopped at the end of the road if the road ends; furthermore, at each point of curvature change, the robot's speed must be less than that allowed by the vehicle's lateral acceleration limit. Ulysses also scans along the right side of the corridor for signs warning of road changes, and creates a speed constraint at the relevant signs.

These constraints—a maximum speed at a point somewhere ahead in the corridor—are typical of the motion

constraints generated by various driving rules. Given the robot's current speed, we could compute a constant acceleration value that would yield the desired speed at the desired point. However, it is also possible to satisfy the constraint by driving faster for a while and then braking hard. Figure 4.4 shows these two possibilities as curves X and Y on a graph of speed versus distance. The figure shows that any speed profile is possible as long as it stays

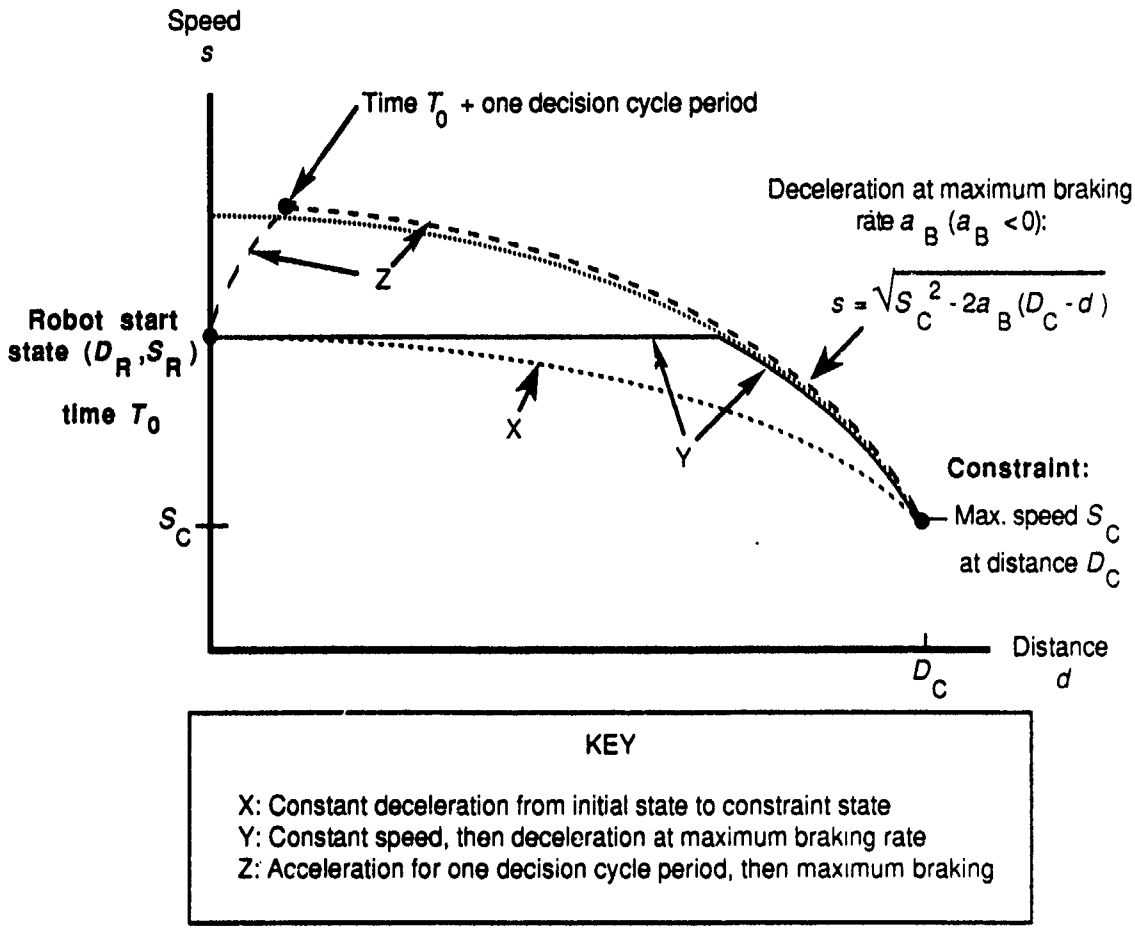

Figure 4.4: Deceleration options plotted on speed-distance graph

below the maximum braking curve. The profile that maximized vehicle speed would rise instantly to the maximum braking curve and then follow the curve to the constraint point. However, the program cannot change the acceleration command at arbitrary times; it looks at situations and changes acceleration only at discrete intervals. Therefore Ulysses computes an acceleration that will cause the robot's speed to meet the maximum deceleration curve exactly at the next decision time. This is curve Z in the figure.

While the high-acceleration, high-deceleration policy shown by curve Z maximizes vehicle speed, it seems to have the potential to cause jerky motion. In fact, the motion is usually smooth because the constraints relax as the robot moves forward. For example, suppose that the robot's sensors could only detect the road 150 feet ahead. Ulysses would constrain the robot to a speed of 0 at a distance of 150 feet. However, when the robot moved forward, more road could be detected, so the constraint point would move ahead. Figure 4.5 shows how this "rolling horizon" affects speed. The robot starts at distance 0 with a speed of 45 fps. A decision interval of 1.0 seconds is assumed in order to show speed changes more clearly. The dashed lines show deceleration constraint curves (-15 fps^2) at the first four decision times. The solid line shows the robot's speed. After a small overshoot, the speed

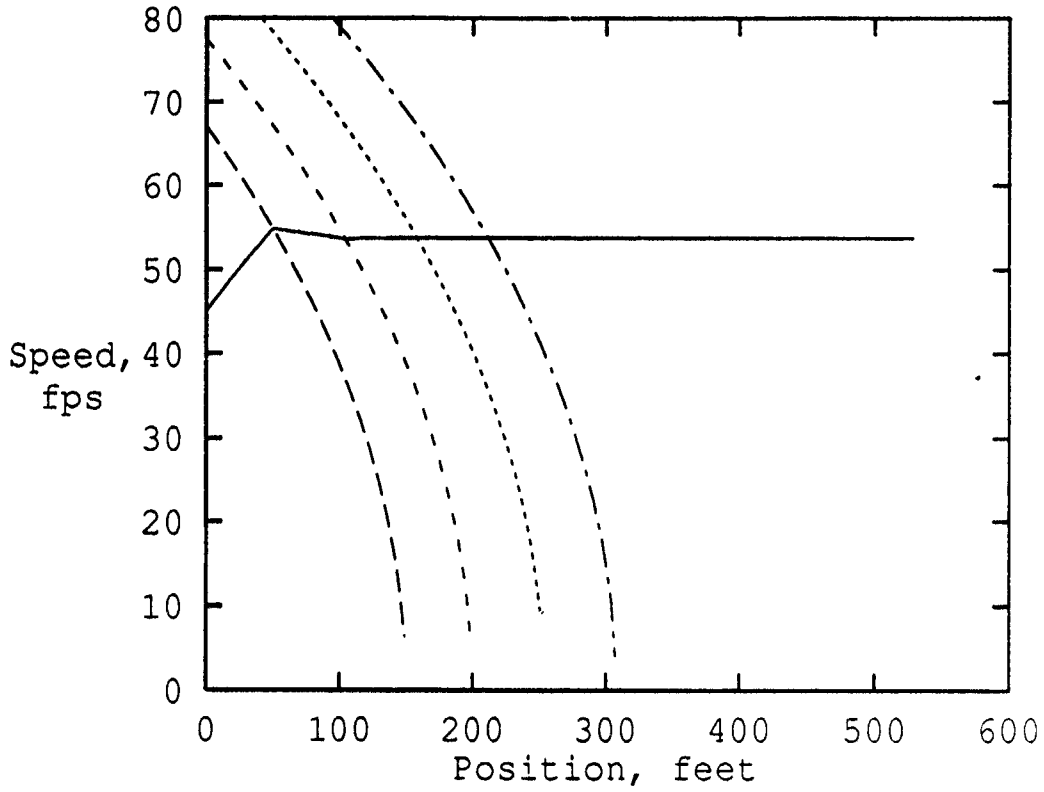

Figure 4.5: Robot speed profile (solid line) as it adjusts to a rolling road horizon. Maximum deceleration is -15.0 fps^2, decision time interval 1.0 sec, horizon at 150 feet. The four dashed lines show, for the first four decision times, the maximum-deceleration profile to the current horizon.

reaches an equilibrium and remains constant.

The next constraint illustrated by Figure 4.3 is that generated by legal speed limits. Ulysses maintains a state variable which records the current speed limit. The vehicle is allowed to accelerate so that it reaches the speed limit in one decision cycle period. Furthermore, Ulysses scans the right side of the corridor for "Speed Limit" signs. Whenever the system detects a speed limit change, it creates an acceleration constraint to bring the robot's speed to the limit speed at the sign (as described above). As the robot nears the Speed Limit sign, Ulysses also updates the speed limit state variable.

The final acceleration constraint is generated by traffic in front of the robot. The safety goal implicit to Ulysses requires that an adequate headway be maintained to the car in front of the robot in the same lane. Ulysses therefore scans the corridor to monitor the next car ahead. If the lead car were to suddenly brake, it would come to a stop some distance ahead. This is the constraint point for computing an acceleration limit. The program uses the lead car's speed, its distance, and its assumed maximum deceleration rate to determine where it would stop. This activity is commonly called "car following."

After all acceleration constraints have been generated, they are combined by taking their logical intersection. The intersection operation guarantees that all constraints are met simultaneously. Figure 4.6 illustrates this process. Since the constraints in effect allow a range of accelerations between the negative limit (the braking capability of the robot) and a computed positive value, the intersection results in a range from the negative limit to the smallest computed positive value. Ulysses chooses the largest allowed acceleration in order to further the implicit goal of

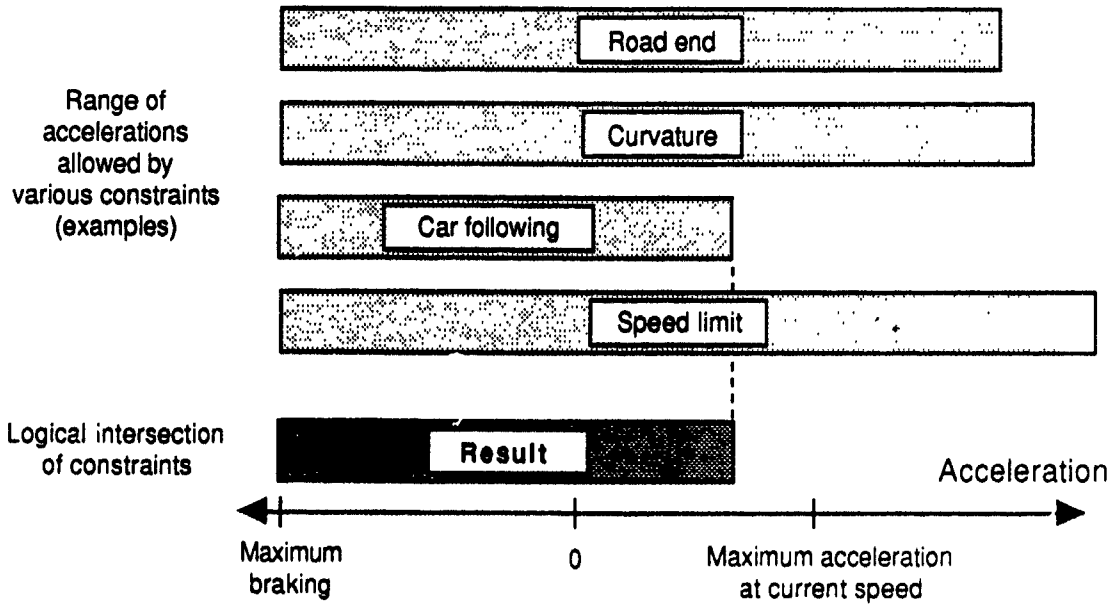

Figure 4.6: Combining acceleration constraints.

getting to the destination as quickly as possible.

The perception system may not be able to detect objects beyond some range. Ulysses deals with the resulting uncertainty by making two assumptions: first, that there is a known range within which perception is certain; and second, that objects and conditions that trigger constraints are always present just beyond this range. This latter assumption is the worst case. For example, Ulysses always assumes that the road ends just beyond road-detection range, that the speed limit drops to zero just outside of sign-detection range, and that there is a stopped vehicle just beyond car-detection range. In this way Ulysses prevents the robot from "over-driving" its sensors.

4.3.1.2 An Intersection Without Traffic

The next traffic scenario we consider is a simple intersection with only one lane on the robot's approach, no other traffic, and no pedestrians. Figure 4.7 illustrates this scenario. Ulysses detects intersections when it visually tracks a lane ahead and finds that the markings end or the road branches. Other clues, such as traffic signals or signs (or cars, in a different scenario), may be detectable at longer ranges; however, since the robot is constrained to stop anyway at the end of the detected road, Ulysses does not consider these clues. Future versions of Ulysses may model the uncertainties of machine perception in more detail and use several clues to confirm observations.

When the robot is actually in an intersection, Ulysses can no longer detect a lane directly in front of the robot. When this first happens, Ulysses changes the In Intersection state variable from Street to Intersection. Later, when there is a lane in front of the robot, the state is changed back again. These state changes mark the robot's progress in its strategic route plan.

Finding the corridor is more difficult at an intersection than it is on a simple highway because the corridor no longer follows clearly marked lanes. The perception system must recognize the other roads at the intersection and identify the one on which the robot's route leaves. Figure 4.8 shows that the perception system must identify the "left" road if the strategic route plan requires the robot to turn left at this intersection. Ulysses can then extend the

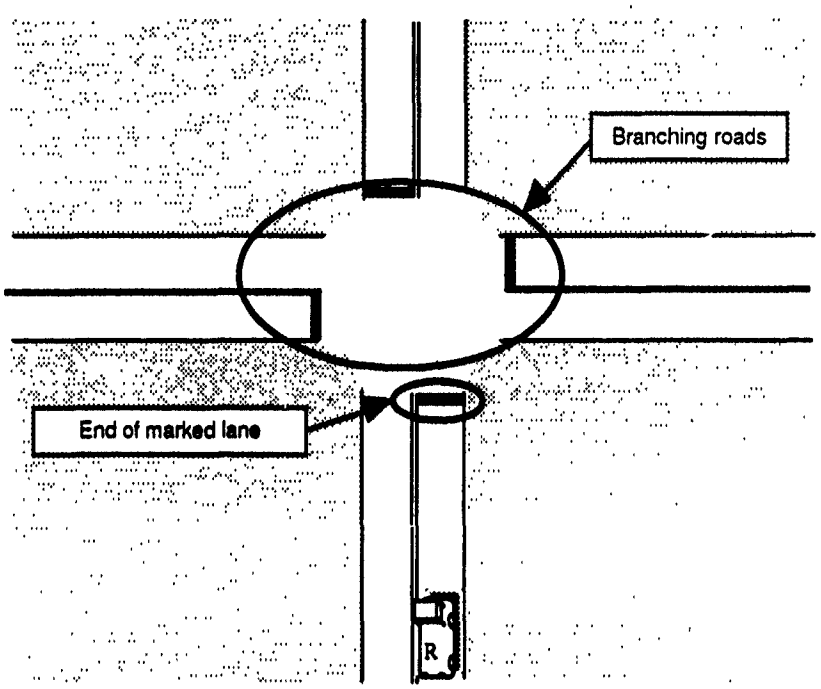

Figure 4.7: An intersection without traffic; detection by tracking lanes.

corridor by creating a path through the intersection from the end of the robot's approach road to the start of the proper lane in the road on the left.

With the corridor established through the intersection, Ulysses generates the same acceleration constraints as for the highway case. Figure 4.9 shows several examples of how these constraints may apply at an intersection. Constraints may apply to conditions before, within, and beyond the intersection.

The next task for the driving program is to determine the traffic control at the intersection. In this scenario the only important TCD's are traffic signals, Stop signs and Stop markings. Thus, as shown in Figure 4.10, Ulysses requests the perception system to look for signs and markings just before intersection and signal heads at various places around the intersection. When the intersection is beyond the given detection range for these objects, Ulysses assumes the worst and constrains the robot to stop at the intersection; however, within the detection range Ulysses assumes that all existing traffic control devices will be found.

Figure 4.11 diagrams the decision process for traffic signals required at this simple intersection. First, Ulysses must determine what the signal indication is. If there is an arrow in the direction of the corridor, the program takes this as the effective signal; otherwise, the illuminated solid signal is used. If the signal indication is red, Ulysses generates an acceleration constraint that stops the robot at the entrance to the intersection. No constraint is generated if the signal is green. If the signal is yellow, then Ulysses determines whether the robot can be stopped at the intersection using a reasonable braking rate. If so, then the program generates a constraint as if the light were red.

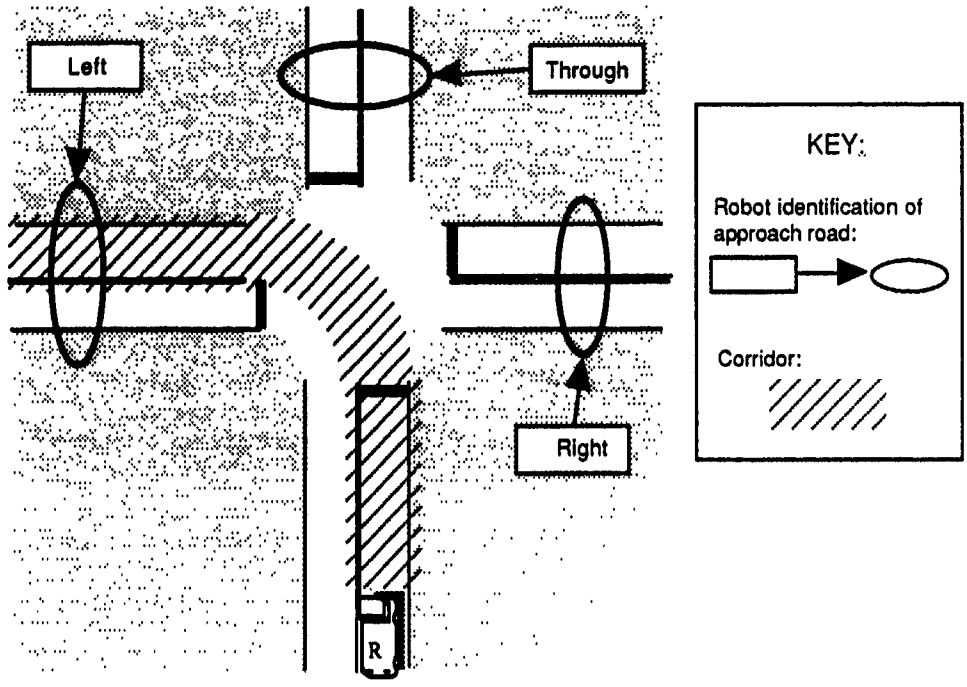

Figure 4.8: Finding the corridor for a left turn.

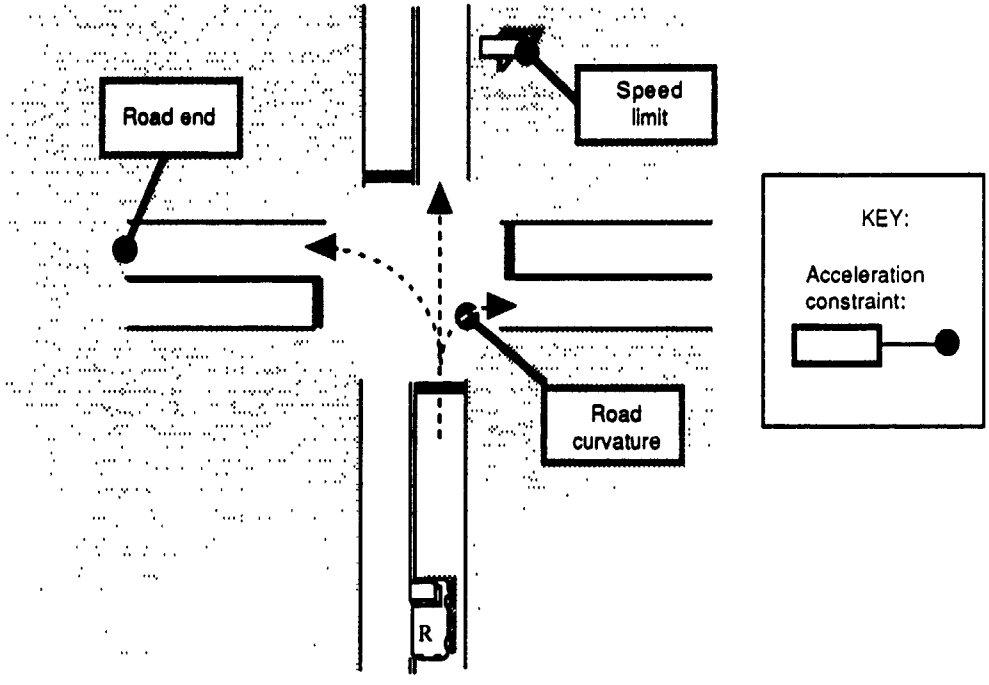

Figure 4.9: Examples of acceleration constraints from road features at an intersection.

Stop signs require not only speed constraints, but a short sequence of actions. A vehicle approaching a stop sign

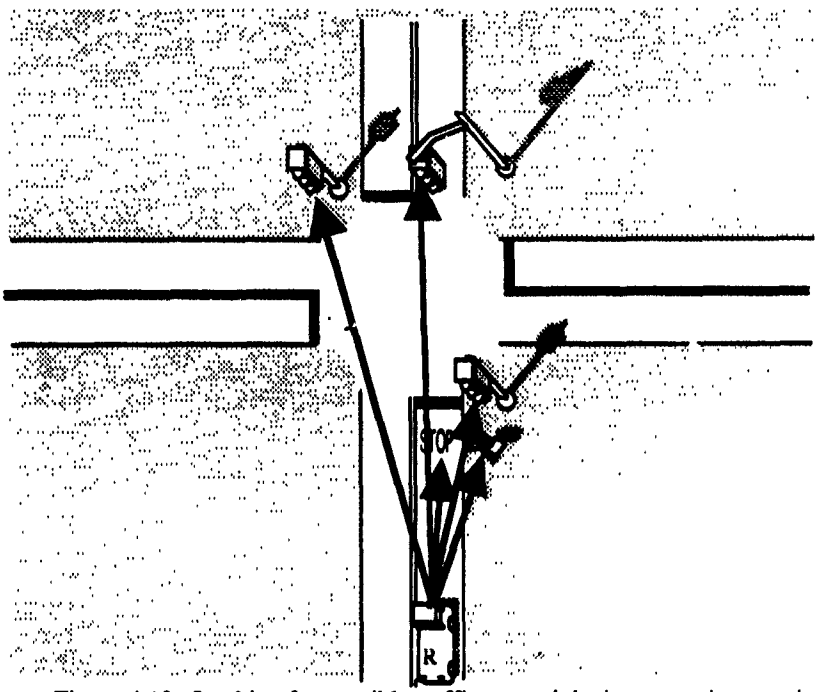

Figure 4.10: Looking for possible traffic control devices at an intersection.

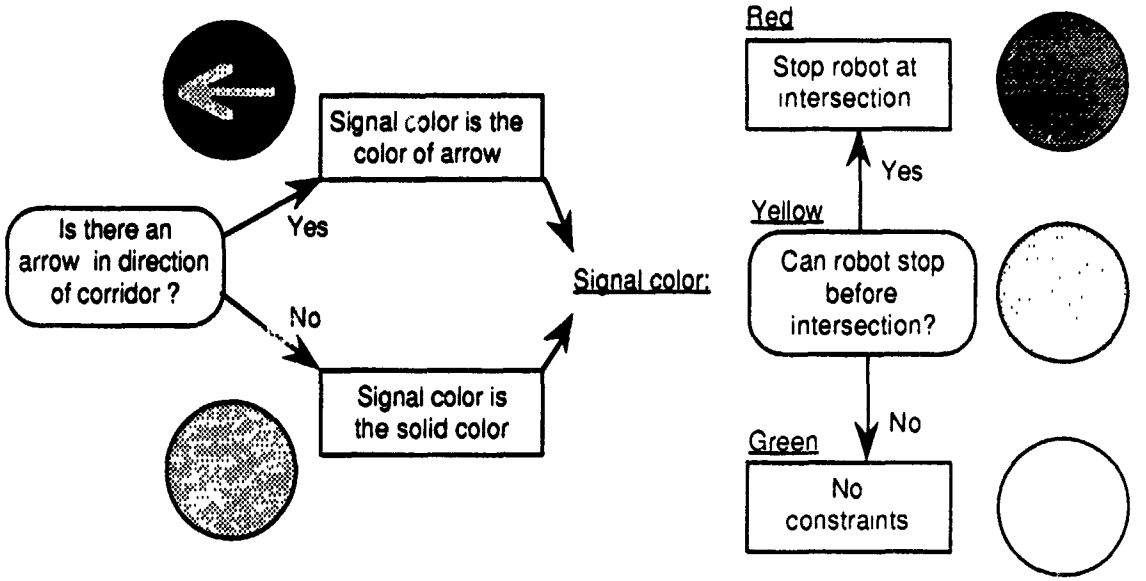

Figure 4.11: Traffic signal logic for intersection without traffic.

must come to a complete stop, look for traffic, and then proceed when the way is clear. Figure 4.12 shows how Ulysses performs these actions with a "Wait" state variable. When a stop sign is detected, Ulysses generates a constraint to stop the robot just before the sign. Later, Ulysses finds that the robot is stopped and that it is very near the sign, so it changes to a "wait for gap" state. In this scenario there is no traffic, so Ulysses immediately moves on to the "accept" state and releases the robot from this traffic control constraint.

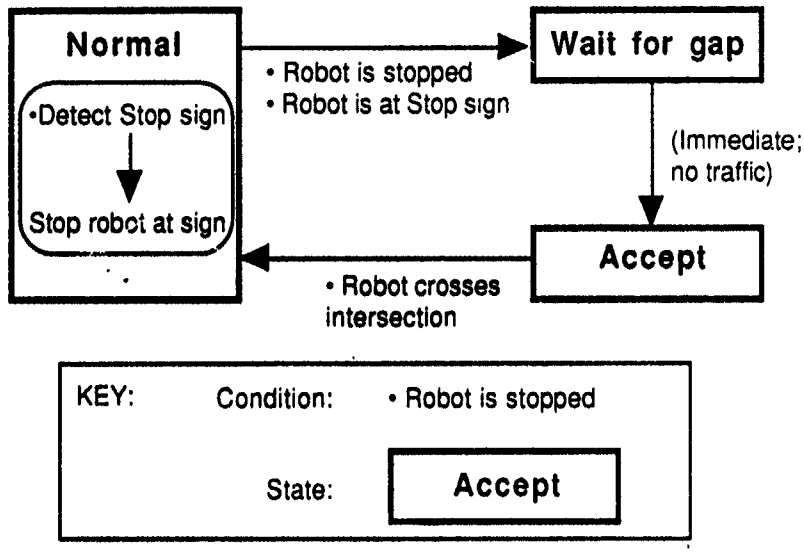

Figure 4.12: State transitions in Stop sign logic.

4.3.1.3 An Intersection with Traffic

We will now add traffic to the simple intersection scenario. Ulysses considers three kinds of traffic at intersections: cars in the same corridor as the robot, which must be given headway; cross traffic blocking the intersection; and cars approaching the intersection on other roads which may have to be given the RoW. Human drivers are sometimes taught to watch the traffic behind them, in case another car is following too closely or approaching very fast. In such a case the driver could accept lower gaps or make more aggressive judgements at an intersection, thereby continuing through the intersection and not stopping quickly in front of the following car. Ulysses does not make such judgements, and thus does not look for traffic behind the robot.

Figure 4.13 illustrates the first kind of traffic that Ulysses considers. The driving program must generate car-following constraints from a lead car either in or beyond the intersection. If the lead car is turning off the robot's path, the robot must still maintain a safe headway until that car is clear of the path. Similarly, the robot must maintain a safe distance to cars that merge into its path.

The second kind of traffic that Ulysses looks for is cross traffic in the intersection. This includes cars sitting across the robot's path or about to cross it, as shown in Figure 4.14. Since the law requires that a vehicle yield the RoW to vehicles already in the intersection, Ulysses looks for such vehicles and stops the robot before the intersection if it finds one. Ulysses does not currently search beyond the closest car to find a gap. Future extensions to Ulysses may try to time the robot's arrival at an intersection to the presence of an upstream gap. However, this type of behavior could only be allowed if it were safe—that is, if the robot could still stop at the intersection if traffic changed unexpectedly.

The third type of traffic is traffic approaching the intersection on other roads. The driving program analyzes nearby TCD's and this approaching traffic to determine if the robot has the RoW. After RoW is determined, Ulysses may generate an acceleration constraint and change the Wait state of the robot. Figure 4.15 illustrates this process.

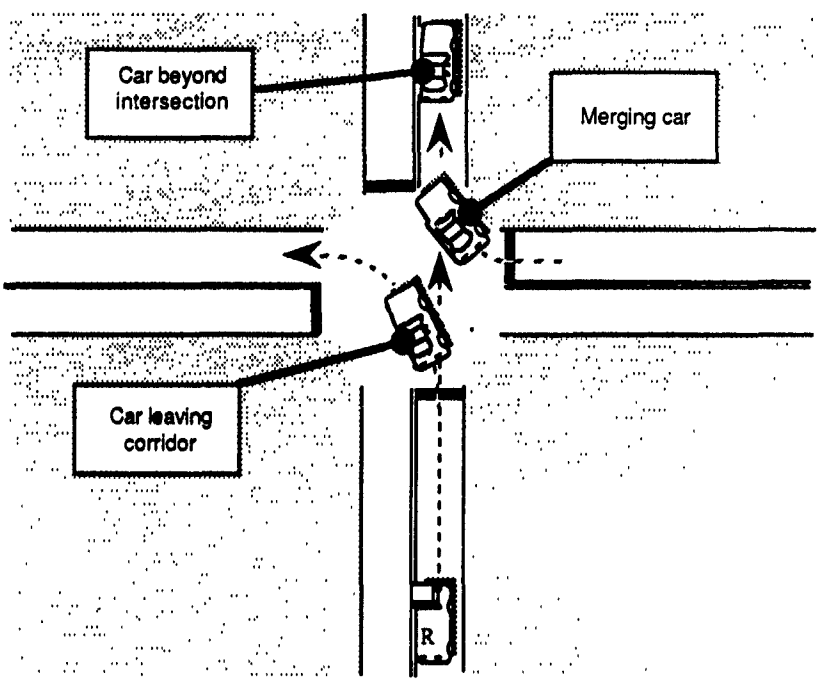

Figure 4.13: Potential car following conditions at an intersection.

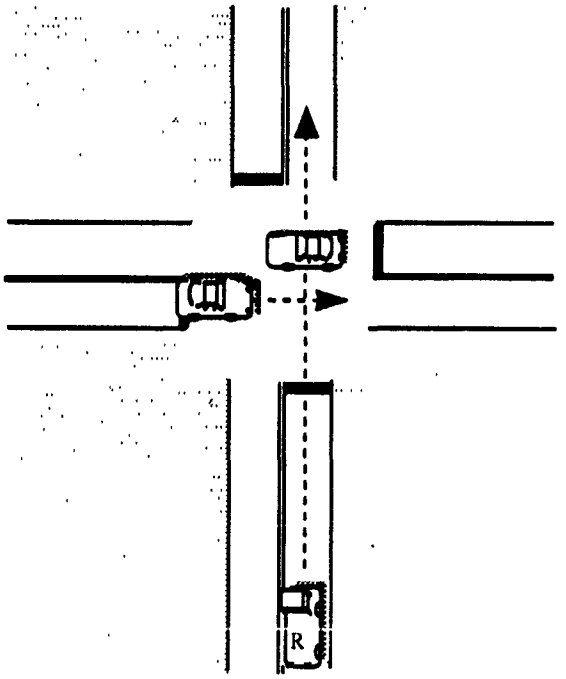

Figure 4.14: Cars blocking an intersection.

Traffic Control Devices. First, Ulysses detects and analyzes signs, markings and traffic lights. In addition to the TCD's needed for the previous scenario, the program now must recognize Yield signs and determine how many lanes are in the roads. The lane count is used to determine if the robot is on a "Minor Road"—that is, if the robot's

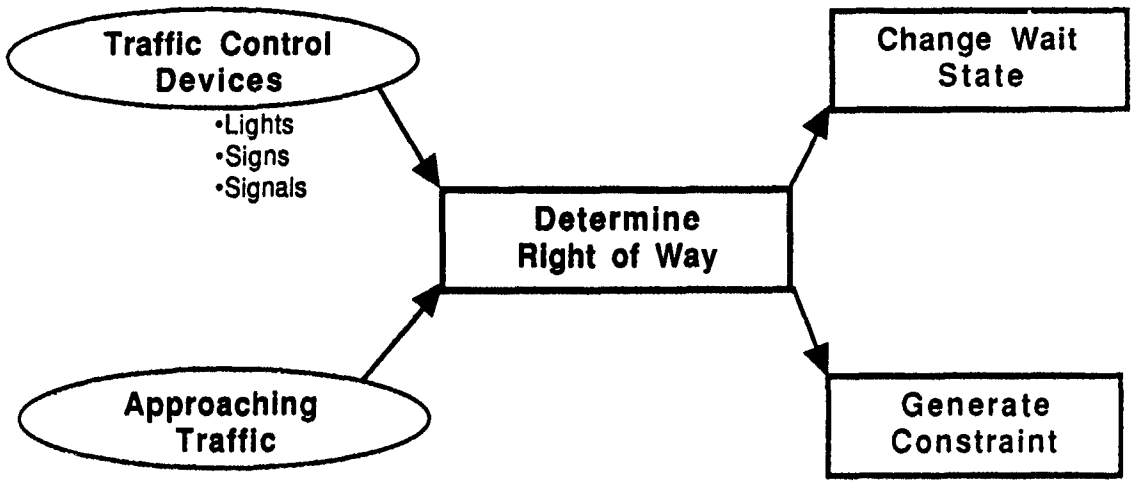

Figure 4.15: Generation of constraints from traffic and traffic control.

road has only one or two lanes and the other road has more lanes. In the United States traffic on a Minor Road generally yields the RoW to other traffic, so in effect has a yield sign. This is a practical rule, not a legal one.

Table 4.3 summarizes the meanings of the various TCD's. The figure groups the TCD's into four equivalence classes. Yellow signals are treated as either red or green, depending on the robot's state and speed. If the robot is in a "wait for gap" state, a yellow signal is always treated as green. This practical rule allows the robot to proceed through an intersection just before the signal turns red. This allowance prevents the robot from being stuck forever in heavy traffic with no gaps. Cars with a given TCD normally yield the RoW to traffic with a TCD in a higher priority class, as will be explained below. Note that some actions in the figure do not depend on other cars; for example, red lights always stop the robot.

Approaching traffic. The second part of RoW evaluation is analyzing the robot's situation relative to other cars. This situation depends on the position and speed of the robot and other cars, and the relative position of the approach roads. Figure 4.16 shows how this information is combined with traffic control information to decide the RoW with respect to each car. For each approach, Ulysses looks up the road to find the first car in each lane. The road to the right is ignored if the robot is turning right, as is the directly opposing road unless the robot or approaching car are turning left. Looking "up the road" essentially requires the perception system to find a corridor along a different road. If the perception system does not find a car, Ulysses makes RoW decisions as if there were a car at the range limit of the sensors or of sight distance. This hypothetical car is assumed to be going a little faster than the prevailing speed of traffic. If the approaching car is going too fast to stop before the intersection (assuming a nominal braking rate), Ulysses always yields the RoW. On the other hand, if the car is very far away from the intersection, Ulysses will ignore it. "Very far away" means that the time it will take the robot to cross the intersection at its current acceleration rate is less than the time it will take for the other car to reach the intersection.

If none of the above conditions exist, then Ulysses further analyzes RoW based on traffic control devices and the movements of the other cars. First, Ulysses guesses the traffic control for the approaching car. To do this, the perception system must look at the side of the approach road for a sign (the back side of a sign). If there is no sign, and the robot is facing a traffic light, Ulysses assumes that the approaching car also has a traffic light. If the car is

Traffic Control	Action
Green signal OR Nothing	Use RoW rules (see Figure 3-15)
Yield sign, OR Nothing and on Minor Rd	Yield to traffic with Green or no traffic control; otherwise use RoW rules (see Figure 3-15).
Stop sign, OR turning right at Red signal when allowed.	Stop at intersection; then proceed using RoW rules (see Figure 3-15)
Red signal	Stop at intersection
Yellow signal	IF Wait-state is "normal" AND robot can stop at intersection THEN treat as Red signal ELSE treat as Green signal.

Increasing priority

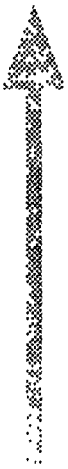

Table 4.3: Actions required by four classes of Traffic Control Devices.

approaching from a cross street, the light is assumed to be red (when the robot's is green), and otherwise green.[2] Once the program has an estimate of the approach car's traffic control, it compares the control to that facing the robot. If they are not equivalent, then the vehicle with the lowest priority signal is expected to yield the RoW.

If the traffic control for the approaching car and the robot are equivalent, Ulysses performs further analysis of the situation. If the approaching car is close to the intersection and stopped, the program assumes that it is waiting for a gap in traffic. In the case of a Stop sign, the robot takes the RoW if the approaching car is not yet waiting. Otherwise, if one or both vehicles are moving, then the robot yields the RoW to cars on the right, and to cars ahead when the robot is turning left. If both the robot and the approaching car are stopped and waiting for a gap, then the drivers must use some deadlock resolution scheme to decide who goes first. In human drivers we have identified four such schemes, as illustrated in Figure 4.17. Humans use different schemes, depending on the local custom and the driver. Ulysses bases its decision only on road configuration; it will use the first-arrive, first-leave technique as well when we better understand how to recognize the same cars in images taken at different times.

After determining the requirements of the traffic control devices and evaluating the traffic situation, Ulysses may

[2]This is a particularly clear example of how the explicit, computational rules in Ulysses elucidate the information requirements of driving. Drivers must make assumptions about the TCD's controlling other cars, and sometimes make errors if their assumptions are wrong

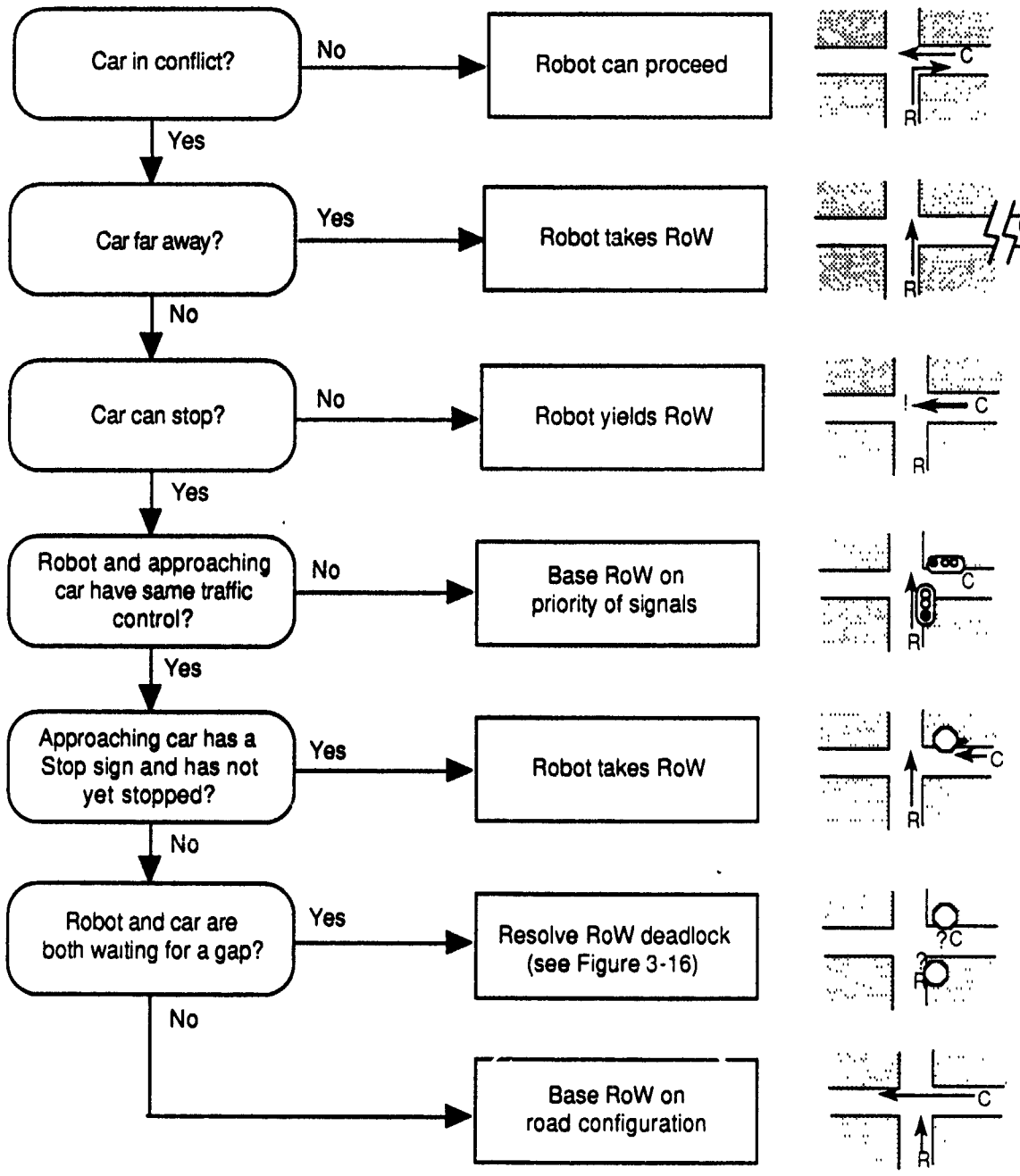

Figure 4.16: Right of Way decision process.
'R' is the robot, 'C' is the other car.

create an acceleration constraint and update the wait state. Figure 4.18 shows the conditions for changing states and for constraining the robot to stop at the intersection. Note that once the program has decided to accept a gap and take RoW, only the presence of new cars in the robot's path will cause it to stop again.

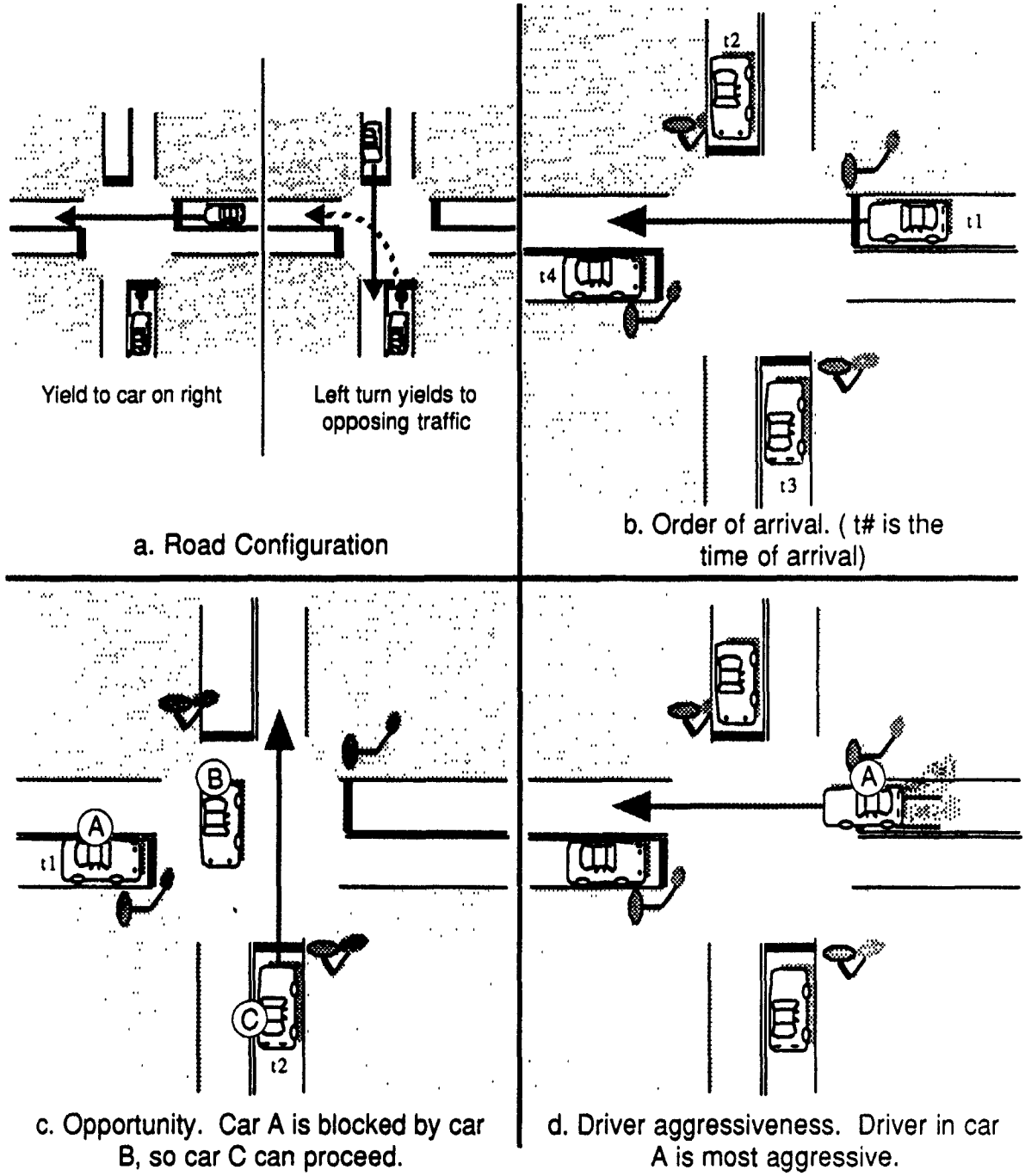

Figure 4.17: Right of Way deadlock resolution schemes.

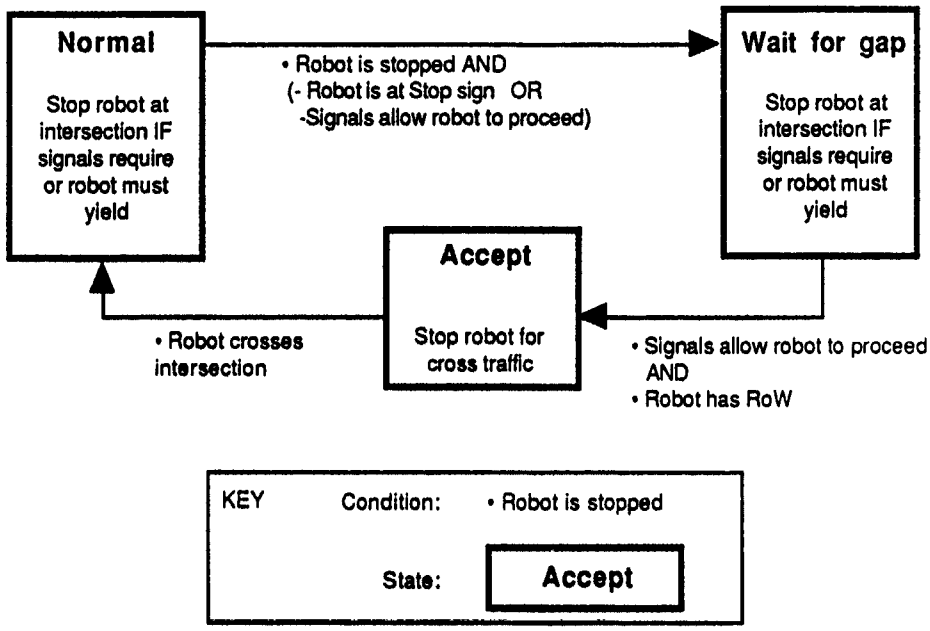

Figure 4.18: Changes in the Wait state at an intersection.

4.3.1.4 A Multi-lane Intersection Approach

The driving situations considered so far have not included streets with multiple lanes. With this complication, Ulysses must generate lane use constraints and make lane selections. We first consider the simple case of multiple lanes at an intersection, as depicted in Figure 4.19. In this scenario there is no other traffic on the same road as the robot.

As the robot approaches an intersection, constraints on turn maneuvers from different lanes—which we generally refer to as lane *channelization*— determine the lane-changing actions that Ulysses can take. Ulysses determines if the channelization of the robot's current lane is appropriate, and looks for a better lane if it is not. Channelization is estimated first by finding the position of the current lane at the intersection. If it is the left-most lane, then the program assumes that a left turn is allowed from the lane; similarly with right turns if it is the right-most lane. Through maneuvers are allowed from any lane by default. Ulysses also looks for signs and road markings to modify its assumptions about channelization.

If the robot's intended maneuver at the intersection is not allowed by the channelization of the robot's current lane, Ulysses generates an acceleration constraint to stop the robot before the intersection. Figure 4.20a illustrates this constraint. Ulysses estimates the minimum distance required to change lanes (from the width of the lanes and the robot's minimum turn radius) and stops the robot that far from the intersection. The program next decides in which direction the robot should move to correct the situation, and looks to see if there is a lane on that side of the robot. If there is a lane, Ulysses constrains the robot to take a lane-change action in that direction. As a practical matter, solid lane lines are ignored, because making a turn from the correct lane is more important than strictly obeying these lane-change restrictions. Since there is only one allowed action, no selection preferences need be considered.

Once a lane-changing action is started, Ulysses makes sure that the robot completes the maneuver before it enters

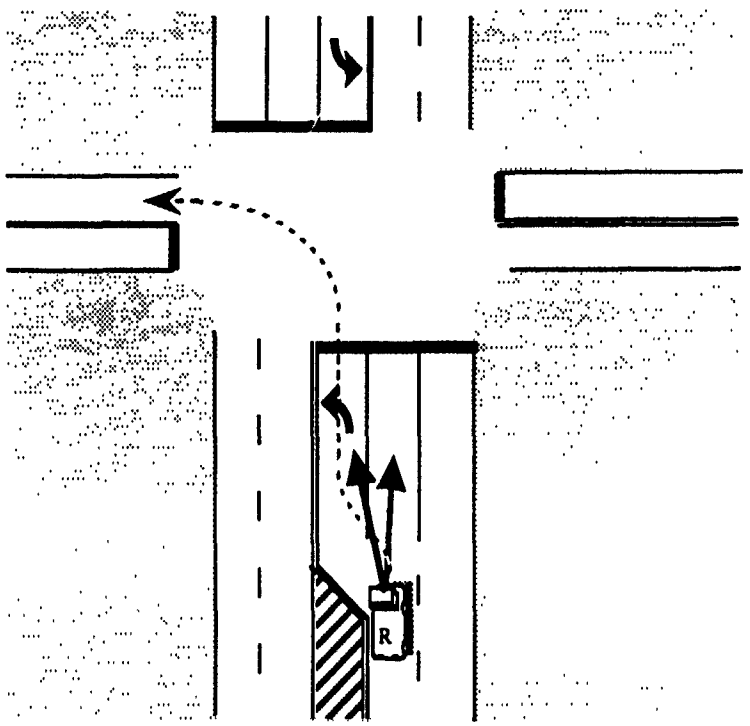

Figure 4.19: Robot observation of lane positions and markings at a multiple lane intersection approach.

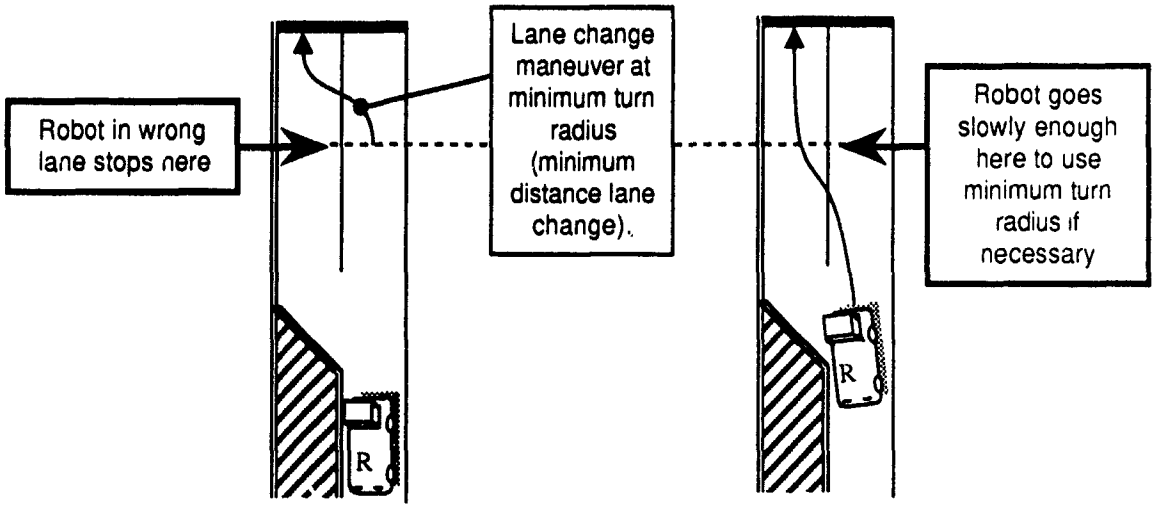

Figure 4.20: Channelization acceleration constraints.

the intersection. The program does this by generating an acceleration constraint that slows the robot to a low speed at the minimum lane changing distance described above. Figure 4.20b shows this constraint. The low speed is set to keep the lateral acceleration on the robot below a certain threshold when turning with minimum radius. The lane-changing constraint is conservative, but our model of operational control does not provide Ulysses with enough information about the lane changing maneuver to predict just when it will be complete (see description of operational level, below). By driving at a speed low enough to use the minimum turn radius while far enough from the intersection, Ulysses guarantees that the maneuver can be completed.

With multiple lanes the driving program recognizes that there may be different signal indications for different lanes. Ulysses looks across the intersection from right to left and attempts to find all of the signal heads. If the robot is turning, Ulysses uses the indication on the head on the side of the turn. Otherwise, Uysses tries to find the head most nearly over the robot's lane.

When Ulysses decides to initiate a lane change, it sets a Lane Position state variable to Init-Left or Init-Right appropriately. Figure 4.21 shows these state transitions. The program does not consider lane selection in future

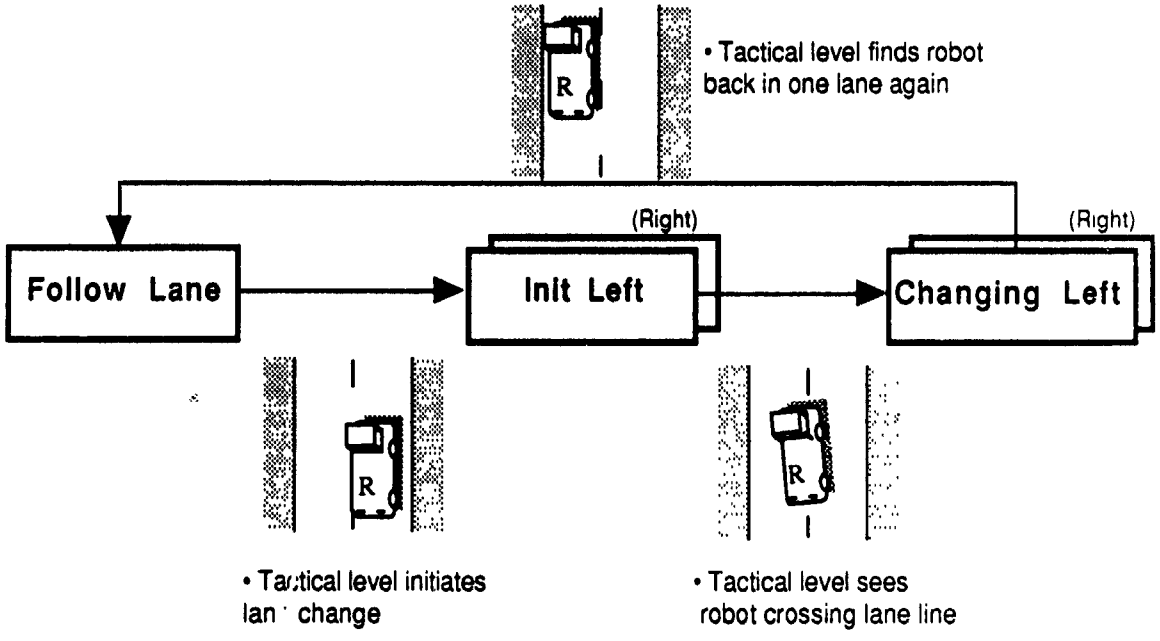

Figure 4.21: State changes during lane changing.

decision cycles while in one of these states. This state variable also helps to guide the perception functions when the robot is between lanes. Once a lane change is initiated, the operational control subsystem moves the vehicle to the new lane without further direction from the tactical level. When the robot is straddling a lane line, the state changes to Changing Left (Right). When tactical perception no longer sees the robot between lanes, the state reverts to Follow Lane.

4.3.1.5 A Multi-lane Road with Traffic

The next scenario is a highway far from an intersection. Unlike the first scenario above, this one is complicated by multiple lanes. Figure 4.22 shows some of the new considerations involved. First, a lane may end even without an intersection. Ulysses detects this in much the same way as it detects a complete road end, and creates an

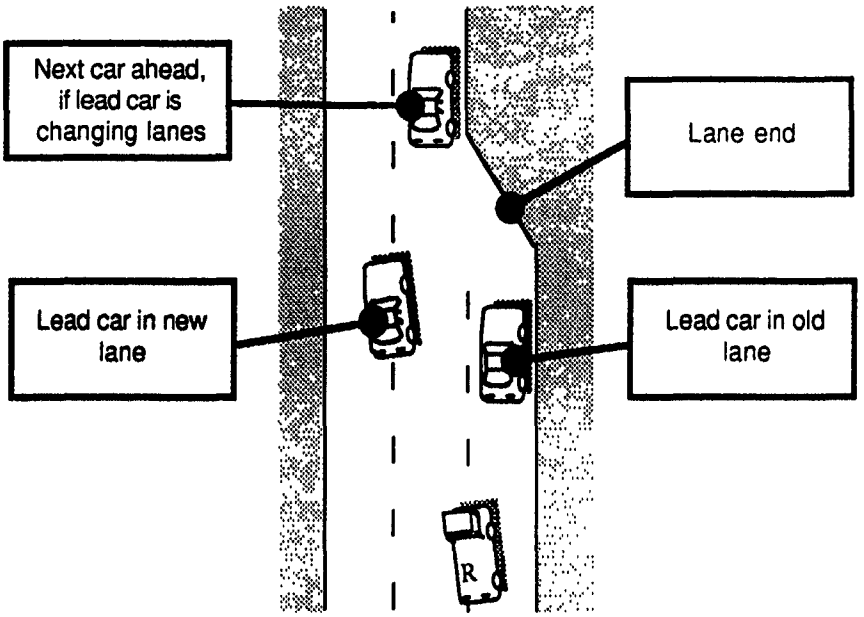

Figure 4.22: Multiple lane highway scenario.

acceleration constraint to stop the robot before the end of the lane. This constraint disappears after the robot changes lanes. Multiple lanes also make car following more complex. If the car in front of the robot is between two lanes, Ulysses maintains a safe headway to that car but also looks for another car in the lane. If the robot is itself changing lanes, the program looks ahead for cars in both lanes until the robot has cleared the old lane.

The three lane actions available to the robot are following the current lane, moving to the right, or moving to the left. Moving to the left does not currently include moving into the opposing lanes; thus Ulysses cannot yet overtake when there is only a single lane in each direction. Ulysses generates contraints and preferences for changing lanes if certain traffic conditions exist. Figure 4.23 shows the important conditions: adjacent lanes, gaps in traffic in adjacent lanes, blocking traffic in the robot's lane and blocking traffic in adjacent lanes. In this scenario, the program does not need to consider channelization.

Table 4.4 shows the constraints and preferences for each traffic condition. The absence of adjacent lanes or broken lane lines or gaps in traffic eliminates the option to move to adjacent lanes. Ulysses generally prefers the rightmost lane to others. Traffic *blocks* the robot if the acceleration allowed by car following is significantly less than acceleration allowed by other constraints. Blocking traffic creates a preference for an adjacent lane if the acceleration constraint in that lane is significantly higher than the car following constraint in the current lane. Ulysses estimates the allowed acceleration in the adjacent lane by hypothesizing what the car following constraint would be and combining this with the speed limit, lateral acceleration and road end constraints. The program combines the constraints from various conditions by taking their logical intersection—retaining only actions that appear in all constraints. If there is more than one lane action available after constraints have been combined, preferences determine which action is chosen. Preferences due to blocking traffic are given priority over the rightmost lane preference.

Ulysses judges gaps for changing lanes based on two criteria: first, the deceleration required of the robot to create a safe headway to the lead car in the other lane; and second, the deceleration required of the following car to leave space for the robot. The program does not search for a gap farther back in traffic if the adjacent one is not big

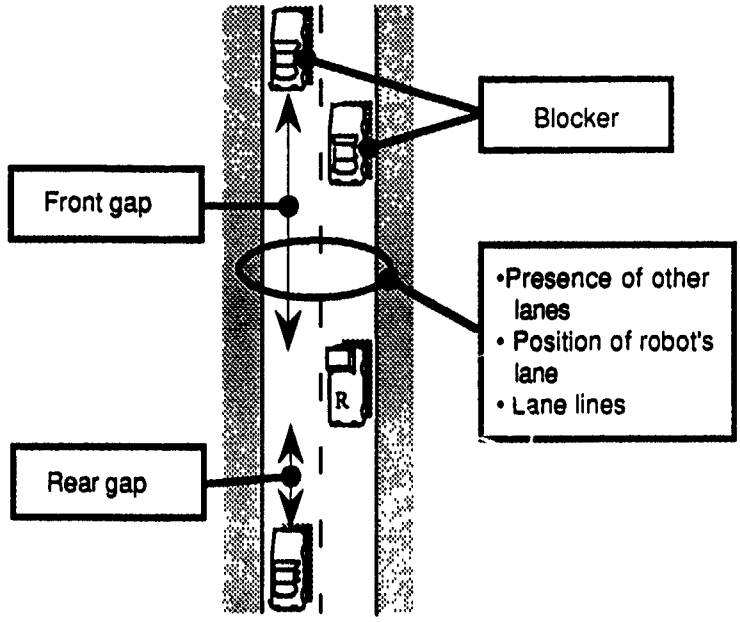

Figure 4.23: Traffic objects that affect lane changing decisions.

enough. However, if the robot is blocked, traffic in the adjacent lane will tend to pass the robot, thereby providing new merging opportunities. Ulysses also does not have the ability to use a physical "language" (beyond directional signals) to communicate to other drivers that it is anxious to change lanes. It is thus possible that the robot will never find a gap if traffic is congested.

4.3.1.6 Traffic on Multi-lane Intersection Approach

The next scenario combines the previous two multi-lane cases. This situation, illustrated in Figure 4.24, adds channelization constraints to traffic considerations. When the adjacent lane does not permit the robot's next turn, Ulysses must decide whether a pass can or should be made. Similarly, if the robot needs to move to a turn lane that has traffic in it, Ulysses must decide whether to merge immediately or wait. Table 4.5 lists the constraints and preferences that must be added to those in Table 4.4. When combining preferences, Ulysses gives the channelization demands the highest priority unless the robot is far from the intersection.

When the robot is near the intersection ($d < D_{Far}$ in Table 4.5), it is not allowed to change lanes to move away from an acceptable ("OK") lane. Thus Ulysses will not attempt to pass a blocking car near an intersection unless multiple lanes are acceptable. This restriction may cause the robot to get stuck behind a parked vehicle, but it avoids the problem of deciding whether the lead vehicle is really blocking the road or just joining a queue that extends all the way to the intersection.

The "Far from intersection" ($d > D_{Far}$) condition in Table 4.5 depends on a distance threshold D_{Far}. When the intersection is at least D_{Far} away from the robot, Ulysses can pass blockers rather than staying in a turn lane. The threshold distance is properly a function of traffic—how far traffic is backing up from the intersection, whether there are gaps in the traffic ahead of the blocker, and how long (distance) the robot would take to complete a pass. Ulysses determines D_{Far} by estimating passing distance and adding a margin to cover the other conditions. The margin is a function of the speed limit, but does not explicitly incorporate downstream queuing conditions. In our simulated world we have found that the margin needed to minimize inappropriate passing maneuvers puts the robot

CONDITION		SET OF ALLOWED ACTIONS	PREFERRED ACTION
Blocking car (Robot blocked by traffic in lane*)	• $L - C > T_1$ Broken lane line	All	Move Left
	• $R - C > T_1$ Broken lane line	All	Move Right
	• $C > R, L$	All	Keep Same
Gap for merging			
•No gap in traffic to left		(Move Right, Keep Same)	—
•No gap in traffic to right		(Move Left, Keep Same)	—
Available lanes			
•There is no lane to the left		(Move Right, Keep Same)	—
•There is no lane to the right		(Move Left, Keep Same)	—
•(There is a lane to the right) AND ($R \geq C$)		All	Move Right
Default		All	Keep Same

Increasing Priority

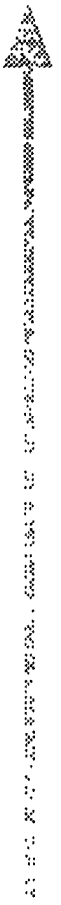

KEY		
	*:	True when (Car following accel) < (Other accel constraints) - T_2
	T_i:	Arbitrary threshold value.
	L, R, C:	Max. acceleration allowed in the lane to the Left, lane to the Right, and Current lane, respectively

Table 4.4: Lane action preferences for a highway with traffic.

in the "near intersection" condition soon after it detects the intersection.

The presence of traffic introduces additional factors into the tests of blocking conditions. When Ulysses determines what acceleration is possible for the robot in an adjacent lane, it must consider constraints from lane channelization and intersection traffic control. In effect, Ulysses must hypothesize the robot in the adjacent lane, look ahead in a new corridor, and recompute all of the acceleration constraints from that lane.

When the robot wishes to change lanes because of channelization, but cannot because that lane change action is not allowed (for example, because a gap in traffic is not available), Ulysses changes the robot's Wait state to "wait

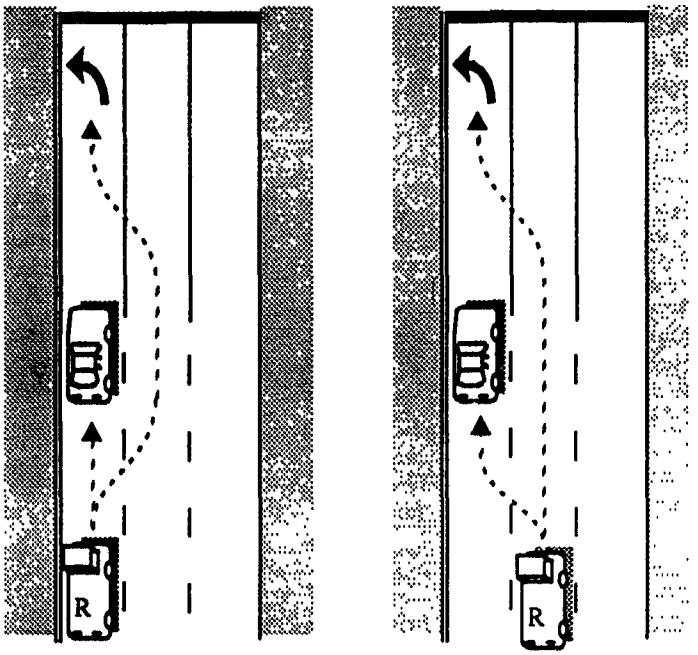

Figure 4.24: Decisions at a multiple lane intersection approach with traffic.

for merge gap." This action signals a standing desire to change lanes. When the robot is in this state, Ulysses adjusts the calculation of the car-following constraint so that extra space is left in front of the robot for maneuvering.

4.3.1.7 Closely spaced intersections

The final complication comes with multiple intersections spaced closely enough together that they all affect the robot. Figure 4.25 depicts multiple intersections ahead of the robot and on cross streets. The driving knowledge already described is sufficient to get the robot through such a situation. This scenario illustrates, though, the necessity of tracing a corridor ahead through multiple intersections, analyzing traffic and traffic control at every intersection along the corridor, and looking through intersections on cross streets for approaching cars.

4.3.2 Tactical Perception

Tactical driving decisions require information about roads, intersections, lanes, paths through intersections, lane lines, road markings, signs, signals, and cars. Our driving model assumes that the robot has a perception subsystem that can detect these traffic objects and determine their location and velocity. In addition, the perception system must estimate the distance to objects, the distance between objects, and the velocity of cars. There is more perception at the operational and strategic levels, but we do not address it in this model.

Tactical driving requires information about spatial relations between objects. When Ulysses looks for an object, it is really interested in objects that have a specific relation to another object. Figure 4.26 illustrates this concept. In the figure, Ulysses is at a point in its analysis where it is looking for *cars* on the *right-hand approach road* at the *second intersection* ahead. There are at least two ways to find the objects in the desired relations. One way would be to detect all cars, and then test each car to see if it was on the road to the right at the intersection. "The road to the right" would itself be found by finding all roads and checking to see if they connected to the the robot's road at the intersection in question. This method would be very difficult because there may be many cars and roads in the robot's field of view, and each one requires significant computation to find and test.

CONDITION		SET OF ALLOWED ACTIONS	PREFERRED ACTION	PRIORITY
Channelization				
• $d < D_{Min}$		Keep Same	—	Highest
• $D_{Min} < d < D_{Far}$	Current lane OK	(Keep Same, Move to <OK lane>)	—	
	Current lane not OK	(Keep Same, Move to <OK lane>)	Move to <OK Lane>	
• $d > D_{Far}$		All	Move to <OK Lane>	Just below **Blocking Car** in Table 3-3
• No intersection visible		All	—	—

KEY		
	d:	Distance from robot to intersection
	D_{Min}:	Minimum distance needed to change lanes.
	D_{Far}:	Range of influence of intersection on upstream traffic
	OK:	Channelization allows robot's intended route

Table 4.5: Lane action constraints and preferences at an intersection with traffic.

Ulysses uses a different technique to relate objects to one another. The perception subsystem uses the reference object and a relation to focus its search for a new object. In the example above the robot would track the corridor ahead to the second intersection, scan to the right to find the approach road, and then look along the road for a car. The car detection process is thus limited to a specific portion of the field of view, determined by the location of the road. All objects found are identified implicitly by their current relation to the robot. (This object identification method has been called "indexical registration" by Agre and Chapman [2].) Ulysses gathers almost all of its data using these *perceptual routines*. Table 4.6 lists the perceptual routines used by the program. Although it may seem that driving decisions could be made with simpler, more general sensing functions, Figure 4.26 shows that very simple sensing is not sufficient; "detect converging objects to the right," for example, cannot distinguish between the two intersections.

The perception subsystem uses *markers* to provide reference points for the perceptual routines. Our simple model of sensing currently assumes that one image—a snapshot picture of the world—is taken each time Ulysses repeats its decisions. Markers are placed in an image as a result of running perceptual routines that can mark cars, lane endings or beginnings, signs, markings, signal heads, or other locations. The markers are essentially names that different perceptual requests can use for the objects in an image. In the example of Figure 4.26, various routines would put markers in the corridor where it enters and leaves intersections. When Ulysses analyzed the second intersection, a routine would mark the approach roads. Finally, when Ulysses had to look for the approaching car at that intersection, it would start a car detection routine and provide the marker for the approach road on the right.

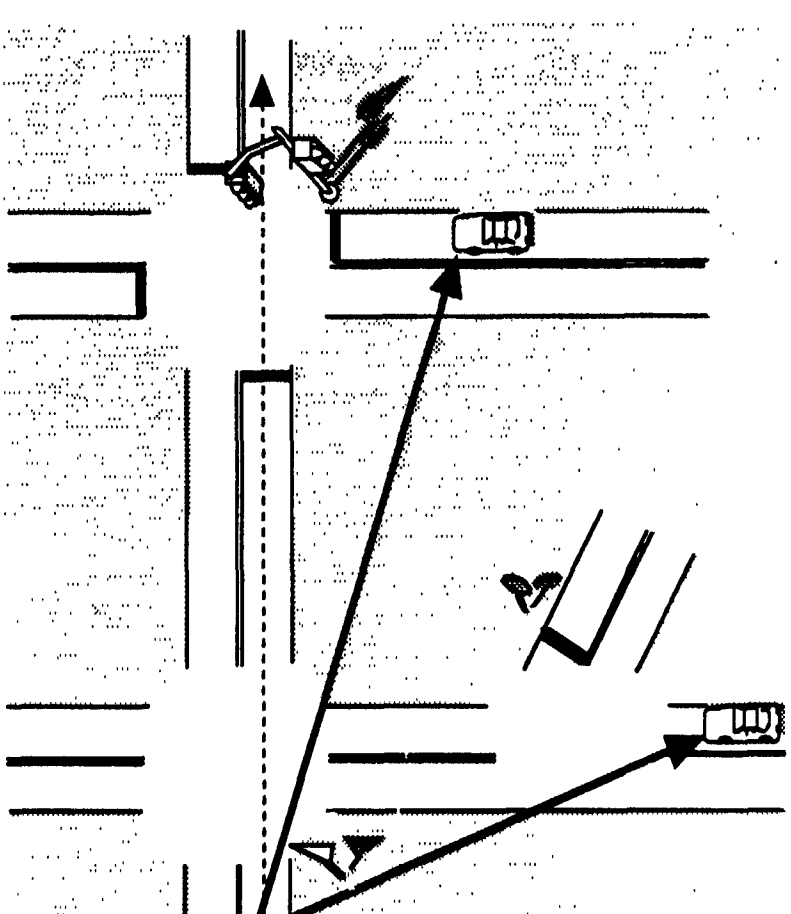

Figure 4.25: Visual search through multiple intersections

Even using the routines described above, perception remains very difficult for a robot. Tactical perception in Ulysses is a focus of our ongoing research.

4.3.3 Other Levels

4.3.3.1 Strategic Level

The strategic level of our model is very simple and serves only to provide a route plan to the tactical level. Figure 4.2 shows that perception at the strategic level looks for landmarks that mark the progress of the robot along the route. Ulysses currently assumes that the route at every intersection is provided by some map-based planner, and therefore uses only intersections as landmarks. A more sophisticated route maintainer would use street signs, road configurations, buildings, etc. to locate the robot in the map.

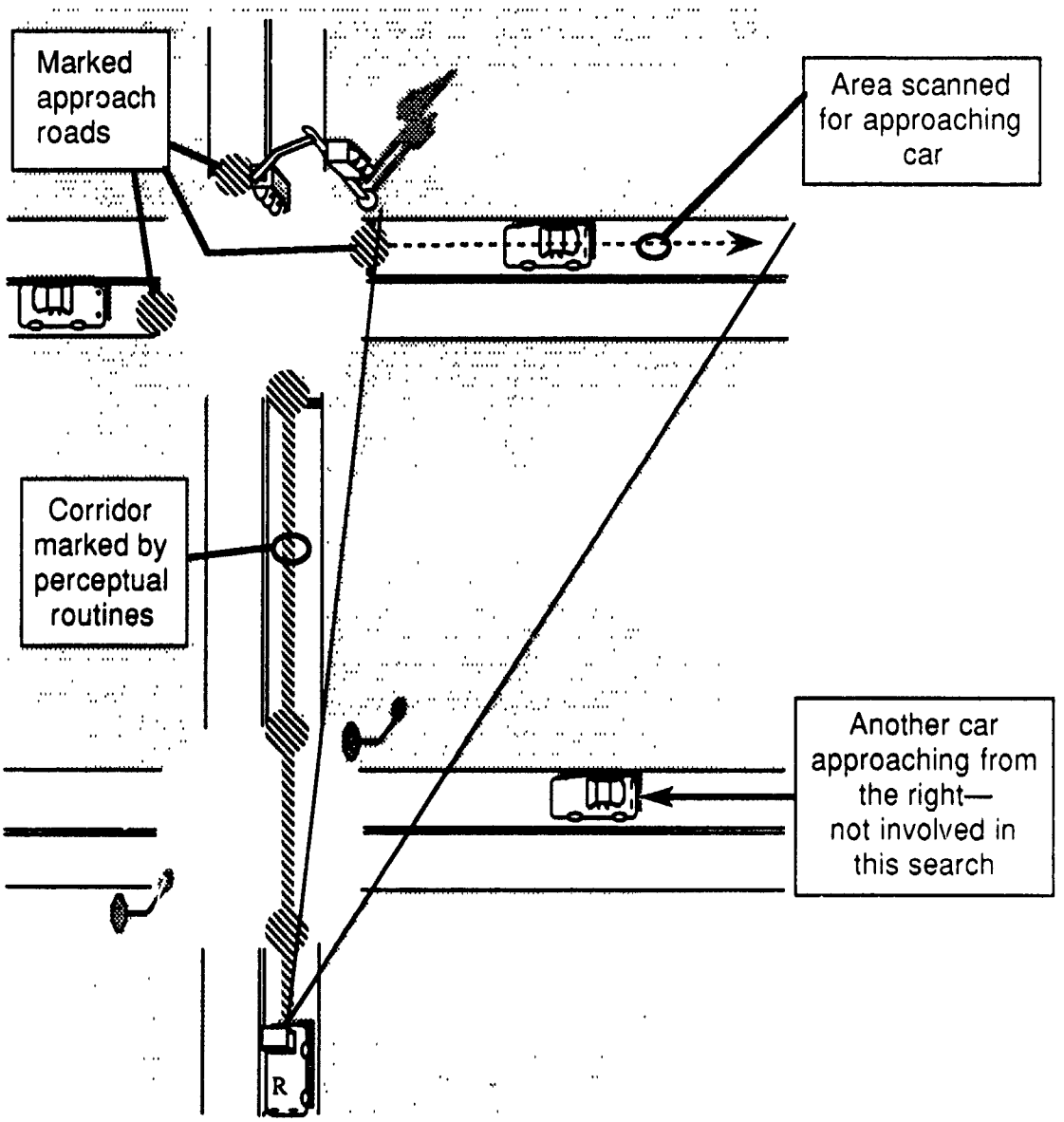

Figure 4.26: Searching for a car approaching a downstream intersection from the right.

4.3.3.2 Operational Level

The operational level makes emergency reactions and executes commands passed down from the tactical level. The operational level is assumed to have its own perception functions to detect emergencies and provide feedback to the actuator controllers. Emergency reactions include avoiding collisions with nearby objects and keeping the wheels away from road hazards. These are considered emergencies because the tactical level is responsible for finding problems in the distance. The tactical model uses four operational functions to execute the commands it generates. These functions are maintaining an acceleration, tracking a lane, changing lanes, and traversing an intersection.

Acceleration. The operational level keeps the vehicle's acceleration at the value commanded by the tactical level.

Find current lane	Find path in intersection
Profile road	Find next car in intersection
Mark adjacent lane	Find intersection roads
Track lane	Find signal
Find next lane mark	Find back-facing signs
FInd next sign	Find crossing cars
Find next car	Distance between marks

Table 4.6: Perceptual routines in Ulysses.

Speed control is not used because an instantaneous change in speed requires an infinite impulse of force, while a change in acceleration requires only a step change in force. Vehicle dynamics dictate that an operational controller is more likely to achieve the latter. The choice of control variables is not crucial to the model. However, we expect that it might be difficult in some robot implementations to provide frequent command updates at the tactical level, so acceleration commands would prove to be more convenient.

Lane Tracking. The operational level is assumed to be able to drive the robot down a lane without intervention from the tactical level. This function involves only steering, as do lane changing and intersection traversal. As described earlier, the tactical level adjusts the speed independently to keep lateral accelerations within limits on turns.

Lane Changing. Lane changing requires the operational level to detect the adjacent lane and begin a double-curve maneuver to move the robot over. When the robot reaches the new lane, lane tracking automatically takes over. At most speeds, the steering angle is adjusted to limit the robot's lateral acceleration to a safe value. This constraint results in a lane change maneuver that takes a roughly constant amount of time, independent of speed. The tactical level can use this fact to estimate the length of a lane change. However, if the robot is changing speeds (e.g., braking while approaching an intersection), it is impossible to predict exactly how far the robot will travel during the maneuver. At low speeds, robot can only increase the steering angle to the physical stops of the vehicle. This angle determines the minimum lane change distance for a given road width.

Intersection Traversal. Since intersections generally do not have marked lanes, the operational system is required to find a path to the given departure lane and drive the robot along the path. As with the other operational functions, there are several ways this may be accomplished. We expect that the robot would follow an imaginary path created from general knowledge about the size of the intersection, and then start up lane tracking when the new lane became clearly visible.

4.3.4 Summary

Ulysses is a computational model of driving implemented as a computer program. It emphasizes the tactical level. Strategic functions are limited to providing a route plan step at every intersection. The operational level abstractly implements tactical commands.

Ulysses can drive the robot in traffic on multi-lane roads, through intersections, or both. Driving knowledge is encoded as constraints and preferences. Ulysses looks for lane endings, curves, speed limit signs, and other cars to constrain the robot's acceleration on a road. When approaching an intersection, the program directs the perception subsystem to look for signs, signals, markings, other roads, and approaching traffic as well as the general road features just mentioned. Ulysses determines the semantics of the traffic control devices and the road configuration and decides whether the robot has the right of way to enter the intersection. Stop signs and conflicting traffic cause the robot stop and then enter a waiting state until traffic clears or the signal changes. The program also evaluates lane channelization, potential speed increases in adjacent lanes, traffic in adjacent lanes, and lane position to decide whether the robot should change lanes. Additional acceleration constraints prevent the robot from approaching the intersection in the wrong lane or in the middle of changing lanes.

Ulysses uses demand-driven perception. The robot looks at the world frequently so that it can respond quickly to changing traffic situations. The model uses perceptual routines and visual markers to find traffic objects with the appropriate spatial relationships to the robot.

4.4 The PHAROS Traffic Simulator

Our motivation for creating a driving model was to describe how to drive an autonomous vehicle. Actually driving a vehicle requires that the driving model be made concrete. The model must specify how all knowledge is encoded and how information is processed. In the preceding section we described how this is done in our model. However, the proof of the pudding is in the eating— descriptions cannot drive real vehicles. Our first step toward using our model on a real robot has been to implement the model in a computer program, Ulysses, and drive a simulated robot in a simulated traffic environment. PHAROS is the traffic simulator we developed for this work.

There are several advantages to driving in simulation before trying to drive an actual vehicle. First, a simulator is flexible. It is possible to generate almost any traffic situation to test various kinds of driving knowledge. These situations can be recreated at will to observe how new driving knowledge changes a vehicle's behavior. Simulators are also convenient, because simulated driving is not dependent on working vehicle hardware, convenient test sites, or weather. Finally, simulated driving is safe and avoids the problem of placing other drivers at risk while testing the robot.

Figure 4.27 shows how PHAROS and Ulysses work together. PHAROS maintains a database describing the street environment and records for each car. PHAROS also controls the behavior of the simulated cars, which we call *zombies*. The simulator executes a decision procedure for each zombie to determine its actions, and then moves it along the street. A robot is simulated by replacing the decision procedure with an interface to Ulysses. Ulysses runs as a separate program—sometimes on a different computer—and gets perceptual information by sending requests to PHAROS. The interface simulates the perceptual routines described earlier. After Ulysses has the information it needs, it sends commands through the interface to the vehicle record. PHAROS then moves the robot using the normal movement routine. The requests for (simulated) perception and the commands for (simulated) control are the *only* communications between Ulysses and PHAROS. This arrangement ensures that Ulysses cannot "cheat" by examining the internal state of the simulator.

The remainder of this section discusses the representation of the street environment, the driving decisions made

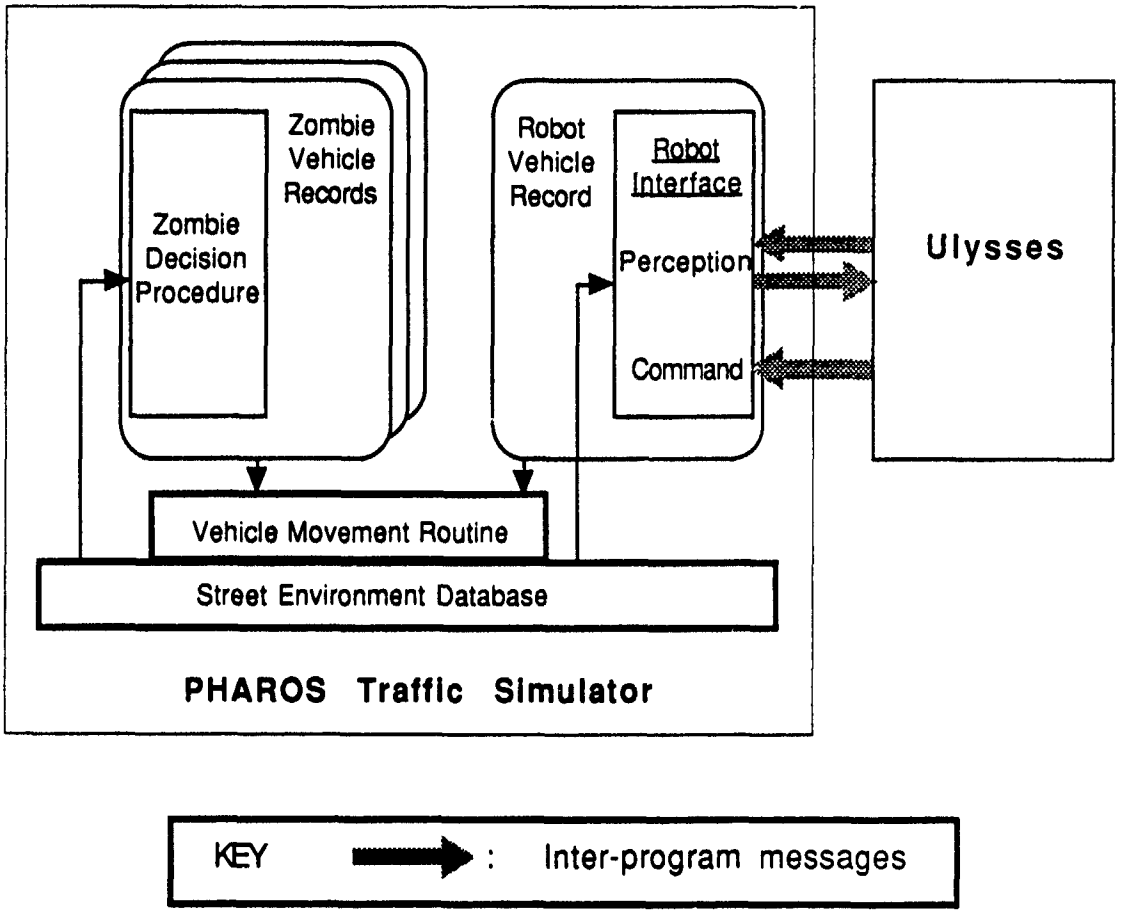

Figure 4.27: Ulysses control of a vehicle in PHAROS.

by the zombies, and the general operation of the simulator.

4.4.1 The Street Environment

PHAROS is a model of the street environment. All models of the world use abstractions so they can capture just the important characteristics of a problem. Model designers must find a compromise between model accuracy and excess complexity. We have attempted to encode many characteristics of the street domain into PHAROS, including enough geometric information to study the perceptual requirements of driving. While PHAROS includes many traffic objects, it uses strong abstraction and structure to simplify their description and use.

PHAROS represents traffic objects with abstract symbols augmented by a few parameters to provide important details. Figure 4.28 illustrates how some objects are encoded. A curved road segment is described by a cubic spline (8 parameters) and a road width. A sign is represented by a type (one of 8), an identifying number, and a position along the road. The general shape and color of the sign is determined by its general type; the lateral distance from the road edge is assumed to vary only a little, so is not encoded at all. PHAROS describes a signal head by its location at the intersection (one of 5 generic positions), whether it is vertical or horizontal, the number of lenses, the

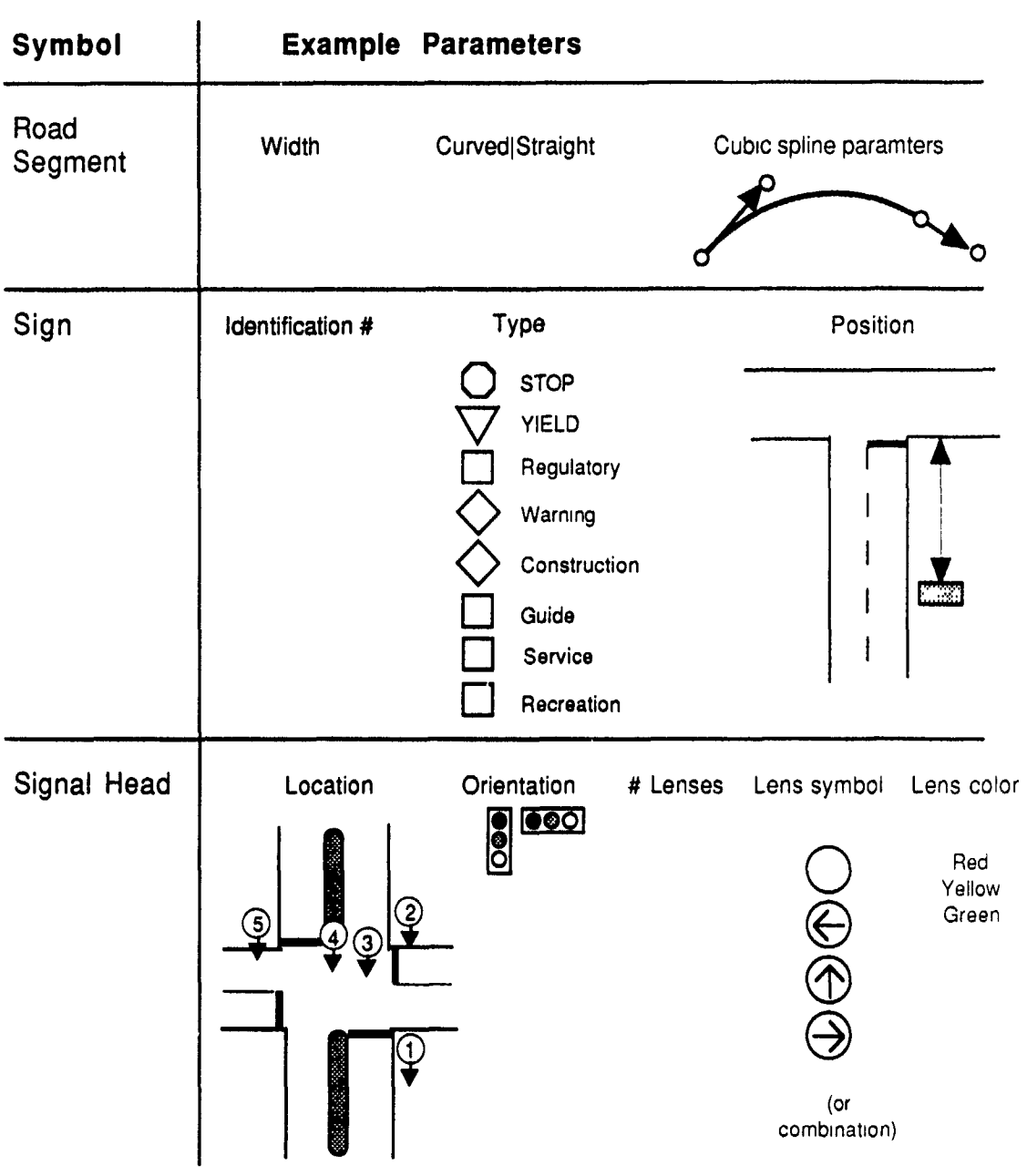

Figure 4.28: Examples of traffic object encodings.

symbols on the lenses, and the color of the lenses.

PHAROS groups traffic object symbols into structures to give them meaning for driving. It would be difficult to determine how streets connected or whether a car could move to an adjacent lane if the lane and line objects in the database were not organized. PHAROS connects objects to one another to form hierarchies and networks of related objects. Figure 4.29 shows how different street objects are connected to one another.

The abstraction and structure used in PHAROS limit the accuracy with which it can simulate the world. For example, PHAROS cannot easily simulate roads without marked lanes. PHAROS vehicles cannot abandon the lane

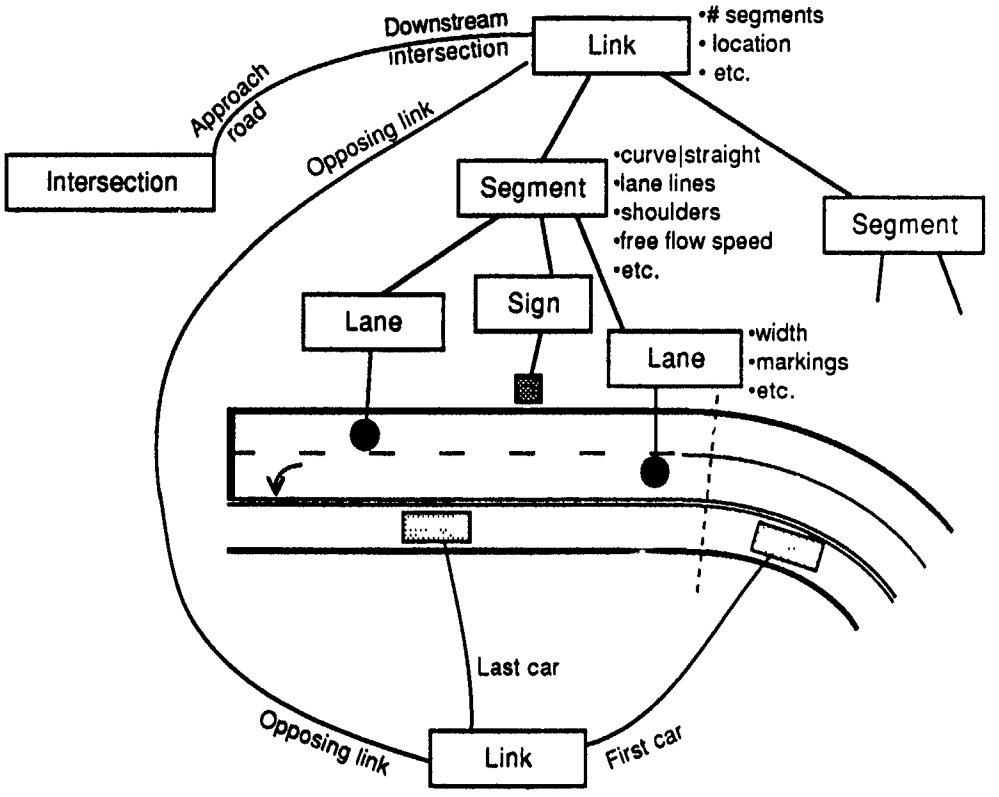

Figure 4.29: Structure of street objects.

abstraction to drive around a broken down vehicle at an intersection. However, our representation scheme does allow PHAROS to simulate many common traffic situations on highways and arterial streets. We also feel that the scheme could be extended to deal with situations that are beyond the current abstraction. Similarly, there are several types of traffic objects missing from PHAROS' world—pedestrians, cyclists, blinking signals, etc. Future versions of PHAROS may include such objects.

4.4.2 PHAROS Driving Model

The driving decisions made by the zombies are based on the logic in the Ulysses driving model. However, there are several differences between Ulysses and the PHAROS-controlled zombies. The key differences are in perception, interpretation, and speed control.

Perception. Zombies are not required to use simulated perception to get information from the simulated world. When PHAROS is running the decision procedure for the zombies, it uses the data structures directly. For example, to find a vehicle across the intersection from a zombie, PHAROS traces symbolic links from the zombie to its road, to the connecting road ahead, and to the rearmost car on that road. Tracing these pointers in the data structures is similar in concept to running perceptual routines, but much simpler in practice.

Interpretation. Several traffic situations that Ulysses encounters are difficult to interpret. Some situations, such as determining the traffic signal for other approaches or the intended turn maneuver of another car, are problematical for Ulysses because they cannot be observed directly. This type of problem is simple for PHAROS, because

zombies have access to the entire database and are not limited by what they can see. This access extends even to examining the internal state of other zombies. Other situations, such as deciding which signal head applies to the robot's lane, require several observations followed by a reasoned guess. Some situations are complex enough that we cannot yet describe how to recognize them. For example, we stated earlier that Ulysses cannot tell whether a blocking car in front of the robot is really broken down or merely part of a queue that extends to the intersection.

PHAROS shortcuts these difficult interpretation problems by encoding the semantics of situations directly into the database. For example, the traffic control for each lane is provided as part of the input data for the simulation and is stored with the other characteristics of the street. Lane channelization is also provided externally and stored. Zombies determine if the car in front of them is in a queue simply by checking that car's "Queue" status; a zombie sets its own status to "enqueued" if it is close to the car in front and the car in front is already in a queue. The direct encoding of interpreted information, as well as the availability of physically unobservable state information, allows PHAROS to move zombies realistically without the complete expertise of a human driver.

Speed control. PHAROS drivers are allowed perfect perception and access to special information so that they can choose actions as realistically—i.e., with human competence—as possible. However, zombies behave unrealistically if they are allowed to control speed too well. Therefore, PHAROS incorporates a reaction delay into zombie speed control. When zombies wish to decelerate quickly, they must switch to a braking "pedal" (state), and when they wish to accelerate again they must switch to an accelerator "pedal." There is a delay of 0.8 s, on average, in switching between pedals. This imposed reaction delay, when combined with the car-following law already discussed, results in fairly realistic behavior during car following, free-flow to car following transitions, free-flow to enqueued transitions, and queue discharge.

4.4.3 Simulator Features

Input. PHAROS generates a street database from a data file that it reads in at the start of each simulator run. Since PHAROS can represent a lot of detail in a variety of traffic objects, the data file can be fairly complex. The PHAROS user must encode the desired street environment into symbols and numbers and type them into the file. Figure 4.30 shows an example of how one face of a traffic signal head is encoded. The terms "face" and "lens" are

```
face vertical 5 L9 LEFT_MARGIN 0 0
        lens  RED_SIGNAL SC_SOLID 8          1 1 1 1 1 0 0 1
        lens AMBER_SIGNAL SC_SOLID 8         0 0 0 0 0 0 1 0
        lens GREEN_SIGNAL SC_SOLID 8         0 0 0 0 0 1 0 0
        lens AMBER_SIGNAL SC_LEFT_TURN 8     0 0 0 0 1 0 0 0
        lens GREEN_SIGNAL SC_LEFT_TURN 8     0 0 0 1 0 0 0 0
```

Figure 4.30: Example of signal head encoding in PHAROS data file.

---

keywords. The first line indicates that there are 5 lenses on this face of the signal head, that they are arranged vertically, and that the head is located on the left shoulder of the street named "L9." If the head were directly over a lane, the last two numbers on the first line would indicate which lane and where along the lane the head was located. The remaining lines describe each lens. The information includes the color, symbol, and diameter of the lens, and whether the lens is lit in each phase.

Encoding and typing this information is tedious and error-prone for multi-intersection networks. A future version of PHAROS should include a graphical input interface that generates the file automatically from pictorial descriptions.

Time. PHAROS has features of both a discrete time and a discrete event simulator. Some events, such as zombie creation and traffic signal changing, happen at irregular intervals; others, such as updating the positions of vehicles,

occur at regular intervals. PHAROS maintains an event queue that keeps track of both types of events. The position-update events compute the vehicles' new positions exactly from their (constant) accelerations over the preceding time interval.

Display and user interaction. The output of PHAROS is an overhead view of the street environment with an animated display of the vehicles. This graphical output provides us with our primary means of evaluating the behavior of both zombies and robots. Figure 4.31 is a picture of the computer screen while PHAROS is running.

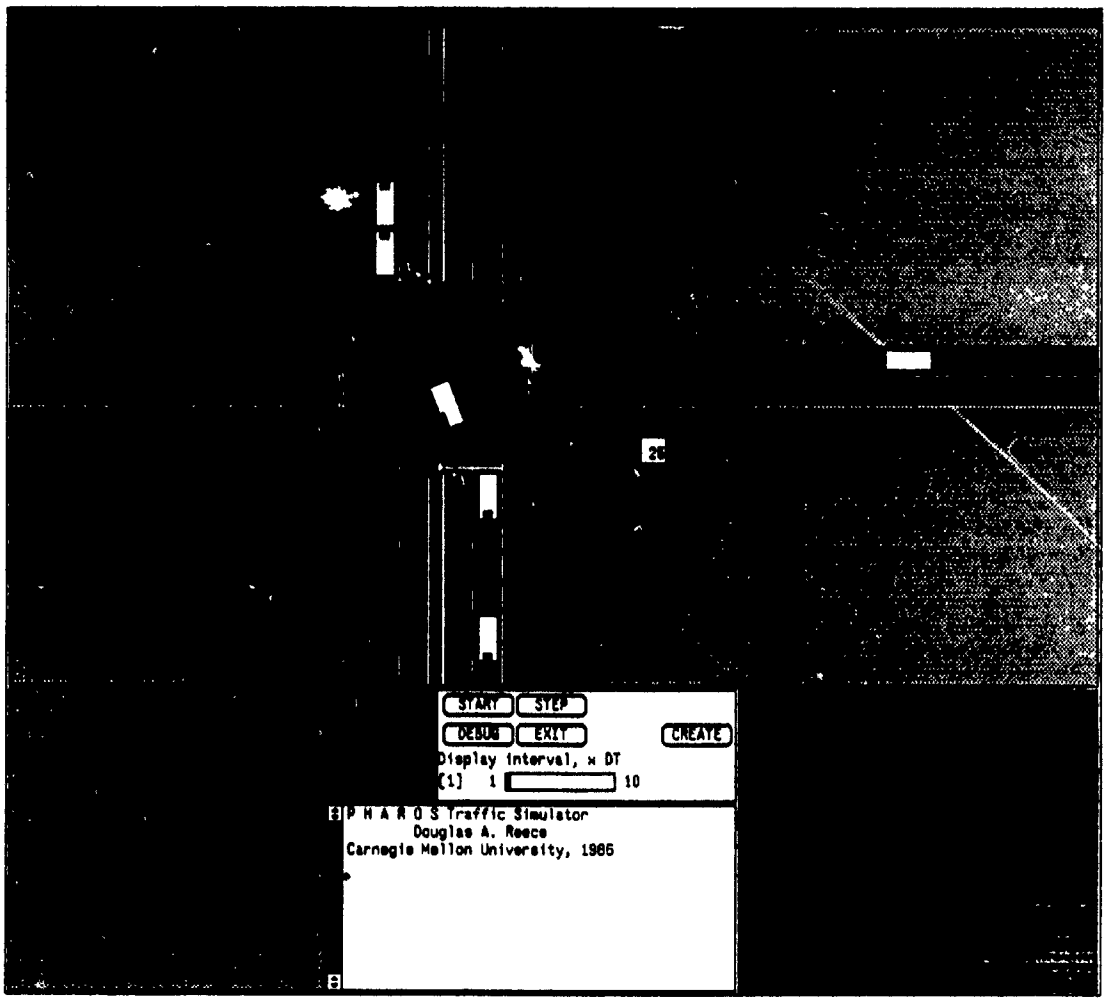

Figure 4.31: The output display of PHAROS.

The figure shows a black-and-white approximation of the computer's high-quality color display. In the lower-left corner is a window showing the entire street network schematically. A portion of the network (enclosed by a small rectangle in the schematic) is drawn at larger scale in the top-center of the screen. Cars are visible as white rectangles, with dark regions at the rear showing brake lights and directional signals. The small window to the right of the network schematic shows simulator time. A user can interactively pan and zoom around the streets to examine various areas in more detail. It is also possible to select individual zombies and trace their decision processes. The simulator can be paused or stepped one decision cycle (100 ms) at a time.

To simulate a robot, a user selects the "button" on the screen marked "create;" PHAROS then pauses and asks where the robot should be injected into the street network. The robot is rendered in a unique color. We have created

various displays to study the activity of Ulysses, including the location of each mark created by the perceptual routines, a count of the number of perceptual requests, and a chart of perceptual activity in each direction.

Performance. The simulator is written in C and runs on a Sun workstation under Sunview. A Sun 4/40 can drive about 30 zombies 3 times faster than real time. With Ulysses driving a robot, the simulation runs much slower than real time. The slowdown is due to the large number of messages that must be passed between the Ulysses and PHAROS and the frequent switching of control between the programs.

PHAROS has be invaluable for us in our research on robot driving. It allows us to test driving decision procedures and examine perception and information flow in Ulysses. PHAROS has been sent to several other sites doing research in driving, robotics, and artificial intelligence.

4.5 Conclusions

Research in autonomous vehicle technology in the past 30 years has provided vehicles that can competently perform operational driving tasks. Although computers can also plan errands and find routes, they cannot make the immediate decisions necessary to drive in traffic. Ulysses is a model for driving that describes how to perform these tactical tasks. Ulysses incorporates driving knowledge that describes how various traffic objects and situations constrain a vehicle's actions. This knowledge recognizes situations from specific relations among physical objects. Ulysses includes tactical perceptual routines for finding these objects in the world and relating them to the vehicle. The model is implemented as a computer program so that it may be developed and tested objectively; it is currently used to drive a robot in the simulated world of PHAROS.

Ulysses was designed to drive safely in the PHAROS world. Our goal was to prevent the simulated robot from having or causing accidents, and from unnecessarily constraining itself to stop. We have achieved this goal for several traffic situations, including different types of intersections, multiple lane roads, and freeway interchanges with light traffic. Future improvements to Ulysses might include new behaviors such as overtaking, improved merging, or "edging" into an intersection while waiting for a gap. A more significant improvement in driving knowledge that we have not yet examined closely is the analysis of nearby traffic to predict how other cars will move. This analysis would involve the detection of many other cars, the *abstraction* the relative motions of the cars, and the projection of the motions into the future. Eventually the model must be combined with a strategic driving program; the parameters in Ulysses would then be determined by variable strategic goals, such as time stress, pleasure in driving, worry about citations, fuel efficiency, etc. PHAROS and Ulysses could also be expanded to include more objects such as blinking signals, activated signals, bicycles, pedestrians, roads without lanes, and different vehicle types.

Rather than adding more sophisticated driving knowledge, our more immediate goal is to determine how a real robot can perform the basic tactical tasks. As Ulysses drives a robot in PHAROS, it generates many perceptual requests. Machine perception is very expensive computationally, so it is important to find ways to minimize the cost of the requests. We are studying ways to take advantage of the coherence of situations over time and the difference in criticality of constraints to eliminate unnecessary requests. In the future we will study how a resource-limited robot might choose the best perception and constraint-generation actions to perform when it cannot perform them all. We would also like to model uncertainty in sensing and interpretation explicitly, and empower Ulysses to choose actions with the maximum expected utility. Finally, a truly intelligent driving model should be able to *learn* how to improve its behavior as it gains experience driving.

Ulysses has four major strengths as a driving model: it comprises many driving tasks; it models individual drivers; it is grounded in (perceived) physical objects and operational maneuvers; and it specifies how to compute actions from perceptions. Of these characteristics, physical grounding and explicit computation are probably the

most important. They allow the model to be designed and used objectively, independent of human interpretation. A computational model can help to detect problems that human designers may not see. For example, we described earlier how Ulysses looks at the backs of Stop signs facing the cars on cross streets. We did not plan to include such a perceptual action in Ulysses, but after the intersection rules were encoded it became clear that this information is necessary for determining right of way. None of the driving task descriptions we studied—including the McKnight analysis [26], and the official driver's manual [8] and vehicle code [25] for our state—call for this action. A model such as Ulysses can predict a driver's real information needs in any situation.

The characteristics described above make Ulysses uniquely suitable for driving an autonomous vehicle. They also give Ulysses the potential to contribute to general driving research. Research in driving seeks to answer many questions that apply equally to a robot and human driver, such as "How can a driver learn to make better decisions?" and "what information should be provided along roads to make driving easier?" We can answer these questions if we have an accurate, concrete driver model. We feel that computational driver models will prove to be invaluable tools for driving research.

References

[1] Aasman, Jans.
Implementations of Car-Driver Behaviour and Psychological Risk Models.
In J. A. Rothengatter and R. A. deBruin (editors), *Road User Behaviour: Theory and Practice*, pages 106-118. Van Gorcum, Assen, 1988.

[2] Agre, P. E. and D. Chapman.
Pengi: An Implementation of a Theory of Activity.
In *Proceedings of the Sixth National Conference on Artificial Intelligence*, pages 268-272. Morgan Kaufman Publishers, Los Altos, 1987.

[3] Belcher, P. L. and Catling, I.
Autoguide Electronic Route Guidance in London and the U.K..
Technical Report 89102, ISATA, June, 1989.

[4] Bender, J. G. and Fenton, R. E.
A Study of Automatic Car Following.
IEEE Transactions on Vehicular Technology VT-18:134 - 140, Nov., 1969.

[5] Cardew, K. H. F.
The Automatic Steering of Vehicles -- An Experimental System Fitted to a Citroen Car.
Technical Report RL 340, Road Research Laboratory, February, 1970.

[6] Chin, H.C.
SIMRO: A Model To Simulate Traffic at Roundabouts.
Traffic Engineering and Control 26(3), March, 1985.

[7] Cro, J. W. and Parker, R. H.
Automatic Headway Control -- An Automobile Vehicle Spacing System.
Technical Report 700086, Society of Automotive Engineers, January, 1970.

[8] Department of Transportation.
Pennsylvania Manual for Drivers (Publication 95)
Commonwealth of Pennsylvania, Harrisburg, PA, 1984.

[9] Dickmanns, E. and Zapp, A.
A Curvature-Based Scheme for Improving Road Vehicle Guidance by Computer Vision.
In *Mobile Robots (Vol. 727)*. SPIE, 1986.

[10] Drew, Donald.
Traffic Flow Theory and Control.
McGraw-Hill Book Company, New York, 1968.

[11] Elliott, R. J. and Lesk, M. E.
Route Finding in Street Maps by Computers and People.
In *Proceedings of AAAI 82*, pages 258 - 261. AAAI, 1982.

[12] FHWA.
Traffic Network Analysis with NETSIM: A User Guide
Federal Highway Administration, Washington, D.C., 1980.

[13] Fenton, R. and Mayhan, R.
Automated Highway Studies at the Ohio State University -- An Overview.
IEEE Transactions on Vehicular Technology 40(1):100 - 113, February, 1991.

[14] Gage, D. W. and Pletta, B. J.
Ground Vehicle Convoying.
In *Mobile Robots II (Vol. 852)*, pages 319 - 328. SPIE, 1987.

[15] Gardels, K.
Automatic Car Controls For Electronic Highways.
Technical Report GMR-276, General Motors Research Labs, Warren, MI, June, 1960.

[16] Gibson, D. R. P.
Available Computer Models for Traffic Operations Analysis.
In *The Application of Traffic Simulation Models. TRB Special Report 194.*, pages 12 - 22. National Academy of Sciences, 1981.

[17] Hayes-Roth, B.
A Blackboard Architecture for Control.
Artificial Intelligence 26:251 - 321, 1985.

[18] Kawashima, H.
Two Major Program Demonstrations in Japan.
IEEE Transactions on Vehicular Technology 40(1):141 - 146, February, 1991.

[19] Kehtarnavaz, N., Lee, J. S., and Griswold, N. C.
Vision-Based Convoy Following by Recursive Filtering.

[20] Kluge, K. and C. Thorpe.
Explicit Models for Road Following.
In *Proceedings of the IEEE Conference on Robotics and Automation.* IEEE, 1989.

[21] Kories, R., Rehfeld, N. and Zimmermann, G.
Toward Autonomous Convoy Driving: Recognizing the Starting Vehicle in Front.
In *Proceedings of the 9th International Conference on Pattern Recognition*, pages 531 - 535. IEEE, 1988.

[22] Kuan, D., Phipps, G, and Hsueh, A-C.
Autonomous Robotic Vehicle Road Following.
IEEE Transactions on PAMI 10(5):648 - 658, 1988.

[23] Laird, John E; Newell, Allen; and Rosenbloom, Paul S.
Soar: an Architecture for General Intelligence.
Artificial Intelligence 33:1 - 64, 1987.

[24] Lang, R. P. and Focitag, D. B.
Programmable Digital Vehicle Control System.
IEEE Transactions on Vehicular Technology VT-28:80 - 87, Feb, 1979.

[25] Legislative Reference Bureau.
Pennsylvania Consolidated Statutes, Title 75: Vehicles (Vehicle Code)
Commonwealth of Pennsylvania, Harrisburg, PA, 1987.

[26] McKnight, J. and B. Adams.
Driver Education and Task Analysis Volume I: Task Descriptions.
Final Report, Department of Transportation, National Highway Safety Bureau, Washington, D.C., November, 1970.

[27] Michon, J. A.
A Critical View of Driver Behavior Models: What Do We Know, What Should We Do?
In L. Evans and R. Schwing (editors), *Human Behavior and Traffic Safety.* Plenum, 1985.

[28] Oshima, R. *et al.*
Control System for Automobile Driving.
In *Proceedings of the Tokyo IFAC Symposium*, pages 347 - 357. , 1965.

[29] Pomerleau, D. A.
ALVINN: An Autonomous Land Vehicle In a Neural Network.
Technical Report CMU-CS-89-107, Carnegie Mellon University, 1989.

[30] Reece, D. A. and S. Shafer.
An Overview of the Pharos Traffic Simulator.
In J. A. Rothengatter and R. A. deBruin (editors), *Road User Behaviour: Theory and Practice.* Van Gorcum, Assen, 1988.

[31] Reid, L. D.; Graf, W. O.; and Billing, A. M.
The Validation of a Linear Driver Model.
Technical Report 245, UTIAS, March, 1980.

[32] Rillings, J. H. and Betsold, R. J.
Advanced Driver Information Systems.
IEEE Transactions on Vehicular Technology 40(1), February, 1991.

[33] T. Rothengatter and R. de Bruin (editor).
Road User Behaviour.
Van Gorcum, 1988.

[34] Shladover, S. E. *et al.*
Automatic Vehicle Control Developments in the PATH Program.
IEEE Transactions on Vehicular Technology 40(1):114 - 130, Feb, 1991.

[35] Sugie, M., Menzilcioglu, O., and Kung, H. T.
CARGuide -- On-board Computer for Automobile Route Guidance.
Technical Report CMU-CS-84-144, Carnegie Mellon University, 1984.

[36] Texas Engineering Experiment Station.
BART. Binocular Autonomous Research Team.
Research brochure, Texas A&M University.
1989

[37] Thorpe, C., Hebert, M., Kanade, T., and Shafer, S.
Vision and Navigation for the Carnegie Mellon NAVLAB.
IEEE Transactions on PAMI 10(3), 1988.

[38] Tsugawa, S., Yatabe, T., Hirose, T., and Matsumoto, S.
An Automobile with Artificial Intelligence.
In *Proceedings of the 6th IJCAI*, pages 893 - 895. IJCAI, 1979.

[39] Turk, M., Morgenthaler, D., Gremban, K., and Marra, M.
Video Road-Following for the Autonomous Land Vehicle.
In *Proceedings of the International Conference on Robotics and Automation.* IEEE, 1987.

[40] van der Molen, H.H., and Botticher, A.M.T.
Risk Models for Traffic Participants: A Concerted Effort for Theoretical Operationalizations.
Road Users and Traffic Safety.
In J. A. Rothengatter and R. A. de Bruin,
Van Gorcum, Assen/Maastricht, The Netherlands, 1987, pages 61-82.

[41] von Tomkewitsch, R.
Dynamic Route Guidance and Interactive Transport Management with ALI-Scout.
IEEE Transactions on Vehicular Technology 40(1):45 - 50, February, 1991.

[42] Waxman, Allen; LeMoigne, Jacqueline J.; Davis, Larry S.; Srinivasan, Babu; Kushner, Todd R.; Liang, Eli and Siddalingaish, Tharakesh.
A Visual Navigation System for Autonomous Land Vehicles.
IEEE Journal of Robotics and Automation RA-3(2), April, 1987.

[43] Wong, Shui-Ying.
TRAF-NETSIM: How It Works, What It Does.
ITE Journal 60(4):22 - 27, April, 1990.

5. Combining artificial neural networks and symbolic processing for autonomous robot guidance

5.1 Introduction

Artificial neural networks are commonly employed as monolithic non-linear classifiers.[1] The technique, often used in domains such as speech, character and target recognition, is to train a single network to classify input patterns by showing it many examples from numerous classes. The mapping function from inputs to outputs in these classification tasks can be extremely complex, resulting in slow learning and unintelligible internal representations.

However there is an alternative to this monolithic network approach. By training multiple networks on different aspects of the task, each can learn relatively quickly to become an expert in its sub-domain. This chapter describes a technique we have developed to quickly train expert networks for vision-based autonomous vehicle control. Using this technique, specialized networks can be trained in under five minutes to drive in situations such as single-lane road driving, highway driving, and collision avoidance.

Achieving full autonomy requires not only the ability to train individual expert networks, but also the ability to integrate their responses. This chapter focuses on rule-based arbitration techniques for combining multiple driving experts into a system that is capable of guiding a vehicle in a variety of circumstances. These techniques are compared with other neural network integration schemes and shown to have a distinct advantage in domains where symbolic knowledge and techniques can be employed in the arbitration process.

5.2 Driving Module Architecture

The architecture for an individual ALVINN driving module is shown in Figure 5.2. The input layer consists of a single 30x32 unit "retina" onto which a sensor image from either the video camera or the laser range finder is projected. Each of the 960 input units is fully connected to the hidden layer of 5 units, which is in turn fully connected to the output layer. The 30 unit output layer is a linear representation of the currently appropriate steering direction. The centermost output unit represents the "travel straight ahead" condition, while units to the left and right of center represent successively sharper left and right turns. The steering direction dictated by the network may serve to keep the vehicle on the road or to prevent it from colliding with nearby obstacles, depending on the type of sensor input and the driving situation the network has been trained to handle.

To drive the Navlab, an image from the appropriate sensor is reduced to 30 x 32 pixels and projected onto the input layer. After propagating activation through the network, the output layer's activation profile is translated into a vehicle steering command. The steering direction dictated by the network is taken to be the center of mass of the "hill" of activation surrounding the output unit with the highest activation level. Using the center of mass of activation instead of the most active output unit when determining the direction to steer permits finer steering corrections, thus improving ALVINN's driving accuracy.

[1] A previous version of this chapter is accepted for publication in the Journal of Engineering Applications of Artificial Intelligence, with the same title, authored by Dean Pomerleau, Jay Gowdy, and Charles Thorpe

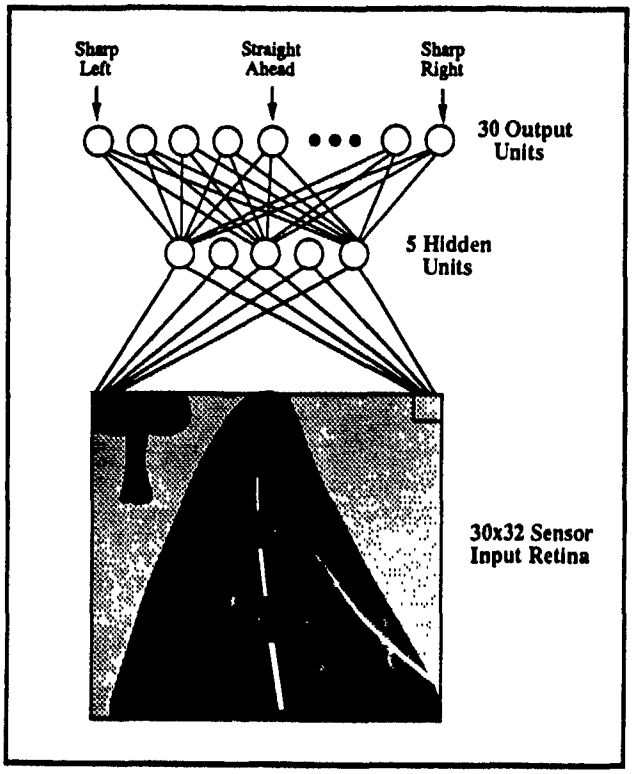

Figure 5.1: The architecture for an individual ALVINN driving module

5.3 Individual Driving Module Training And Performance

We have developed a scheme called training "on-the-fly" to quickly teach individual modules to imitate the driving reactions of a person. As a person drives, the network is trained with back-propagation using the latest video camera image as input and the person's current steering direction as the desired output. To facilitate generalization to new situations, additional variety is added to the training exemplars by shifting and rotating the original camera image in software to make it appear that the vehicle is situated differently relative to the environment (See Figure 5.3). The correct steering direction as dictated by the driver for the original image is altered for each of the

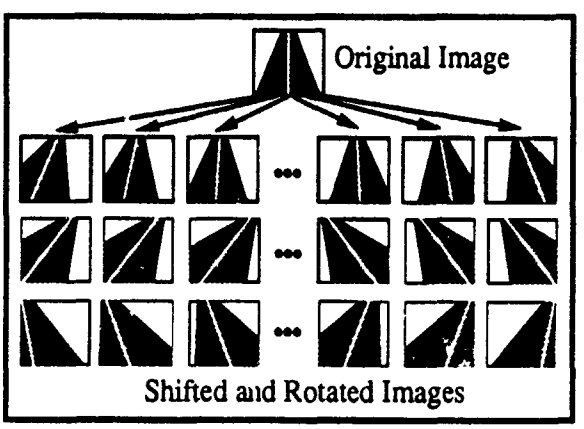

Figure 5.2: The single original video image is shifted and rotated to create multiple training exemplars in which the vehicle appears to be at a different locations relative to the road.

transformed images to account for the altered vehicle placement. Adding these transformed patterns to the training set allows the network to learn to recover from driving mistakes, without requiring the human trainer to explicitly stray from the road center and then return. For more details about the technique and purpose of training on-the-fly, see [7].

Running on three Sun-4 Sparcstations, training on-the-fly requires about five minutes during which a person drives the Navlab at about six miles per hour over a 1/4 to 1/2 mile stretch of training road. Once it has learned, the network can accurately traverse the length of road used for training and also generalize to drive along parts of the road it has never encountered under a variety of weather conditions. In addition, since determining the steering direction from the input image merely involves a forward sweep through the network, the system is able to process 20 images per second, allowing it to drive at up to the Navlab's maximum speed of 20 miles per hour\footnote{The Navlab has a hydraulic drive system that allows for very precise speed control, but that prevents the vehicle from driving over 20 miles per hour.}. This is over twice as fast as any other sensor-based autonomous system has driven the Navlab [6, 3].

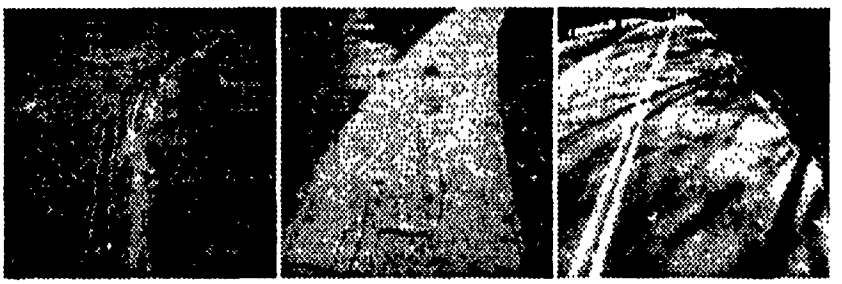

Figure 5.3: Video images taken on three of the roads ALVINN modules have been trained to handle. They are, from left to right, a single-lane dirt access road, a single-lane paved bicycle path, and a lined two-lane highway.

The flexibility provided by training on-the-fly has facilitated the development of individual driving networks to handle numerous situations. Using video camera images as input, networks have been trained to drive on single-lane dirt roads, single-lane paved roads, two-lane suburban neighborhood streets, and lined two-lane highways (See Figure 5.3).

By replacing the video input with alternative sensor modalities, ALVINN has learned other interesting behaviors. One such sensor onboard the Navlab is a scanning laser range finder. The range finder provides images in which pixel values represent the distance from the range finder to the corresponding area in the scene. Obstacles such as trees and cars appear as discontinuities in depth, as can be seen in the simulated range finder image at the bottom of Figure 5.3. Using this sensor, separate ALVINN modules have been trained to avoid collisions in obstacle-rich environments and to follow alongside rows of parked cars.

A third type of image used as input to ALVINN modules comes from a laser reflectance sensor. In this type of image, a pixel's value corresponds to the amount of laser light that reflects off the corresponding point in the scene and back to the sensor. The road and off-road regions reflect differently, making them distinguishable in the image (see Figure 5.3). Laser reflectance images in many ways resemble black and white video images, but have the advantage of being independent of ambient lighting conditions. Using this sensor modality, we have trained a network to follow single-lane roads in total darkness.

Figure 5.4: Images taken of a scene using the three sensor modalities the system employs as input. From left to right they are a video image, a laser range finder image and a laser reflectance image. Obstacles like trees appear as discontinuities in laser range images. The road and the grass reflect different amounts of laser light, making them distinguishable in laser reflectance images.

5.4 Symbolic Knowledge And Reasoning

Despite the variety of capabilities exhibited by individual driving networks, until recently the system has been far from truly autonomous. First, the one driving network architecture shown in Figure 5.2 was capable of driving only on the type of road on which it was trained. If the road characteristics changed, ALVINN would often become confused and stray from the road. In addition, a real autonomous system needs to be capable of planning and traversing a route to a goal. The neural network driving modules are good at reactive tasks such as road following and obstacle avoidance, but the networks have a limited capability for the symbolic tasks necessary for an autonomous mission. The system of networks cannot decide to turn left at an intersection in order to reach a goal. After making a turn from a one lane road to a two lane road, the system does not know that it should stop listening to one network and start listening to another. Just as a human needs symbolic reasoning to guide reactive processes, the networks need a source of symbolic knowledge to plan and execute a mission.

Ideally, the symbolic knowledge source would reason like a person. It would use its knowledge of the world to plan a sequence of observations and corresponding actions to traverse the route. For instance, to achieve the goal of reaching a friend's house, the mission description might be a sequences like, "Drive until the sign for Seneca Road is seen, and turn left at that intersection. Then drive until the third house on the left is seen, and stop in front of it."

In this ideal system, once the mission is planned, the symbolic knowledge source would rely entirely on perception to control the execution of the mission. In other words, the symbolic resource module would be able to recognize events and use what it sees to guide the interaction of the networks. The symbolic resource module would be capable of reading the street sign at an intersection and making the appropriate turn to continue on to its destination. It would also be able to identify the new road type and choose the appropriate network for driving on that kind of road. Unfortunately, the perception capabilities required by such a module are beyond the current state of the art.

In order to bridge the gap between mission requirements and perception capabilities, we use additional geometric and symbolic information stored in an "annotated map". An annotated map is a two dimensional data structure containing geometrical information about the area to be traversed, such as the locations of roads and landmarks. In addition, each object in the map can be annotated with extra information to be interpreted by the clients that access the map. For example, as far as the annotated map is concerned, a mailbox is simply a two dimensional polygon at a particular location with some extra bits associated with it. The "extra bits" might represent the three dimensional shape of the the mailbox, or even the name of the person who owns it. The module which manages the annotated map does not interpret this extra information, but rather provides a mechanism for client modules to access the

annotations. This reduces the knowledge bottleneck that can develop in large, completely centralized systems.

The annotated map is not just a passive geometric database, but instead is an active part of our system. Besides having a 2D representation of the physical objects in a region, annotated maps can contain what are called alarms. Alarms are conceptual objects in the map, and can be lines, circles, or regions. Each alarm is annotated with a list of client modules to notify and the information to send to each when the alarm is triggered. When the annotated map manager notices that the vehicle is crossing an alarm on the map, it sends the information to the pertinent modules. Once again, the map manager does not interpret the information: that is up to the client modules.

Alarms can be thought of as positionally based production rules. Instead of using perception based production rules like, "If A is observed, then perform action B", an annotated map based system has rules of the form, "If location A is reached, then perform action B". Thus we reduce the problem of making high level decisions from the difficult task of perceiving and reacting to external events to the relatively simple task of monitoring and updating the vehicle's position.

The first step in building an annotated map is collecting geometric information about the environment. We build our maps by driving the vehicle over roads and linking the road segments together at intersections. At the same time, a laser range finder is used to record the positions of landmarks such as mailboxes and telephone poles. Planning a particular mission requires adding specific instructions to the map in the form of "trigger annotations". This is currently a process performed by the person planning the mission. For example, the human expert knows that when approaching an intersection, the vehicle should slow down, so the expert chooses the appropriate location to put the trigger line. The trigger line goes across the road at that point, and is annotated with a string of bits that represents the new speed of the vehicle. During the run, when the vehicle crosses the trigger line, the map manager sends the string of bits to a module that interprets the information and slows the vehicle to the desired speed. In the current system, alarms are interpreted as commands, but there is no predefined "correct" way for a module to react to an alarm. Depending on its content, an alarm could also be interpreted as a wakeup call, or even as simply advice.

Because position information is so critical to an annotated map system, we use multiple techniques to determine the vehicle's current location. We use an Inertial Navigation System (INS) which can determine the vehicle's location with an error of approximately 1\% of distance traveled [1]. To eliminate positioning error that accumulates over time in the INS data, the annotated map system also uses information from perception modules. For example, since the driving networks presumably keep the vehicle on the road, lateral error in the vehicle positioning system relative to the road can be identified and eliminated. In addition, a module using the laser range finder compares the landmarks it sees to the landmarks collected when the map was built, and triangulates the vehicle's position on the map. These techniques allow perception modules to provide useful positioning information {\em without} requiring them to explicitly recognize and interpret particular objects such as street signs. The position corrections provided by perception modules are interpreted as a change in the transform between the location that the INS reports and the real vehicle position on the map. A separate module, called the navigator, is in charge of maintaining and distributing this position transform.

Annotated maps provide the system with the symbolic information and control knowledge necessary for a fully autonomous mission. Since the control knowledge is geometrically based, and since planning is done before the mission starts, runtime control comes at a low computational cost. Figure 5.4 shows the structure and interaction of the annotated map system's components. It also illustrates the annotated map system's interaction with the other parts of the system, including the perceptual neural networks and the arbitrator (discussed below). Figure 5.4 shows a map and annotations for a mission segment.

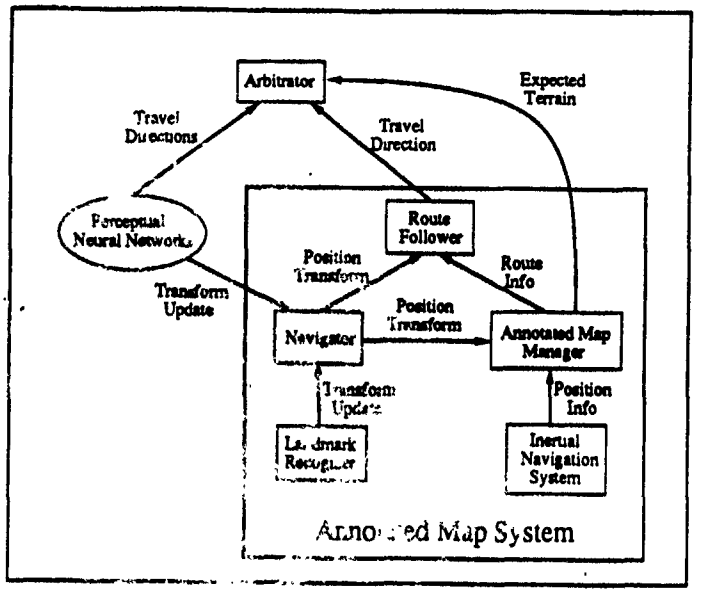

Figure 5.5: The components of the annotated map system and the interaction between them. The annotated map system keeps track of the vehicle's position on a map. It provides the arbitrator with symbolic information concerning the direction to steer to follow the preplanned route and the terrain the vehicle is currently encountering. The neural network driving modules are condensed for simplicity into a single block labeled perceptual neural networks.

5.5 Rule-Based Driving Module Integration

We use the symbolic knowledge provided by the annotated map system to help guide the interaction of the reactive driving neural networks. Figure 5.5 shows the system architecture with emphasis on the neural networks. Whereas Figure 5.4 subsumed the neural network systems into one unit labeled "perceptual neural networks", Figure 5.5 subsumes the annotated map system into one package. In this diagram, each box represents a separate process running in parallel. Images from the three onboard sensors are provided to the five driving networks shown in the second row of the diagram. The driving networks propagate activation forward through their weights, with each determining what it considers to be the correct steering direction. These steering directions are sent to the arbitrator, which has the job of deciding which network to attend to and therefore now to steer.

The arbitrator makes use of both the geometric and control information provided by the annotated map system to perform a mission autonomously. First, the route following module within the annotated map system uses the geometric information in the annotated map to recommend a vehicle steering direction. The direction recommended by the route follower is the direction it thinks the vehicle should steer in order to follow the preplanned route. When the vehicle is driving down a road, the route follower queries the annotated map for the position of the road ahead of the vehicle. The route follower uses this geometric information to generate a steering direction.

The annotated map system also provides the arbitrator with information about the current driving situation, including what type of road the vehicle is on, and whether there is an intersection or dangerous permanent obstacle ahead. For example, suppose during the planning phase the human expert notices that at a particular point the road changes from one lane to two. The expert would set a trigger line at the corresponding point on the map and

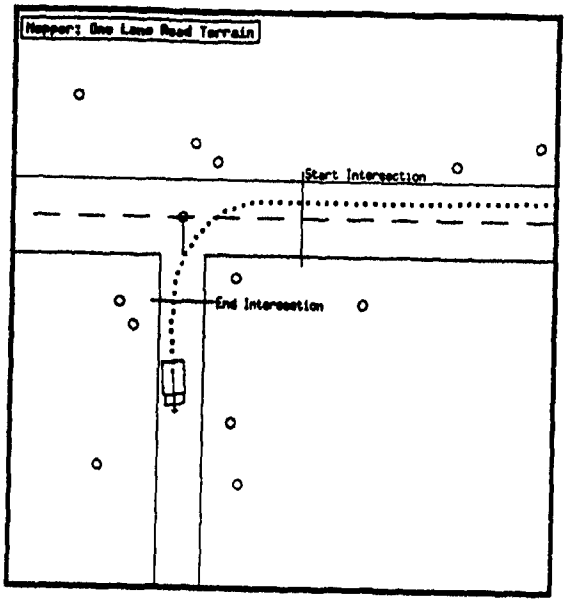

Figure 5.6: A section of a map created and maintained by the annotated map system. The map shows the vehicle traversing an intersection between a single- and a two-lane road. The lines across the roads are alarms which are triggered when crossed by the vehicle. Triggering an alarm results in a message being passed from the map manager to the arbitrator indicating a change in terrain type. The circles on the map represent the positions of landmarks, such as trees and mailboxes. The annotated map system uses the locations of known landmarks to correct for vehicle positioning errors which accumulate over time.

annotate it with a message that will tell the arbitrator to stop listening to the one lane road following network and start listening to the two lane road following network. When the alarm is triggered during the run, the arbitrator combines the advice from the annotated map system with the steering directions of the neural network modules using a technique called relevancy arbitration.

Relevancy arbitration is a straightforward idea. If the annotated map system indicates the vehicle is on a two-lane road, the arbitrator will steer in the direction dictated by the two-lane road driving network, since it is the relevant module for the current situation. If the annotated map system indicates the vehicle is approaching an intersection, the arbitrator will choose to steer in the direction dictated by the annotated map system, since it is the module that knows which way to go in order to head towards the destination. In short, the arbitrator combines symbolic knowledge of driving module capabilities with knowledge of the present terrain to determine the relevant module for the current circumstances.

The relevancy of a module need not be based solely on the current terrain information provided by the annotated map system. Instead, the arbitrator also employs rules for determining a module's relevancy from the content of the module's message. The obstacle avoidance network has one such rule associated with it. The obstacle avoidance network is trained to steer straight when the terrain ahead is clear and to swerve to prevent collisions when confronted with obstacles. The arbitrator gives low relevancy to the obstacle avoidance network when it suggests a straight steering direction, since the arbitrator realizes it is not an applicable knowledge source in this situation. But when it suggests a sharp turn, indicating there is an obstacle in the vehicle's path, the urgency of avoiding a collision takes precedence over other possible actions, and the steering direction is determined by the obstacle avoidance network. This priority arbitration is similar in many ways to the subsumption architecture [2], although the most

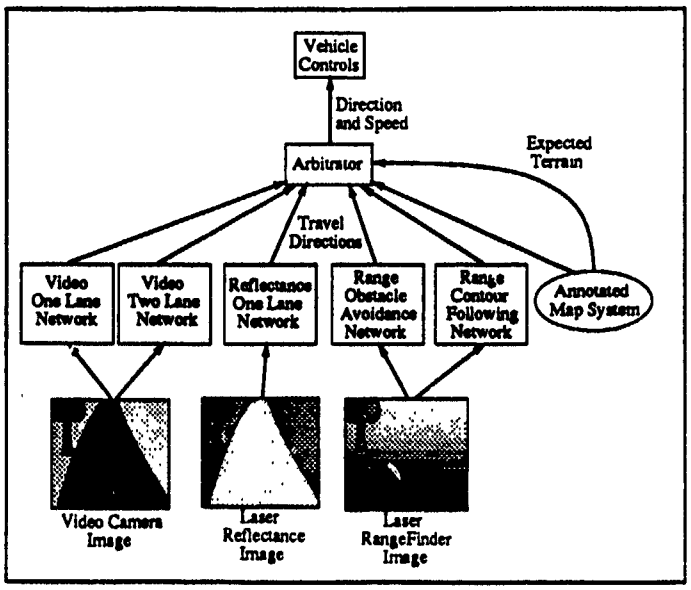

Figure 5.7: The integrated ALVINN architecture. The arbitrator uses the terrain information provided by the annotated map system as well as symbolic models of the driving networks' capabilities and priorities to determine the appropriate module for controlling the vehicle in the current situation.

common interaction between behaviors in Brooks' systems is for higher level behaviors to override less sophisticated, instinctual ones.

By combining map-related knowledge about the current driving situation with knowledge about abilities and priorities of individual driving modules, the integrated architecture provides the system with capabilities that far exceed those of individual driving modules alone. Using this architecture, the system has successfully followed a 1/2 mile path through a suburban neighborhood from one specific house to another. In navigating the route, the system was required to drive through three intersections onto three different roads while swerving to avoid parked cars along the way. At the end, the vehicle came to rest one meter from its destination.

5.6 Analysis And Discussion

Rule-based integration of multiple expert networks has significant advantages over previously developed connectionist arbitration schemes. One such advantage is the ease of adding new modules to the system. Using rule-based arbitration, the new module can be trained in isolation to become an expert in a new domain, and then integrated by writing rules for the arbitrator which specify the new module's area of expertise and its priority. This is in contrast to other connectionist expert integration techniques, such as the task decomposition architecture [5], connectionist glue [8] and the meta-pi architecture [4]. To combine experts using these techniques requires the training of additional neural network structures, either simultaneously with the training of the experts in the case of the task decomposition architecture, or after expert training in the case of the connectionist glue and meta-pi architectures. Adding a new expert using these techniques requires retraining the entire integrating structure from scratch, which involves presenting the system patterns from each of the experts' domains, not just the new one. This large scale retraining is particularly difficult in a task like autonomous navigation because it requires either driving over all the experts' domains again, or storing a large number of domain-specific images for later reuse.

Another significant advantage of rule-based arbitration is the ease with which non-neural network knowledge sources can be integrated into the system. Symbolic tasks such as planning and reasoning about a map are currently difficult to implement using neural networks. In the future, it should be possible to implement more and more symbolic processing using connectionist techniques, but until then, rule-based arbitration provides a way of bridging the gap between neural networks and traditional AI systems.

The technique is not without shortcomings however. The current implementation relies too heavily on the accuracy of the annotated map system, particularly for negotiating intersections. The question might be asked, why is the mapping system required for intersection traversal in the first place? Why can't the driving networks handle intersections? The answer is that when approaching an intersection, an individual driving network will often provide ambiguous steering commands, since there are multiple possible roads to follow. If left on its own, a road-following network will often alternately steer towards one or the other road choices, causing the vehicle to oscillate and eventually drive off the road. In addition, even if the network could learn to definitively choose one of the branches to follow, it still wouldn't know which is the (\it appropriate) branch to choose in order to head toward the destination. In short, the mapping modules can be viewed both as a useful source of high level symbolic knowledge, and as an interim solution to the difficult perceptual task of intersection navigation.

The annotated map system as currently implemented is not a perfect solution to the problem of high level guidance because it requires both detailed knowledge of the route, and an accurate idea of the current vehicle position. In certain controlled circumstances, such as rural mail delivery, the same route is followed repeatedly, making an accurate map of the domain feasible. However a system capable of following less precise directions, like "go about a half mile and turn left on Seneca Road", is clearly desirable. Such a system would require more reliance on observations from perception modules and less reliance on knowledge of the vehicle's exact position when making high level decisions.

Conceptually, this shift towards reliance on perception for high level guidance could be done in two ways. First, observations of objects like the Seneca Road street sign, could be used to update the vehicle's position on the map. In fact, position updates based on perceptual observations are currently employed by the annotated map system when it triangulates the vehicle's location based on the positions of known landmarks in laser range images. But position updates are only helpful when the observations are location specific. For observations of objects like stop lights, or arbitrarily located objects like "road construction ahead" signs, the system's response should be independent of the vehicle's location.

These location independent observations could be modeled as positionless alarms in the annotated map. When a perception module sees an object like a "road construction ahead" sign, it would notify the map manager. The map manager would treat the sighting as an alarm, distributing the information associated with the alarm to the pertinent modules. Perception triggered alarms would allow the system to transition between its current perceptual abilities and future, more advanced capabilities.

Although the system is not yet capable of identifying and reading individual signs, we have had preliminary success in using neural network perceptual observations to help guide high level reasoning. The technique relies on the fact that when the vehicle reaches an intersection, the output of the driving network becomes ambiguous. This ambiguity manifests itself as an output vector with more than one active steering direction corresponding to the multiple possible branches to follow. This output ambiguity has been successfully employed to update the vehicle's position and to follow coarse directions. As the vehicle approaches an intersection, the annotated map system signals the arbitrator that an intersection is coming up and that the vehicle should follow the right-hand branch in order to head towards the goal. This level of detail does not require either a highly accurate map or precise knowledge of the vehicle's current position. The arbitrator takes the annotated map system's message as a signal to

watch the output of the current driving network carefully. When the driving network's output becomes ambiguous, the arbitrator signals the annotated map system that the vehicle has reached the intersection and to update the vehicle's position accordingly. The arbitrator also uses the "turn right" portion of the annotated map system's message in order to choose the correct steering direction from the driving network's ambiguous output vector. This closer interaction between the perception networks and the annotated map allows the system to use perception for intersection traversal, instead of relying solely on knowledge from the map for guidance.

Another shortcoming of rule-based arbitration as currently implemented its binary nature. Currently, a module is deemed by the annotated map system as either appropriate or inappropriate for the current road type. This binary decision does not address the question of intelligently combining modules trained for the same domain, such as the video-based single-lane driving network and the laser reflectance-based single-lane driving network. There are obviously some situations, such as night driving, when one network is better suited than the other. To take more subtle circumstances into account when weighting the steering directions dictated by multiple networks, we are developing augmented arbitration rules that consider more context than just the current road type. We are also currently working on connectionist techniques that can determine a network's reliability directly from its output alone. Preliminary results in this area look very promising.

One final drawback of the current system is the need for a human expert to preplan the mission by providing map annotations. In the future, we will replace the human expert with an expert system capable of annotating the map appropriately. We understand the techniques the human expert uses to find the shortest route and to annotate the map, so automating the process should not be difficult.

In conclusion, a modular architecture permits rapid development of expert neural networks for complex domains like autonomous navigation. Rule-based arbitration is a simple and efficient method for combining these experts when symbolic knowledge is available for reasoning about their appropriateness. Rule-based arbitration also permits the combination of neural network experts with non-neural network processing techniques such as planning, which are difficult to integrate using other arbitration schemes.

5.7 Acknowledgements

This work would not have been possible without the input and support provided by Dave Touretzky, John Hampshire, and especially Omead Amidi, James Frazier and rest of the CMU ALV group.

The principle support for the Navlab has come from DARPA, under contracts DACA76-85-C-0019, DACA76-85-C-0003 and DACA76-85-C-0002. This research was also funded in part by a grant from Fujitsu Corporation.

5.8 References

[1] O. Amidi and C. Thorpe.
Integrated mobile robot control.
In *Proceedings SPIE Mobile Robots V*, pages 504-524. 1990.

[2] R.A. Brooks.
A Robust Layered Control System for a Mobile Robot.
IEEE Journal of Robotics and Automation RA-2(1):14-23, April, 1986.

[3] Jill D. Crisman and Charles E. Thorpe.
Color Vision for Road Following.
Vision and Navigation: The Carnegie Mellon Navlab.
In Charles E. Thorpe,
Kluwer Academic Publishers, 1990, Chapter 2.

[4] J. B. Hampshire and A.H. Waibel.
The Meta-Pi Network: Building Distributed Knowledge Representations for Robust Pattern Recognition.
Technical Report CMU-CS-89-166-R, Carnegie Mellon, August, 1989.

[5] R.A. Jacobs, M.I. Jordan and A.G. Barto.
Task Decomposition Through Competition in a Modular Connectionist Architecture: The What and Where Vision Tasks.
Technical Report 90-27, Univ. of Massachusetts Computer and Information Science, March, 1990.

[6] Karl Kluge and Charles E. Thorpe.
Explicit Models for Robot Road Following.
Vision and Navigation: The Carnegie Mellon Navlab.
In Charles E. Thorpe,
Kluwer Academic Publishers, 1990, Chapter 3.

[7] D. Pomerleau.
Efficient Training of Artificial Neural Networks for Autonomous Navigation.
Neural Computation 3(1), March, 1991.

[8] A. Waibel.
Modular Construction of Time Delay Neural Networks for Speech Recognition.
Neural Computation 1(1), March, 1989.